Regulating cationic polymerization: from structural control to life cycle management

Lianqian Wu<sup>1</sup>, Brayan Rondon<sup>1</sup>, Shoshana Dym<sup>1</sup>, Wenqi Wang<sup>1</sup>, Kuiru Chen<sup>1</sup>, Jia Niu<sup>1\*</sup>

1. Department of Chemistry, Boston College, Chestnut Hill, Massachusetts 02467, United States

\* Correspondence to: jia.niu@bc.edu

Abstract

Cationic polymerization is a powerful strategy for the production of well-defined polymers and advanced materials. In particular, the emergence of living cationic polymerization has enabled pathways to complex polymer architectures inaccessible before. The use of light and electricity as an external stimuli to regulate cationic polymerization represents another advance with increasing applications in surface fabrication and patterning, additive manufacturing, and other advanced material engineering. The past decade also witnessed vigorous progress in stereoselective cationic polymerizations, allowing for the dual control of both the tacticity and the molecular weight of vinyl polymers towards precision polymers. In addition, in addressing the plastics pollution crisis and achieving a circular materials economy, cationic polymerization offers unique advantages for generating chemically recyclable polymers, such as polyacetals, polysaccharides, polyvinyl ethers, and polyethers. In this review, we provide an overview of recent developments in regulating cationic polymerization, including emerging control systems, spatiotemporally controlled polymerization (light and electricity), stereoselective polymerization, and chemically recyclable/degradable polymers. Hopefully, these discussions will help to stimulate new ideas for the further development of cationic polymerization for researchers in the field of polymer science and beyond.

**Keywords** 

Living polymerization, Organocatalysis, Photocontrolled polymerization, Electrocontrolled polymerization, Stereoselective polymerization, Sustainable materials.

1

# **Table of Contents**

1. Introduction	5
2. General features of cationic polymerization	6
3. Emerging control systems	9
3.1. Cationic RAFT polymerization	9
3.2 Organocatalytic cationic polymerization	16
3.2.1 Organic Brønsted acid assisted cationic polymerization	16
3.2.2 Organic Lewis acid assisted cationic polymerization	23
3.3. Spatiotemporally controlled cationic polymerization	30
3.3.1 Photocontrolled/photoinitiated cationic polymerization	30
3.3.2 Electrocontrolled cationic polymerization	41
4. Stereocontrolled cationic polymerization	46
4.1 Stereoselective cationic polymerization of vinyl ethers	47
4.2 Stereoselective cationic polymerization of other monomers	57
5. Chemically recyclable/degradable polymers	60
5.1 Polyacetals	61
5.2 Polysaccharides and carbohydrate polymers	71
5.3 Polyvinyl ethers and polyethers	73
6. Conclusion and outlook	77

#### **Abbreviations**

 $\alpha$ -MeSt  $\alpha$ -Methylstyrene

AIBN Azobisisobutyronitrile

Ane trans-Anethole

BDE Bond dissociation energy

BVE *n*-Butyl vinyl ether

BzF Benzofuran

 $\varepsilon$ -CL  $\varepsilon$ -Caprolactone

CEVE 2-Chloroethyl vinyl ether

CHVE Cyclohexyl vinyl ether

cPPA Cyclic PPA

CTA Chain transfer agent

 $C_{\rm tr}$  Chain transfer constants

DBPDA *N,N'*-Di-sec-butyl-1,2-phenylenediamine

DDQ 2,3-Dichloro-5,6-dicyano-1,4-benzoquinone

DEP Diethyl phthalate

DHF 2,3-Dihydrofuran

DOLO 1,3-Dioxolan-2-one

DOP 1,2-Dioxepane

DOX 1,3-Dioxane

*DP*<sub>n</sub> Number-average degree of polymerization

*DP*<sub>w</sub> Weight-average degree of polymerization

DXL 1,3-Dioxolane

ee Enantiomeric excess

 $E_{\rm r}$  Reduced modulus

EPE Ethyl-1-propenyl ether

EVE Ethyl vinyl ether

Fc Ferrocene

H Hardness

HBD Hydrogen bond donor

HNTf<sub>2</sub> Trifluoromethanesulfonimide

IBVE Isobutyl vinyl ether

IDPi Imidodiphosphorimidate

IPVE Isopropyl vinyl ether

LA Lactide

MA Methyl acrylate

MAO Methylaluminoxane

MDOL 2-Methyl-1,3-dioxolane

MesSt 2,4,6-Trimethylstyrene

MOMBr Bromomethyl methyl ether

MOTP 2-methyl-1,3-oxathiepane

MOVE 2-Methoxyethyl vinyl ether

MSA Methanesulfonic acid

NVC *N*-Vinylcarbazole

*o*-PA *o*-Phthalaldehyde

PADIs N,N'-Bis(triflyl)phosphoramidimidates

PCCP 1,2,3,4,5-Pentacarbo-methoxycyclopentadiene

pCSt 4-Chlorostyrene

PDXL Poly(1,3-dioxolane)

*p*FSt 4-Fluorostyrene

PLA Polylactic acid

*p*MOS 4-Methoxystyrene

*p*MeSt 4-Methylstyrene

*p*MeBzA 4-Methylbenzaldehyde

PMP *p*-methoxyphenyl

PMPDOL 2-(4-Methoxyphenyl)-1,3-dioxolane

PVE *n*-Propyl vinyl ether

PTH 10-Phenylphenothiazine

RAFT Reversible addition-fragmentation chain transfer

ROP Ring opening polymerization

St Styrene

TADDOL Tetraaryl-1,3-dioxolane-4,5-dimethanol

TBVE *tert*-Butyl vinyl ether

TEMPO (2,2,6,6-Tetramethylpiperidin-1-yl)oxy

TFA Trifluoroacetic acid

TfOH Triflic acid

*t*-HBD *trans*-Hexahydro-1,3-benzodioxole

TMSVE Trimethylsilyl vinyl ether
UTS Ultimate tensile strength

VAc Vinyl acetate

#### 1. Introduction

Despite its important commercial applications, e.g., the production of polybutene-based butyl rubbers and polyvinyl ethers, cationic polymerization was considered to be highly prone to side reactions, challenging to control, and only applicable to a limited subset of monomers. This pessimistic view was proven to be grossly inaccurate when the living cationic polymerization was first reported by Higashimura and Sawamoto in the 1970s [1-4], as well as the subsequent report of living cationic polymerization of isobutylene by Faust and Kennedy [5,6]. Since then, the field has undergone rapid developments, and several reviews that focus on significant aspects of living cationic polymerization, such as Lewis acid-catalyzed controlled cationic polymerization [7-10], the living cationic polymerization mediated by reversible addition-fragmentation chain transfer (RAFT) mechanism [11], and photoinitiated and photocontrolled cationic polymerization [12-15], have already been published. To complement those seminal works, this review will attempt to not only provide a summary of recent advances in new initiation and control strategies for cationic polymerization, but also connect these methodology innovations to emerging applications in stereochemical control, biopolymer synthesis, and sustainability (Fig. 1). In doing so, we hope to introduce a broader perspective that advances in fundamental polymer chemistry can create exciting opportunities for accessing new materials with structures and functions beyond the realm of traditional synthetic polymers.

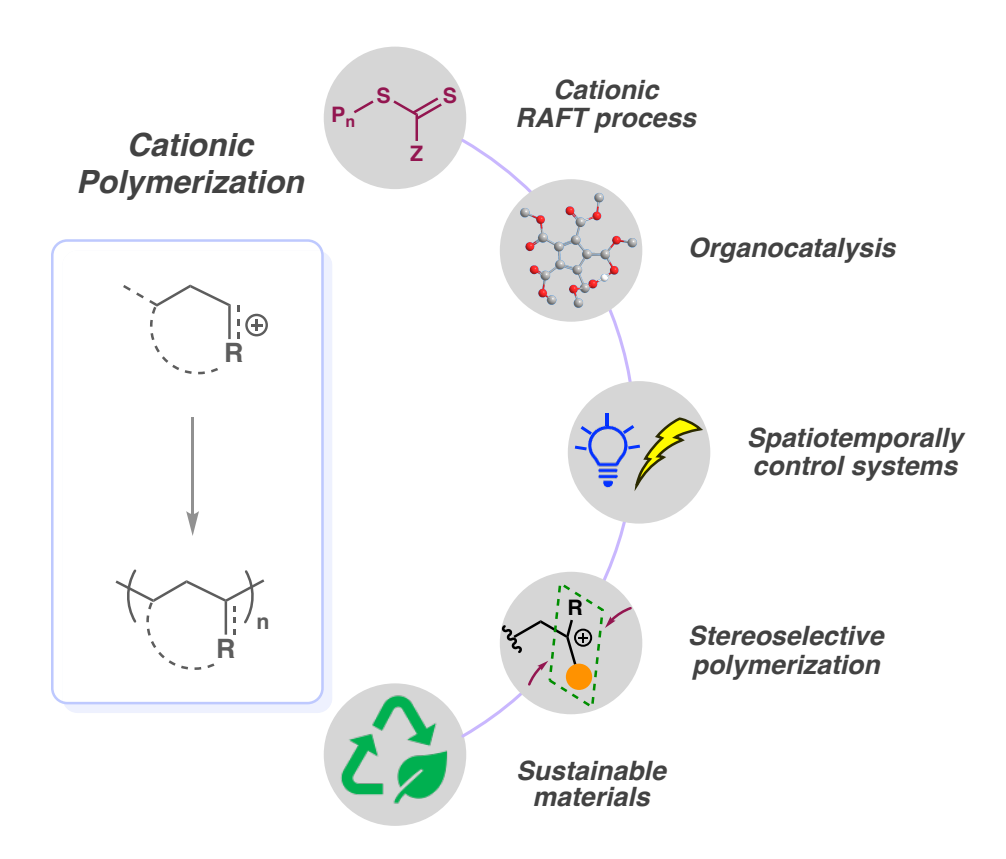


Fig. 1. Recent developments in cationic polymerization.

### 2. General features of cationic polymerization

**Monomer scope.** Cationic polymerization generally requires monomers with electron-donating substitutions that can stabilize the propagating cation, *e.g.*, vinyl ethers, 2,3-dihydrofuran (DHF), benzofuran (BzF), styrene (St), styrene derivatives, isobutene (IB), *N*-vinylcarbazole (NVC), lactones, isocyanides, *o*-phthalaldehyde (*o*-PA), cyclic acetals, and anhydrosugars (**Fig. 2**). This requirement makes the monomer scope of cationic polymerization distinct from, and largely complementary to, the radical polymerization, which is commonly used to polymerize monomers with electron-withdrawing substitutions such as (meth)acrylates, (meth)acrylamides, and styrenics. In particular, vinyl ethers [16], anhydrosugars [17,18], and NVC [19] have demonstrated the best versatility in living cationic polymerization thus far, due to their abilities to form long-lived propagating cationic species in polymerization.

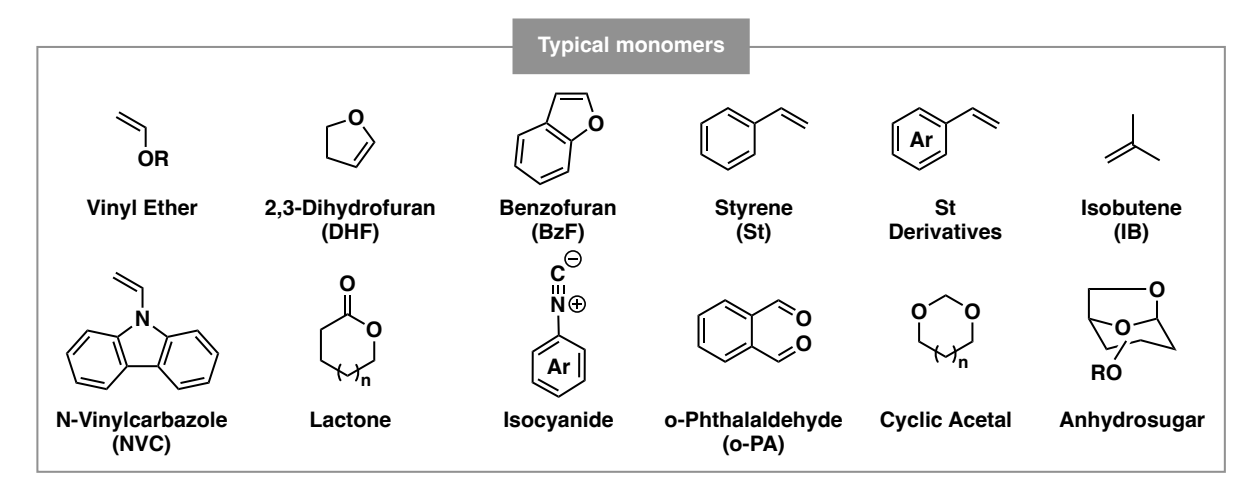


Fig. 2. Typical monomers for cationic polymerization.

Initiating method. In classic cationic polymerization, the cations are typically generated from the reaction between an initiator and a Lewis or Brønsted acid [7-10]. In cationic RAFT polymerization, cationic species are produced through the reaction between a chain transfer agent (CTA) and a Brønsted or Lewis acid catalyst (Fig. 3) [11]. These initiators are often also referred to as cationogens. Typical initiators (cationogens) for cationic polymerization are listed in Fig. 3, including organohalides, esters, sulfonates, thioethers, selenoethers, phosphates and thiocarbonylthio compounds. It is noteworthy that Lewis bases such as ethers, esters, and amides are sometimes used in conjunction with Lewis acids to regulate the initiation or reversible deactivation process for improved control over the cationic polymerization. Furthermore, recent works on photocontrolled and electrochemically controlled cationic polymerization suggest that one-electron oxidation of the CTA by photocatalysts or electrochemistry can also be used to produce cationic species, allowing for preparation of precise polymer in a spatiotemporal manner [14,15].

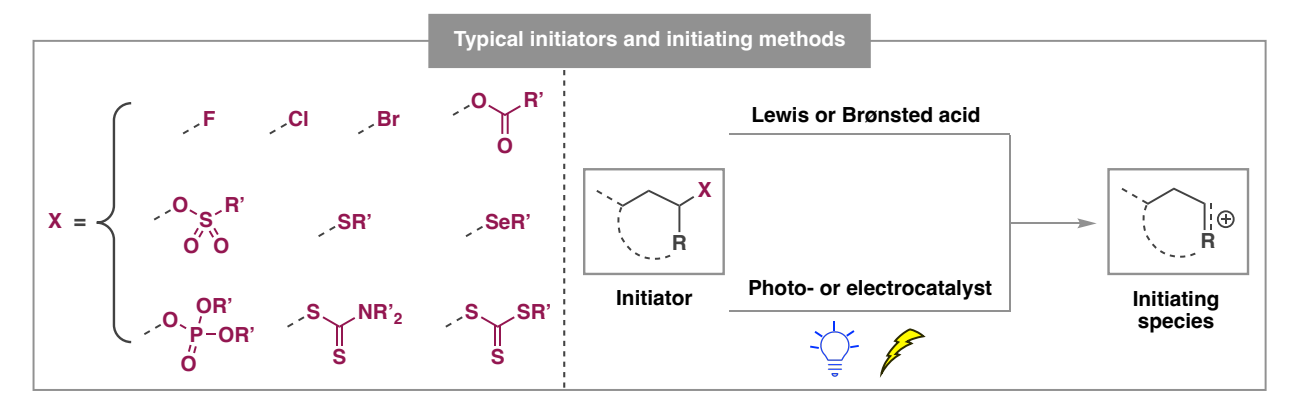


Fig. 3. Typical initiators and initiating methods for cationic polymerization.

**Propagating species.** A hallmark of cationic polymerization is the propagating cations, such as carbenium, oxocarbenium, oxonium, iminium, and sulfonium. Firstly, different classes of propagating species display different reactivities. For example, compared with carbenium species, oxocarbenium and iminium species are less reactive because of the  $\pi$ -donation of heteroatoms (oxygen or nitrogen). Moreover, the counteranions, forming by the leaving groups of initiators and Lewis/Brønsted acid catalysts, also play a significant role in the propagation step. Furthermore, both the cationic propagating species and the counteranions are typically solvated by solvent molecules. Therefore, solvents have profound impacts on the reactivity of propagating cations and are often strategically chosen for regulating cationic polymerization. It should also be noted that the propagating cations are highly electrophilic. As a result, they are more prone to side reactions, such as E1-type elimination,  $S_N1$ -type substitutions by water or other environmental nucleophiles. The high reactivity of cation species also means that its half-life is relatively short, and controlling this propagating species through a reversible deactivation mechanism is challenging.

(a) 
$$\cdots P_m - X + Cat$$
  $\longrightarrow$   $X - Cat + \cdots P_m^{\oplus}$   $M$ 

(b)  $\cdots P_m - X + \cdots P_n^{\oplus}$   $\longrightarrow$   $\cdots P_m - X - P_n \cdots$   $\longrightarrow$   $\cdots P_m^{\oplus} + \cdots P_n - X$  transient adduct

Fig. 4. General scheme for counteranion-rebound and RAFT process in cationic polymerization.

Control mechanism. Key to controlling the intrinsically unstable propagating cation in living cationic polymerization is to establish an efficient reversible deactivation process, in which the

equilibrium between the dormant species and the propagating species strongly favors the former to keep the concentration of the propagating cations low. Two main control mechanisms have been explored: counteranion-rebound and RAFT. In the counteranion-rebound cationic polymerization [7-10], activation of the chain-capping group (e.g., halide) by catalyst (e.g., metal catalyst) produces an ion pair of the propagating carbocation and a counteranion. The rebound of the counteranion reversibly deactivates the carbocation and regenerates the dormant species (Fig. 4a). In cationic RAFT polymerization [11], a dormant chain end can readily undergo reversible nucleophilic addition to the propagating carbocation to form a transient adduct, which then undergoes fragmentation to regenerate the propagating carbocation and the dormant species (Fig. 4b). Therefore, a reversible chain transfer process is established to exert control over the polymerization.

#### 3. Emerging control systems

The past decade has witnessed the rapid development of control strategies for living cationic polymerization. New catalytic systems that show remarkable reactivity and higher selectivity were reported [15]. This section will start with a cationic RAFT polymerization mechanism, followed by a comprehensive summary of the recent advances in organocatalytic cationic polymerization, and end with an overview of the spatiotemporally controlled polymerizations through light and electricity.

#### 3.1. Cationic RAFT polymerization

RAFT polymerization was first reported in 1998 as a radical polymerization method and represents one of the most powerful strategies in living radical polymerization [20-22]. In 2015, RAFT polymerization was further developed into an elegant method for controlled cationic polymerization [11,23] (**Fig. 4b**). In the cationic RAFT polymerization, the propagating cation ( $P_n^{\oplus}$ ) readily undergoes reversible addition-fragmentation chain transfer with another dormant polymer chain end ( $P_m$ -X, X indicates the chain end group) to generate the other cationic propagating polymer chain ( $P_m^{\oplus}$ ) and another dormant polymer chain ( $P_n$ -X). During a productive RAFT process, the rate of the addition/fragmentation equilibrium is higher than that of

propagation, thus making all polymer chains grow at similar rates and imposing control over the polymerization. A key component in cationic RAFT polymerization is the nature of CTAs employed (**Fig. 5**). Therefore, this section will discuss different CTAs that have been examined thus far, as well as their chain-transfer constants ( $C_{tr}$ ).

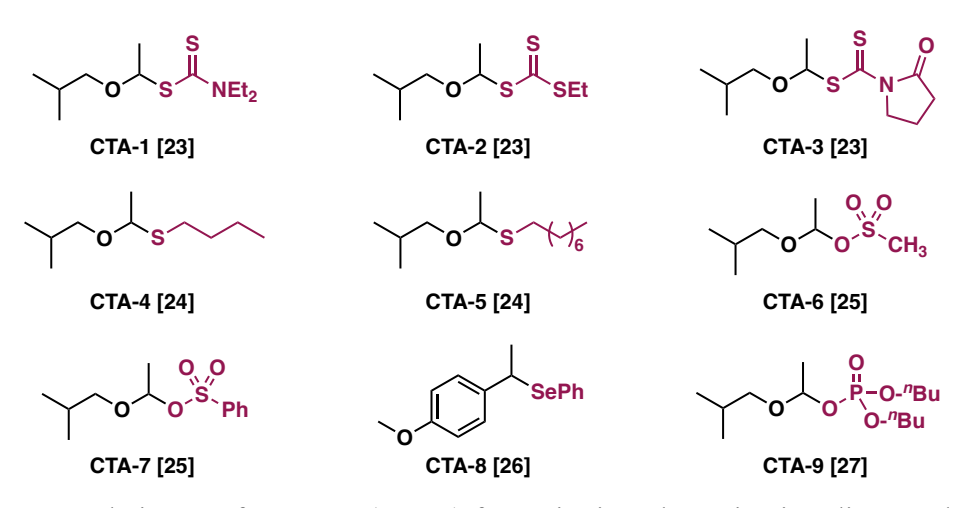
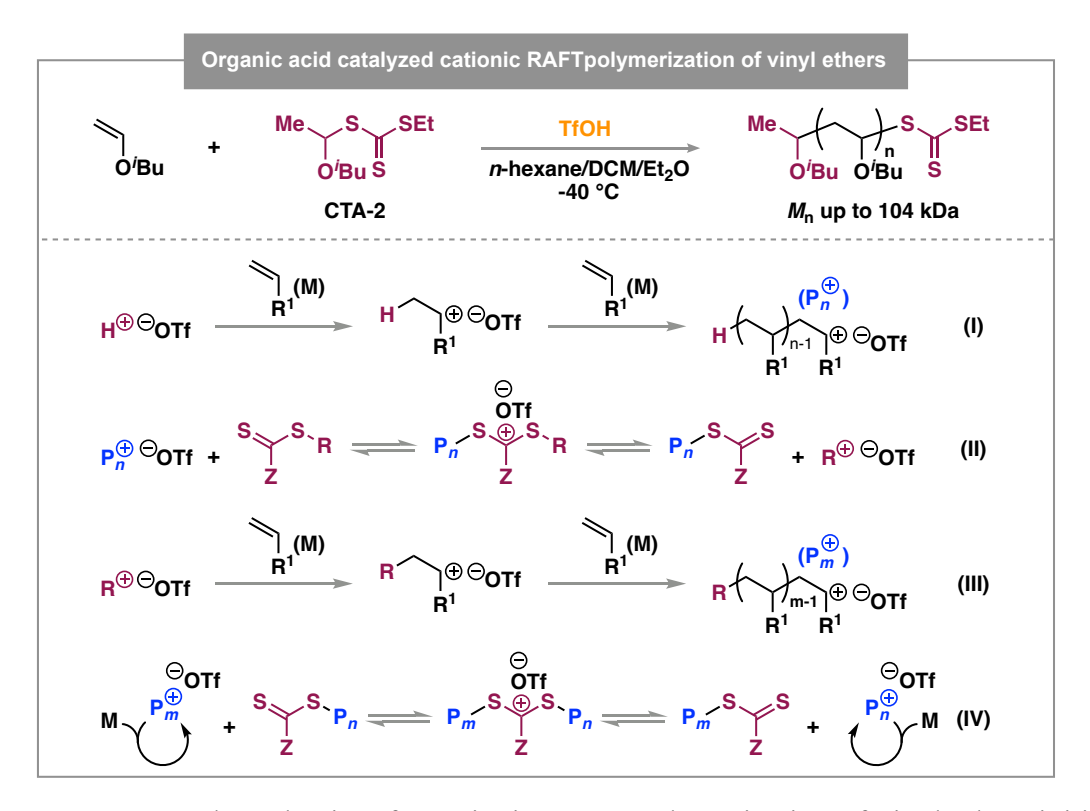


Fig. 5. Chain transfer agents (CTAs) for cationic polymerization discussed in this review.

Building on the reversible addition-fragmentation between sulfur-based nucleophiles and carbocation, in 2015, Kamigaito and coworkers investigated the potential of thiocarbonylthio compounds for gaining control over cationic polymerizations (Fig. 6) [23]. They screened several thiocarbonylthio derivatives for the polymerization of isobutyl vinyl ether (IBVE) with triflic acid (TfOH) as the catalyst. Among them, dithiocarbamate compounds provided the best control over polymerization. A well-defined polymer ( $M_n = 5.1 \text{ kDa}$ , D = 1.08) was obtained when CTA-1 was used. In contrast, loss of control was observed in the absence of CTA-1 ( $M_n = 24.6 \text{ kDa}$ , D = 3.58). They also found that trithiocarbamate CTA-2 gave a comparable performance ( $M_n = 5.0 \text{ kDa}$ , D= 1.18). However, CTA-3 with an electron-withdrawing pyrrolidione group gave higher dispersity (D > 1.80). Additionally, a high molecular weight polymer  $(M_n = 104 \text{ kDa}, D = 1.23)$  was obtained by fixing the [M]<sub>0</sub>/[CTA-2]<sub>0</sub> to be 1000. Based on these results, the authors claimed that the electronic effects of the nitrogen groups on the CTAs play the key role in the controlled polymerization, as more electron-donating substituents in the CTAs can stabilize the formed cationic intermediate, thereby allowing for control over polymerization. The living nature of the polymerization was confirmed by the linear relationship between  $M_n$  and monomer conversion, <sup>1</sup>H NMR identification of the ω-chain end, and successful chain extension experiments [23]. The

versatility of CTA-2 was also demonstrated by block copolymerization of ethyl vinyl ether (EVE) with methyl acrylate (MA). Poly(EVE-b-MA) ( $M_n = 12.4$  kDa, D = 1.32) was successfully prepared, showcasing the ability to combine cationic and radical RAFT for the synthesis of block copolymers previously difficult to access. The comprehensive mechanistic studies revealed that a distinct cationic RAFT mechanism was responsible for the controlled polymerization (**Fig. 5**). Polymerization was initiated by the protonation of the monomer by TfOH, forming the cationic propagating species  $P_n^{\oplus}$  (I). The cationic species  $P_n^{\oplus}$  then could undergo reversible chain transfer with the CTAs to form a dormant polymer chain and a cation  $R^{\oplus}$  (II). The cationic fragment  $R^{\oplus}$  (re)initiated polymerization by adding to the monomer, generating another propagating cationic species  $P_n^{\oplus}$  (III). The propagating species  $P_n^{\oplus}$  then underwent reversible chain transfer with another dormant polymer chain, generating another cationic propagating species  $P_n^{\oplus}$  and another dormant polymer chain (IV).



**Fig. 6.** General mechanism for cationic RAFT polymerization of vinyl ethers initiated by TfOH and mediated by a thiocarbonylthio-type CTA. [11,23], Copyright 2022. Adapted with permission from Elsevier Science Ltd.

Compared with thiocarbonylthio compounds, thioacetals are easier to prepare and have more stable C-S bonds. Kamigaito and coworkers proposed that a more stable sulfonium intermediate would be formed, allowing for faster chain transfer, and thus exerting better control over the polymerization. Accordingly, they discovered that thioacetals could mediate the chain transfer process during the polymerization of IBVE with trace amounts of TfOH as the catalyst (**Fig 7a**) [24]. Using thioacetal **CTA-4**, a well-defined poly(IBVE) ( $M_n = 3.3 \text{ kDa}$ , D = 1.18) was obtained when IBVE was polymerized at -40 °C. Additionally, by increasing the [M]<sub>0</sub>:[I]<sub>0</sub> ratio to 1000 and lowering the temperature to -78 °C, a high molecular weight polymer ( $M_n = 117 \text{ kDa}$ , D = 1.24) was obtained while achieving full conversion. Furthermore, **CTA-4** also displayed excellent control in the polymerization of EVE ( $M_n = 4.7 \text{ kDa}$ , D = 1.11). However, loss of control was observed for the bulky monomers, such as cyclohexyl vinyl ether (CHVE) ( $M_n = 6.6 \text{ kDa}$ , D = 1.63), presumably was due to the increased steric hinderance preventing formation of the sulfonium intermediate.

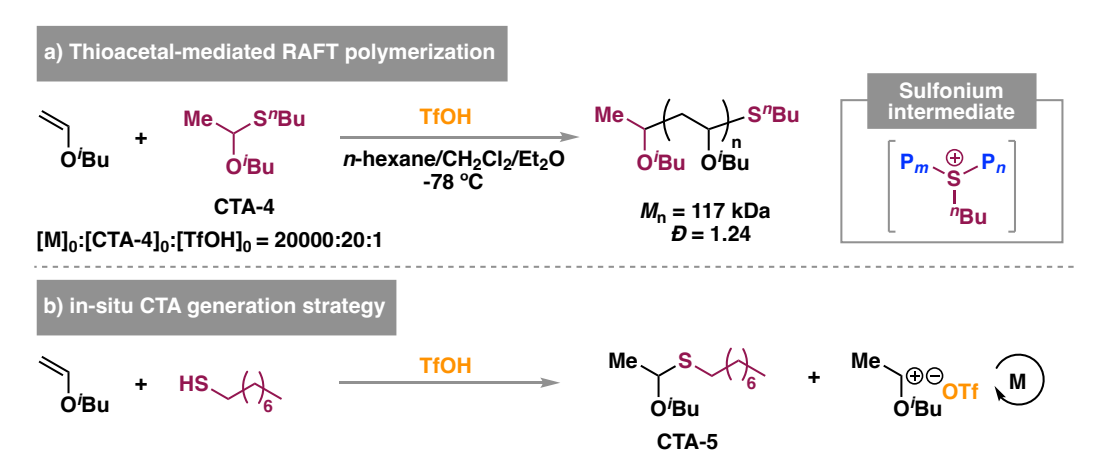


Fig. 7. Cationic RAFT polymerization of IBVE mediated by thioacetal-type CTA [24,25].

Interestingly, these thioacetal CTAs can also be generated *in situ* by combining a weakly acidic thiol precursor with TfOH (**Fig. 7b**) [25]. The vinyl ether monomer can undergo an electrophilic addition by the 1-octanethiol to form its CTA adduct (**CTA-5**). The triflic acid fills its usual role of activating the monomer and initiating polymerization. This system efficiently generated a polymer with full conversion in 24 hours with excellent molecular weight control ( $M_n = 5.6 \text{ kDa}$ , D = 1.12). The sulfur atom was demonstrated to be the key for the controlled polymerization. Polymerization of IBVE with 1-octanol instead 1-octanethiol under the same conditions yielded a

polymer with full conversion but significantly higher molecular weight and dispersity ( $M_n = 10.8$  kDa, D = 2.83).

Using the weak/strong acid pairing method, sulfonic acids were also investigated for the polymerization of IBVE (**Fig. 8**) [25]. TfOH is used as a catalyst to generate the adduct (**CTA-6**) of IBVE and sulfonic acids *in situ*. Kamigaito and coworkers found that there was a significant improvement when using CH<sub>3</sub>SO<sub>3</sub>H ( $M_n = 5.5 \text{ kDa}$ , D = 1.51) instead of PhSO<sub>3</sub>H ( $M_n = 5.6 \text{ kDa}$ , D = 2.51). The authors proposed that the methyl group was extra stabilizing for the chain transfer intermediate through electron-donation, making the reversible deactivation faster. Additionally, acetic acid and trifluoroacetic acid (TFA) were not as effective as sulfonic acids, as demonstrated by unpredictable molecular weight and high dispersity ( $M_n > 10 \text{ kDa}$ , D > 3.0). The poor performance of acetic acid derivatives as CTAs might be due to the inability of ester groups to stabilize the positive charge, further suggesting that sulfonic acid (sulfonate group) is important for chain transfer process.

**Fig. 8.** Cationic RAFT polymerization of IBVE mediated by a methane sulfonic acid-derived CTA generated *in situ* by TfOH [25].

In 2020, Tanaka and You demonstrated that selenoethers can also be used to achieve controlled cationic RAFT polymerization of vinyl ether and electron-rich styrene monomers (**Fig. 9**) [26]. In this work, controlled polymerization of 4-methoxystyrene (pMOS) ( $M_n = 12$  kDa, D = 1.38) was achieved in the presence of benzeneselenol as **CTA-8** precursor. These results were an improvement over those when using thiophenol as the CTA precursor. Preliminary experiments

suggested that the good control was due to the high nucleophilicity of selenium atom, as it could readily attack the stabilized propagating carbocation species during the propagation of pMOS.

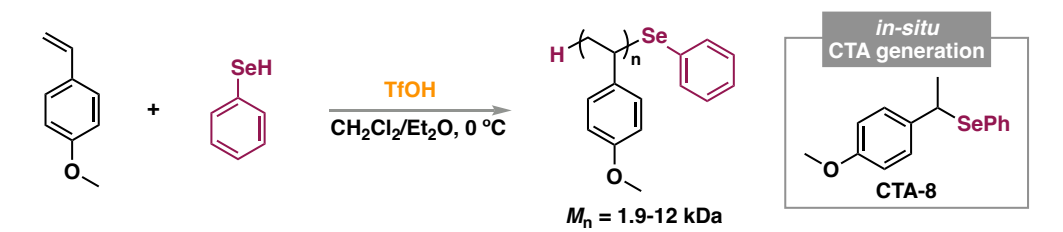
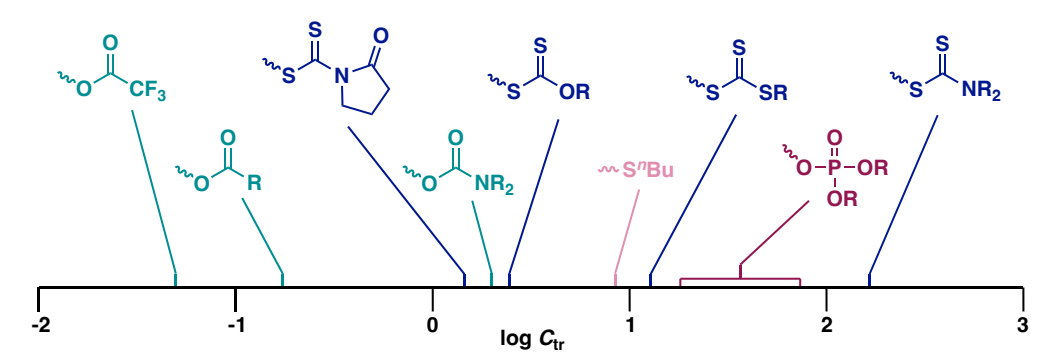


Fig. 9. Cationic RAFT polymerization of pMOS mediated by a selenoether-type CTA generated in situ [26].

Although sulfur has been the typical heteroatom involved in RAFT chemistry, sulfur-containing CTAs tend to have undesired odors and colors, impacting polymer application. As a result, efforts have been made toward developing CTAs bearing other elements. Kamigaito and coworkers demonstrated that phosphoric and phosphonic acid-based initiators could offer an alternative route to controlled cationic polymerization (**Fig. 10**) [27]. Polymerization of IBVE in the presence of phosphate-type **CTA-9** and TfOH was highly efficient, yielding a polymer with quantitative conversion in 30 minutes and excellent control ( $M_n = 2.8$  kDa and D = 1.10). Notably, a high molecular weight polymer ( $M_n = 102$  kDa and D = 1.13) was obtained within three hours. The reversible chain transfer between the dormant phosphate chain end and the propagating species proceeds through a phosphonium intermediate with resonance stabilization, providing improved control compared with previous CTAs employed.

**Fig. 10.** Cationic RAFT polymerization of IBVE mediated by a phosphate-type CTA and initiated by TfOH. [27], Copyright 2016. Adapted with permission from The Royal Society of Chemistry.

The reactivities of different CTAs in the polymerization of IBVE were compared by measuring their chain transfer constants ( $C_{tr}$ ), which were estimated from  $DP_w/DP_n$  (the weight-average and number-average degree of polymerization, respectively), conversion, [catalyst]<sub>0</sub>:[CTA]<sub>0</sub> and [M]<sub>0</sub>:[CTA]<sub>0</sub> [27,28]. In these circumstances, higher  $C_{tr}$  values resulted in lower  $DP_w/DP_n$  values, which correlated with better control over the cationic RAFT polymerization (**Fig. 11**). Dithiocarbamates with alkyl and aryl substituents have the highest  $C_{tr}$  values, which exhibit excellent control over the cationic RAFT polymerization. Electron-donating groups likely promote chain transfer because they can stabilize the cationic intermediate. On the other hand, CTAs with electron-withdrawing groups, such as carboxylate and trifluoroacetate groups, have significantly lower  $C_{tr}$  values, therefore generating much broader MW distribution. Although these  $C_{tr}$  values were obtained from the polymerization of IBVE, the same trend might also work for other typical monomers for cationic polymerization, such as NVC, St, and isobutene, etc.



**Fig. 11.** The logarithmic chain-transfer constants  $C_{tr}$  of different CTAs in the cationic RAFT polymerization of IBVE. [11], Copyright 2022. Adapted with permission from Elsevier Science Ltd.

### 3.2 Organocatalytic cationic polymerization

Metal-based Lewis acids are typically utilized in living cationic polymerization to mediate the reversible equilibrium between the carbocationic species and dormant covalent bonds (C-X, X = halogen, carboxylate, phosphate, etc.) [8]. However, metal residues are usually challenging to remove from the desired polymers, which limits their application scope, particularly in the field of biomedicine, microelectronic, cosmetics and food packaging. Driven by this, metal-free cationic polymerization has been developed since the 1980s [29,30]. Although organocatalysts have numerous advantages, such as excellent air- and moisture-stability and facile preparation, metal-free catalytic systems are often inferior to metal-catalyzed systems in terms of reaction rates and monomer scope [31]. Therefore, developing organic Brønsted/Lewis acidic catalysts that display comparable performance to metal-based Lewis acid in controlled cationic polymerization is in highly demand [32]. This section will highlight the most recent advances in organocatalytic cationic polymerization, and different catalytic models, namely, activated monomer mechanism, hydrogen bonding catalysis, halogen bonding catalysis, and chalcogen bonding catalysis, will be discussed in detail.

## 3.2.1 Organic Brønsted acid assisted cationic polymerization

In 2000, Endo and co-workers reported the first living cationic ring opening polymerization (ROP) of  $\varepsilon$ -caprolactone ( $\varepsilon$ -CL) using HCl•Et<sub>2</sub>O as a metal-free catalyst and n-butyl alcohol as an initiator

(Fig. 12) [33]. A library of poly(ε-CL) with molecular weights ranging from 3.0 kDa to 10 kDa could be readily obtained by adjusting the feed ratio of the monomer and initiator. Moreover, this work described the facile preparation of diblock copolymers consisting of lactones and cyclic carbonates by chain extension. Since then, a variety of organic acids, such as TfOH [34], trifluoromethanesulfonimide (HNTf<sub>2</sub>) [35], methanesulfonic acid (MSA) [36], and carboxylic acids [37], were disclosed to show excellent control over the ROP of lactones, lactides (LA), and cyclic carbonates. The activated monomer mechanism was suggested in these organic Brønsted acids catalyzed polymerizations. The acidic catalysts functioned as a hydrogen donor that preferentially activates the monomer compared with the polymer chain, followed by a nucleophilic attack of the hydroxy group of the propagating chain end onto the carbonyl of the activated monomer, leading to controlled chain growth and avoiding the transesterification reactions.

Fig. 12. The first example of living cationic ROP of  $\varepsilon$ -caprolactone and proposed activated monomer mechanism [33].

Inspired by great advances in organocatalysis [38-40], various phosphate-based Brønsted acids featuring bifunctional active site were designed and showed remarkable reactivity in the polymerization of lactones or LA [41-45]. In a pioneering example, Bourissou and co-workers applied the phosphoramidic acids as bifunctional catalysts for the ROP of lactones (**Fig. 13**) [46]. Poly( $\varepsilon$ -caprolactone) with controllable molecular weight ( $M_n = 1.2-18.3$  kDa) and low dispersity (D = 1.06-1.22) could be readily obtained from the living cationic ROP of  $\varepsilon$ -CL. Computational calculations disclosed a bifunctional activation mode, in which the acidic site of the catalyst operated as a hydrogen-bond donor to activate the monomer and the basic P=O moiety behaved as a hydrogen-bond acceptor to deprotonate the alcoholic  $\omega$ -chain end. This appealing bifunctional

activation model was further supported by the <sup>1</sup>H NMR titration experiments between catalyst and initiator or monomer. Although numerous catalysts have been designed and showed excellent control over the cationic polymerization, the early catalytic systems usually were limited to lactone polymerization. Therefore, developing organic Brønsted/Lewis acidic catalysts that showed broader monomer scope, particularly the vinyl monomers, is highly desirable.

Bifunctional activation model

$$O + ^nPen-OH$$
 $O + ^nPen-OH$ 
 $O + ^nPen-OH$ 

Fig. 13. Living cationic ROP of ε-caprolactone using a bifunctional catalyst [46].

Brønsted acid organocatalysts were also found to exert excellent control over the polymerization of vinyl monomers. In an early example, the Gates group developed a novel Brønsted acid catalyst featuring a unique hexacoordinate phosphorus (V) anion, which can act as a weakly coordinating anion during the polymerizations (**Fig. 14**) [47]. This initiating system provided an efficient method to polymerize monomers such as *n*-butyl vinyl ether (BVE), isoprene,  $\alpha$ -methylstyrene ( $\alpha$ -MeSt), and St. However, the optimal reaction conditions required low temperatures (-78 to -38°C) and often resulted in polymers with low to moderate dispersity (D = 1.11 - 1.94). Nonetheless, high molecular weight polymer was achievable. Particularly, BVE and  $\alpha$ -MeSt demonstrated good yields (74 - 89%) at various [M]<sub>0</sub>/[I]<sub>0</sub> ratios (200 - 1200), affording polymers with moderate to high molecular weights ( $M_n$  up to 122 kDa). Additionally, St and isoprene exhibited modest yields (47 - 89%), affording polymers moderate molecular weight ( $M_n = 37 - 55$  kDa,  $M_n = 11 - 77$  kDa, respectively).

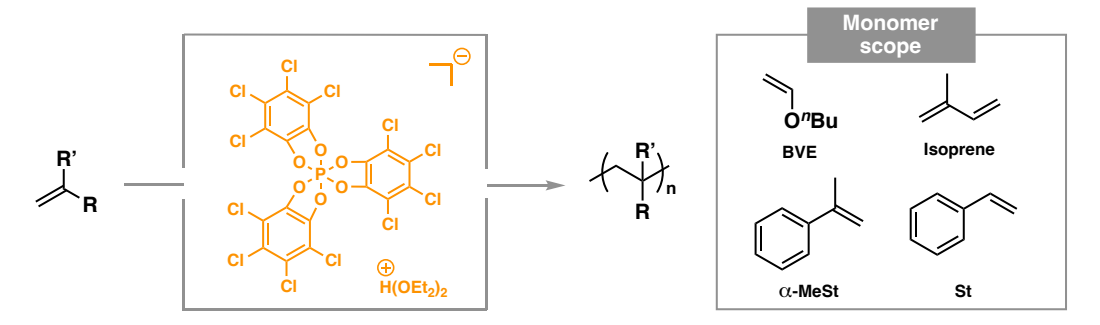


**Fig. 14.** H(OEt<sub>2</sub>)<sub>2</sub>[P(1,2-O<sub>2</sub>C<sub>6</sub>Cl<sub>4</sub>)<sub>3</sub>] as a single-component initiator for cationic polymerization [47].

In 2016, Tang and others reported a single component mediated polymerization of IBVE using HNTf<sub>2</sub> [48], a strong brønsted acid, as initiator and organocatalyst. Polymerizations exhibited excellent living characteristics as molecular weight increased linearly with monomer conversion. Furthermore, polymerizations reached quantitative conversion within 10 seconds, affording polymers with a broad range of molecular weights ( $M_n = 3.5 - 60 \text{ kDa}$ ), all in alignment with their predicted molecular weights while maintaining low dispersity (D < 1.21).

In 2019, Fors and Lambert reported a well-designed organic acid that can mediate the controlled cationic polymerization of vinyl ethers under ambient conditions without the need for extensive monomer purification, low temperatures, or anhydrous conditions (Fig. 15) [49]. Polymerizations were carried out in the presence of catalytic amounts of 1,2,3,4,5-pentacarbo-methoxycyclopentadiene (PCCP), which has been previously reported as a strong Brønsted acid catalyst in numerous small molecule transformations [50]. The proposed mechanism of this system involves the initial protonation of a vinyl ether monomer with PCCP catalyst to form an adduct, which can further participate in an equilibrium with a propagating oxocarbenium species and a cyclopentadienyl anion, and thus meditating the polymerization. The excellent living characteristics of this system are attributed to the stabilizing hydrogen bonding interactions present in the transition state of polymerization between the PCCP anion and the propagating chain end/monomer. In addition, the strong tight-ion pair formed provides a method of slowing down propagation while suppressing terminating and chain transfer events. Furthermore, this system could polymerize various vinyl ethers with different alkyl substitutions. Surprisingly, a disubstituted ethyl-1-propenyl ether (EPE) and DHF were also able to be polymerized at low

temperatures (0°C) and nitrogen atmosphere, while maintaining moderate dispersity (D < 1.33) and moderate molecular weights ( $M_n = 5.4$  - 49 kDa). Nonetheless, when a higher degree of polymerization was targeted (DP > 100), a significant amount of elimination and chain transfer events were observed. These side reactions were evidenced by the deviation from the first-order kinetics during polymerization, resulting in polymers with lower  $M_n$  and higher dispersity, likely due to the intermolecular deprotonation of a propagating chain end by the cyclopentadienyl anion resulting in regeneration of PCPP and a terminated chain.

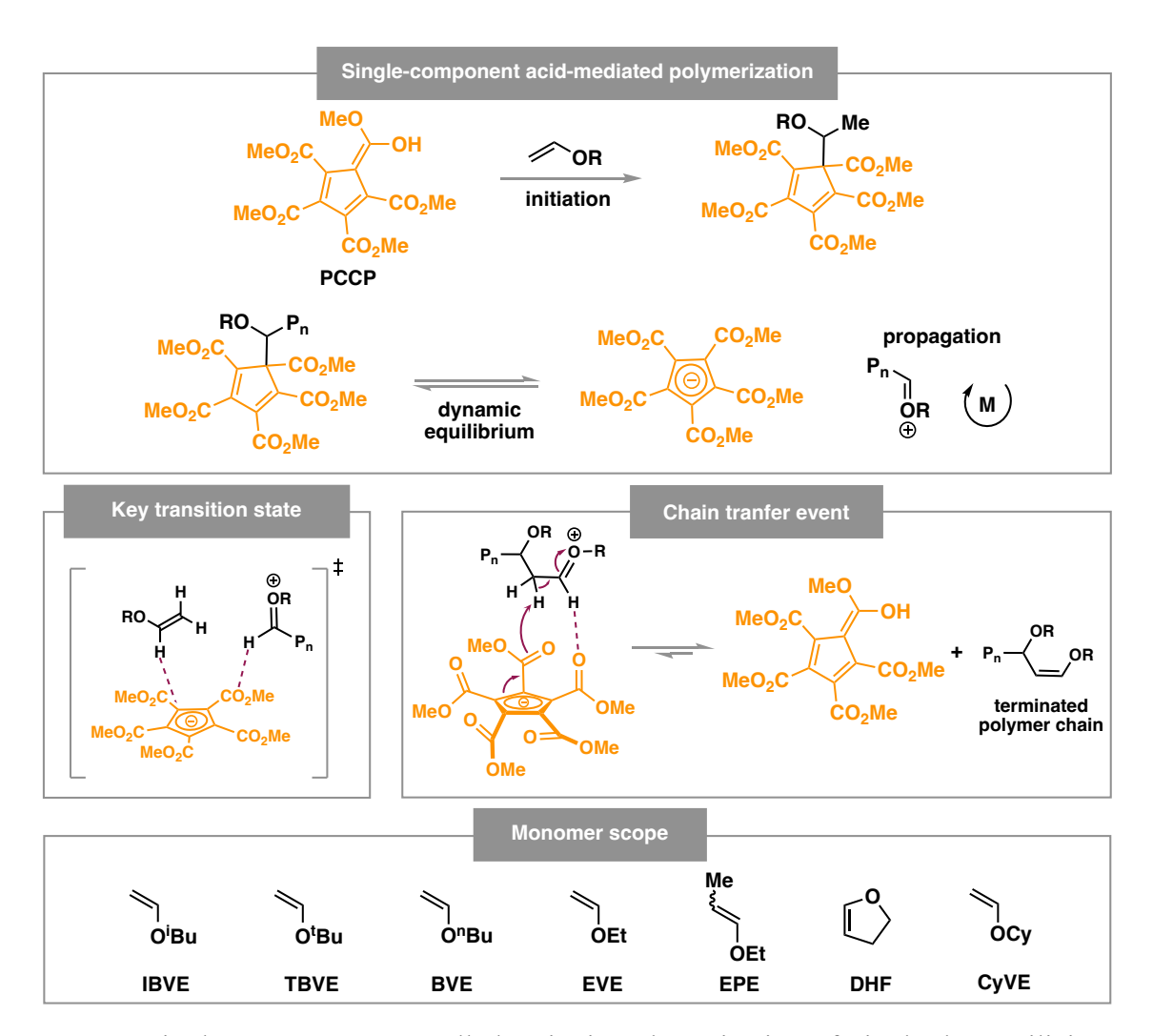


**Fig. 15.** Single-component controlled cationic polymerization of vinyl ethers utilizing PCCP as the catalyst. [49], Copyright 2019. Adapted with permission from American Chemical Society.

To address this concern, follow up work was conducted by introducing hydrogen bond donors (HBD) as co-catalysts to posit further stabilization of the cyclopentadienyl anion. Polymerization of IBVE was probed in the presence of **HBD 1-6**, aiming to suppress the intermolecular elimination event at the propagating chain end (**Fig. 16**) [51]. Notably, **HBD-4** exerted good control over the polymerization ( $M_n = 29.8 \text{ kDa}$ , D=1.16), likely because of being able to provide three hydrogen-bonding interactions to the PCCP anion. Moreover, the introduction of hydrogen-bonding donor co-catalysts provided faster polymerization rates as well as higher molecular weights ( $M_n$  up to 66 kDa). Further work also demonstrated this system is compatible with conventional RAFT methods [52], thus providing further moisture tolerance and broader monomer scope.

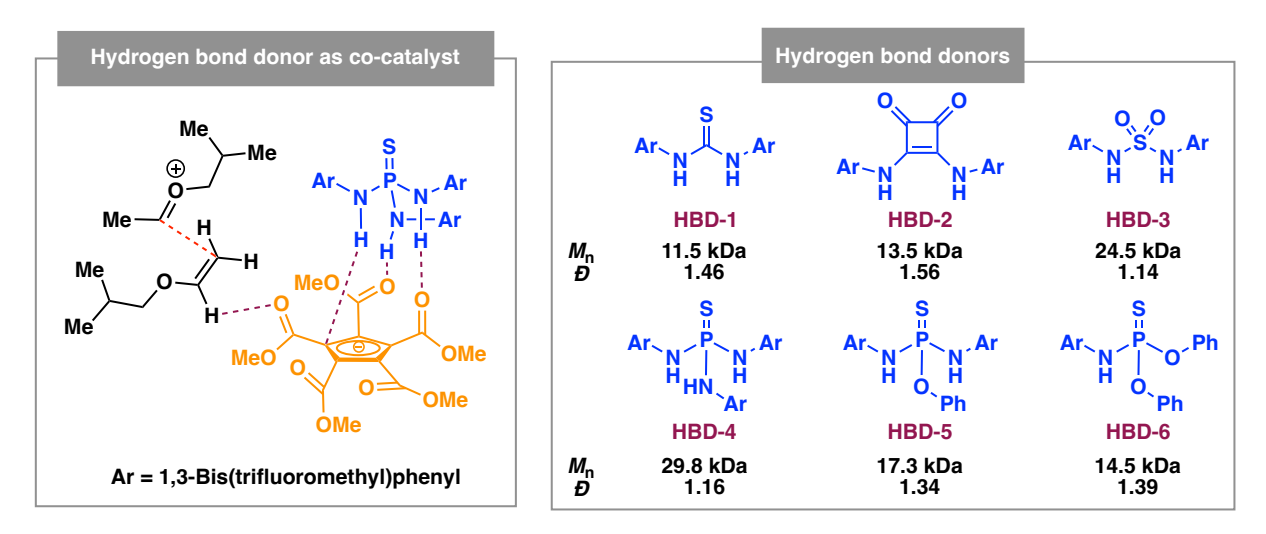


**Fig. 16.** Hydrogen bond donor assisted controlled cationic polymerization of vinyl ethers utilizing PCCP as the catalyst. [51], Copyright 2020. Adapted with permission from John Wiley & Sons Inc.

In 2022, Tao and co-workers designed an elegant selenocyclodiphosph(V)azane hydrogen-bond donor catalyst to achieve precise control over the polymerization of a series of electron-rich vinyl monomers (**Fig. 17**) [53], including vinyl ethers, DHF, and NVC. The polymerization of IBVE proceeded in a fine-controlled fashion, as confirmed by the linear increase of  $M_n$  over monomer conversion, predictable molecular weight proportional to [M]<sub>0</sub>/[I]<sub>0</sub> ratio and narrow and unimodal MW distribution. The well-defined structure of obtained poly(IBVE) was demonstrated by <sup>1</sup>H NMR and MALDI-TOF MS analysis, successful chain extension further verified the excellent fidelity of the  $\omega$ -chain end. The evaluation of a library of selenocyclodiphosph(V)azanes catalysts

revealed that the strong Cl<sup>-</sup> affinity and/or acidity of catalysts is crucial for efficiently promoting the cationic polymerization. The comprehensive experimental and computational studies revealed a novel polymerization mechanism, wherein catalyst and dormant species form a polarized covalent complex, followed by a dynamic anion binding process to regulate the chain growth (**Fig. 17**). The formation of polarized covalent complex is responsible to produce extremely low concentration of cationic active species, leading to excellent control over the polymerization under mild conditions. Notably, the polymerization was highly practical and user-friendly, no compromise on control over molecular weight and dispersity was observed when using unpurified monomer and solvent under ambient atmosphere. Furthermore, the catalyst could be readily recovered without compromising its performance on the controlled polymerization (*e.g.*, virgin catalyst: 99% conversion,  $M_n = 9.5$  kDa, D = 1.11; recycled catalyst: 99% conversion,  $M_n = 9.2$  kDa, D = 1.14).

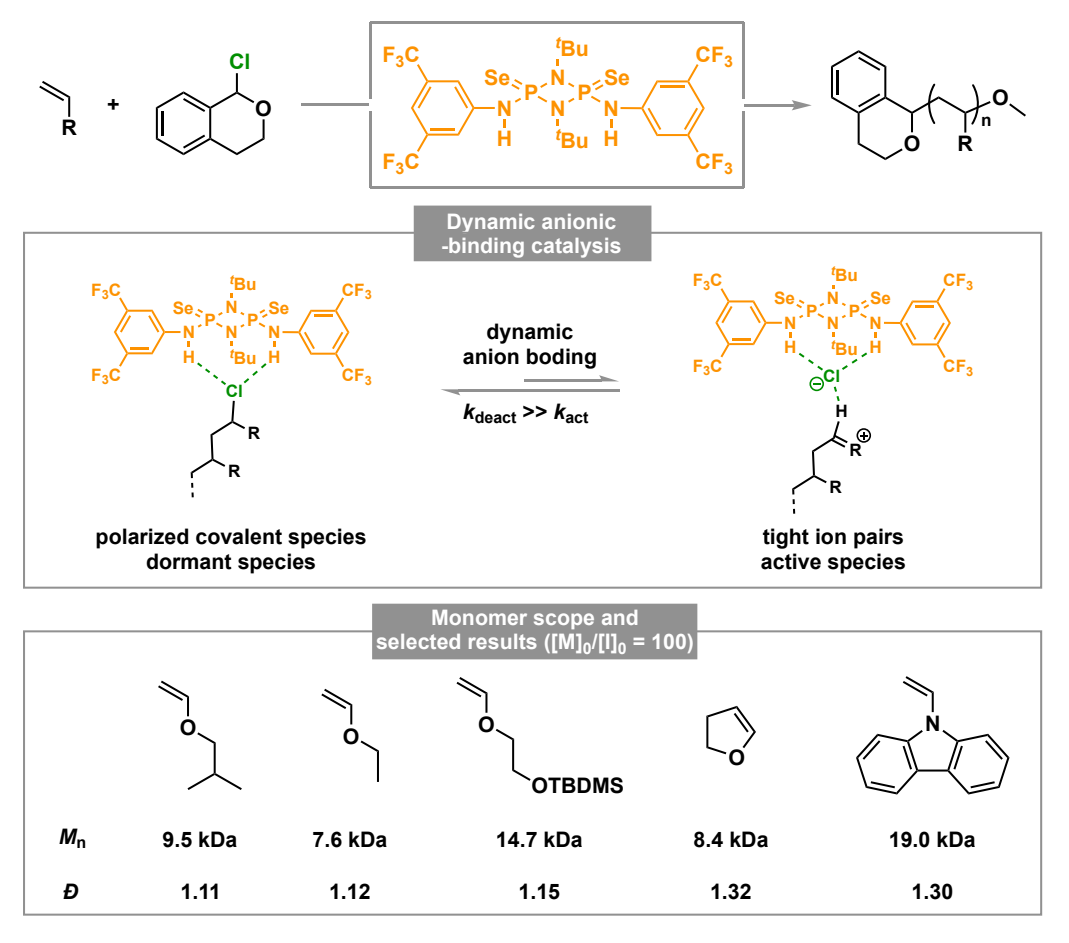


**Fig. 17.** Living cationic polymerization of vinyl monomers enabled by anion-binding catalysis. [53], Copyright 2022. Adapted with permission from Springer Nature Limited.

#### 3.2.2 Organic Lewis acid assisted cationic polymerization

In 2023, Zhou and co-workers employed a stable and inexpensive organic Lewis acid trityl tetrafluoroborate (TrBF<sub>4</sub>) in the controlled polymerization of  $\varepsilon$ -CL (**Fig. 18**) [54]. A series of poly( $\varepsilon$ -CL) with predictable molecular weight and low dispersity were obtained by changing the feed ratio between the monomer and methanol initiator. The linear relationship between the molecular weight and monomer conversion, linear pseudo-first-order kinetic plot, together with successful chain extension by  $\varepsilon$ -CL indicated a well-controlled polymerization was achieved (*e.g.*, before chain extension:  $M_n = 8.4$  kDa; after chain extension:  $M_n = 17.1$  kDa). The monomer was activated through the coordination of carbonyl oxygen and trityl cation, thereby facilitating the nucleophilic attack of the hydroxy group of the polymer chain end. Then the sequential steps of a

proton transfer and ring opening process furnish the chain growth process, and the regenerated trityl cation will continue to activate the next monomer until the completion of the polymerization.

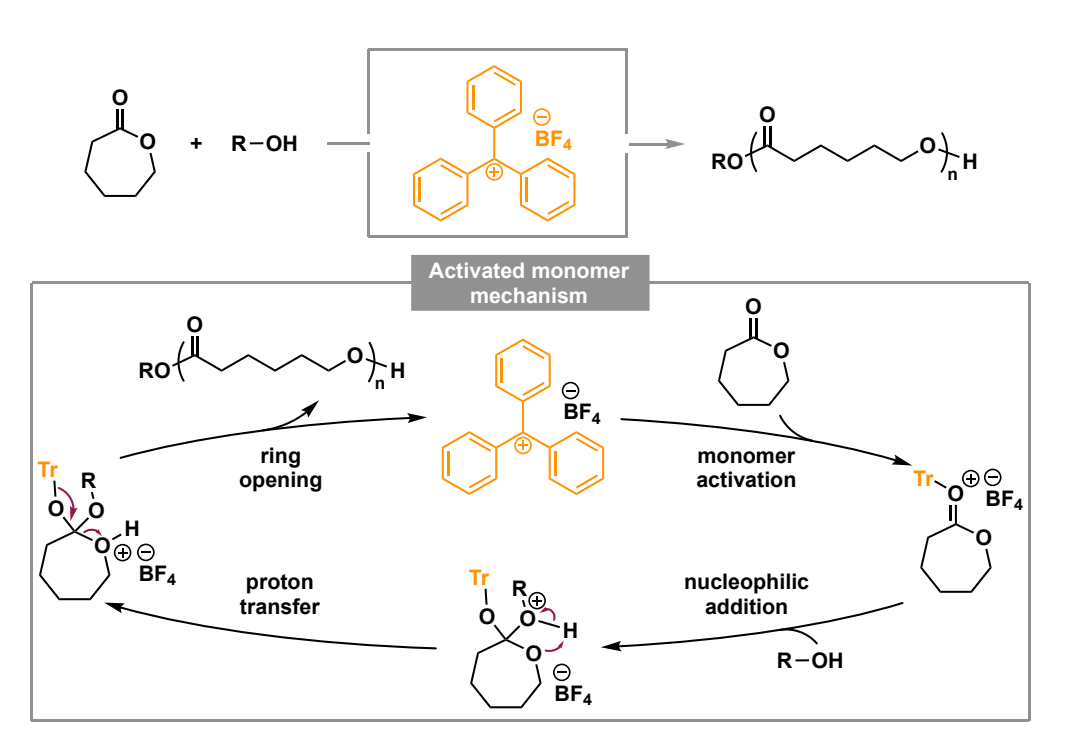


**Fig. 18.** Living cationic polymerization of ε-CL using trityl tetrafluoroborate. [54], Copyright 2023. Adapted with permission from American Chemical Society.

Interestingly, Li and Dong reported a unique metal-free polymerization of aryl isocyanides, affording optically active helical polymers (**Fig. 19**) [55]. This polymerization was initiated by a common borate compound, [Ph<sub>3</sub>C][B(C<sub>6</sub>F<sub>5</sub>)<sub>4</sub>], in chlorobenzene at 25 °C. Moderate to good yields of helical polymers were obtained with varying molecular weights ( $M_n = 30\text{-}180 \text{ kDa}$ ), although relatively high dispersity was observed (D > 3.0). The copolymerization of chiral and achiral monomers resulted in helical polymers, as characterized by circular dichroism spectroscopy (CD) with molar circular dichroism values ( $\Delta \epsilon_{364}$ ) ranging from 0.61 to 15.47 M<sup>-1</sup> cm<sup>-1</sup>. The proposed mechanism begins with addition of an aryl isocyanide monomer to the [Ph<sub>3</sub>C]<sup>+</sup> species, granting propagation via a cationic addition of the monomer. Further, the chains can be terminated by C-H activation of the aryl isocyanide monomer, resulting in a terminated chain and H<sup>+</sup>, which can reinitiate the polymerization. The termination and chain transfer events were responsible for the

resulting high dispersity. Additionally, high resolution ESI-MS of oligomers obtained confirmed the chain ends corroborating the proposed mechanism.

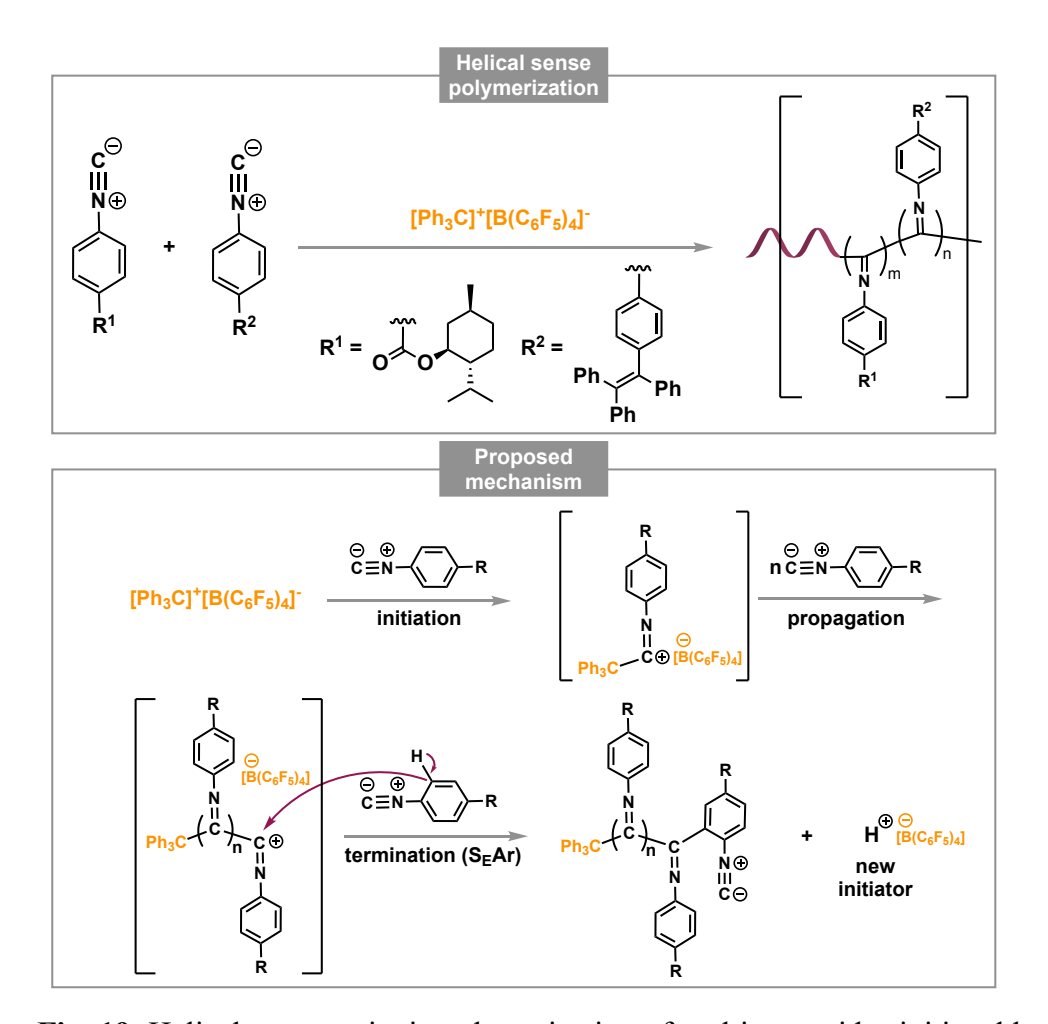


**Fig. 19.** Helical-sense cationic polymerization of aryl isocyanides initiated by  $[Ph_3C][B(C_6F_5)_4]$ . [55], Copyright 2018. Adapted with permission from John Wiley & Sons Inc.

Halogen (XB) and chalcogen-bonding (ChB) have emerged as attractive tools to regulate the reactivity and selectivity of organocatalytic systems [56,57]. These catalysts feature an electropositive Lewis acidic region on the heteroatom (Br, I, Te), so called  $\sigma$ -hole. The non-covalent interaction between the  $\sigma$ -hole and a Lewis base is responsible for catalysis (**Fig. 20**). This subsection will provide an overview of recent developments in XB and ChB catalyzed cationic polymerization.

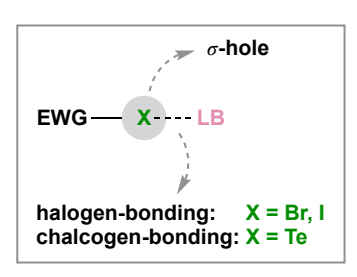


Fig. 20. Halogen (XB) and chalcogen-bonding (ChB).

Pioneering work of Higashimura and Sawamoto in the 1970-1980s first studied the halogenbonding catalysis for controlled cationic polymerizations of a series of vinyl monomers, including styrenic monomers [1], alkyl vinyl ethers [2,3], and NVC [4]. For instance, linear increase of  $M_n$ over conversion was achieved for the polymerization of IBVE, and nearly monodispersed polymer ( $D \sim 1.1$ ) can be obtained when used HI/I<sub>2</sub> as a binary catalytic system (**Fig. 21**). Key to these controlled cationic polymerizations was the use of a dual catalytic system of HI/I<sub>2</sub>. The monomer undergoes addition by HI, resulting in a monomer-HI adduct. Followed by activation by I<sub>2</sub>, resulting in a triiodide species and a cationic species that can undergo chain propagation.

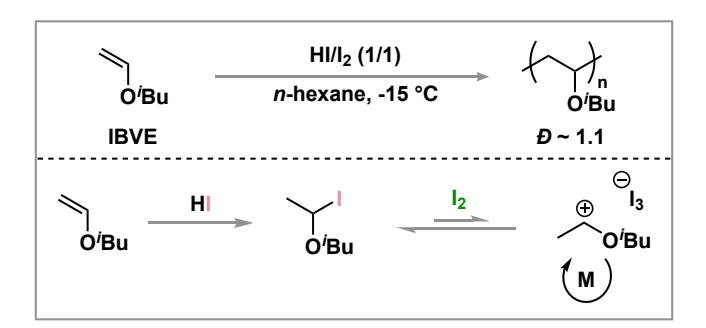
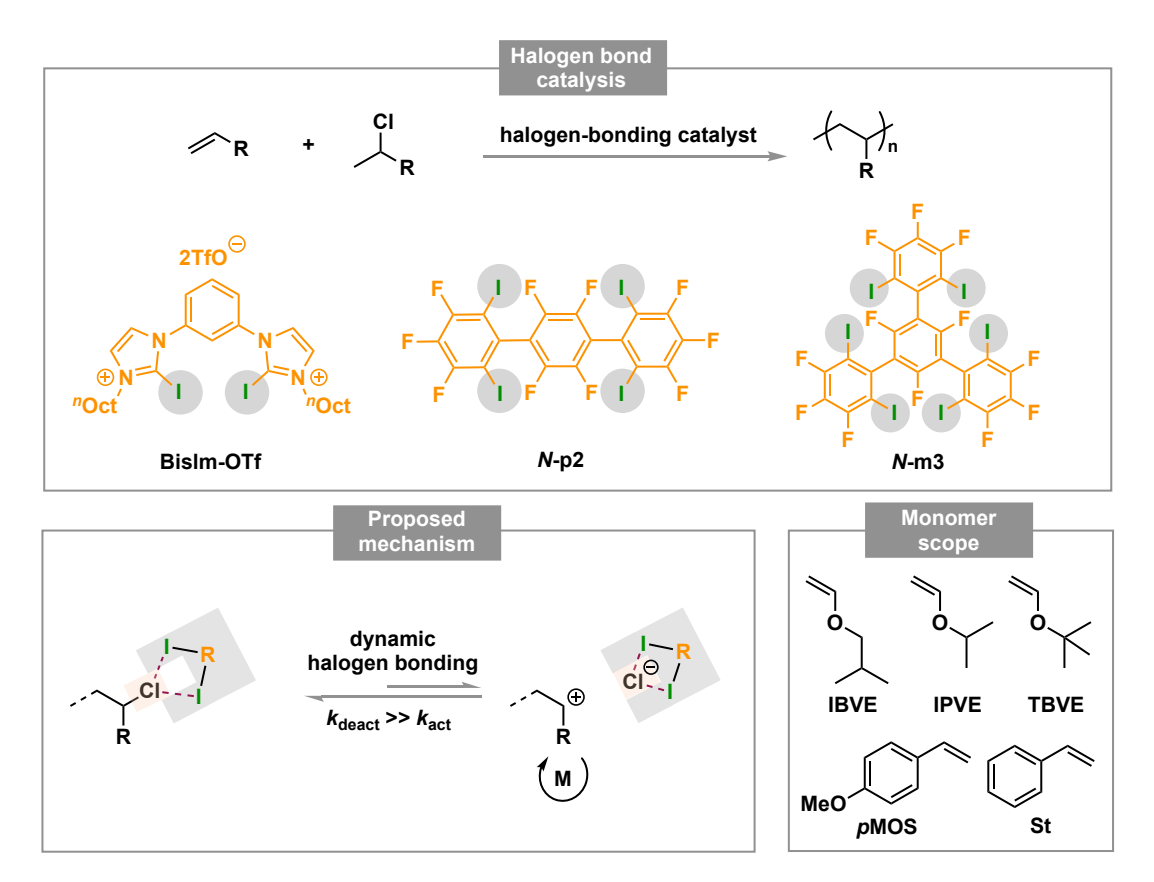


Fig. 21. HI/I<sub>2</sub>-catalyzed controlled cationic polymerization of vinyl ethers [2].

In 2017, Takagi and others applied halogen bonding catalysis to control the polymerization of IBVE (**Fig. 22**) [58]. This novel approach harnesses the non-covalent interactions between a halogen bonding catalyst and the halogenated chain end of the dormant species, forming a reversible equilibrium and thus controlling the polymerization. In the presence of bidentate Bislm-OTf catalyst at -10 °C, IBVE could be readily polymerized to give polymers with predictable molecular weight and moderate dispersity ( $M_n = 5.0 \text{ kDa}$ , D = 1.52). Of note, control experiments using hydrogen analog of Bislm-OTf catalyst resulted in no polymerization, respectively,

indicating that the halogen bonding catalysis is crucial for the control of polymerization. Follow-up work in 2020 further extended this chemistry by exploring non-ionic halogen bond catalyst N-p2 and N-m3 [59], obviating solubility, and decomposition issues. Additionally, other vinyl monomers were explored as well, and notably, the polymerization of pMOS was conducted to yield poly(pMOS) (M<sub>n</sub> = 4.3 kDa, D = 1.3), demonstrating the broad monomer scope of this system.



**Fig. 22.** Halogen-bonding controlled cationic polymerization of vinyl ethers and styrenic monomers [58,59].

In their following work, the Takagi lab found that halogen-bonding catalysis could also be applied in the cationic polymerization of n-hexyloxyallene (**Fig. 23**) [60]. The screening of a series of halogen-bonding organocatalysts revealed that the iodine-carrying bidentate catalyst demonstrated the best performance, giving corresponding polymer with  $M_n$  of 2.4 kDa and moderate dispersity of 1.63. Additionally, the regioselectivity of the polymerization was found to be 3:1, with 1,2-addition preferentially occurred. Despite of poor control over the molecular weight and

regioselectivity, elaborate catalyst design and condition optimization might solve the problems to generate these reactive and functional polyallene materials.

$$\frac{3}{2} \stackrel{?}{=} \stackrel{?$$

Fig. 23. Cationic polymerization of *n*-hexyloxyallene using halogen-bonding organocatalyst [60].

Independently, Aoshima and co-workers discovered that diaryliodonium salts could also act as halogen-bonding organocatalysts to perform the cationic living polymerization of vinyl monomers (Fig. 24) [61]. The polymerization of IBVE proceeded efficiently and reached 97% conversion in 15 min at -40 °C. The SEC traces of the polymer exhibited narrow molecular weight distribution (D < 1.1), and the molecular weight estimated from SEC was also consistent with the theoretical values ( $M_n = 11.7 \text{ kDa}$ ,  $M_{n,\text{theo}} = 11.2 \text{ kDa}$ ). Additionally, this new methodology showed broad monomer scope. Polymerization of other functionalized vinyl ethers, such as 2-chloroethyl vinyl ether (CEVE) and 2-methoxyethyl vinyl ether (MOVE), and less-reactive styrene derivatives, such as pMOS and 4-methylstyrene (pMeSt), was also feasible to give corresponding polymer in predictable MW and relatively low dispersity (D = 1.10-1.69). The evaluation of the substituents group on the catalysts was investigated, catalysts with electron-withdrawing group (i.e., fluorine) exhibited much higher reaction rates ( $k_{\rm app} = 5.9 \times 10^{-3} \, {\rm s}^{-1}$ ) than that with methyl substituent groups  $(k_{\rm app} = 1.9 \times 10^{-4} \, \rm s^{-1})$ . Accordingly, a possible mechanism was proposed, in which the central iodine atom of diaryliodonium salts acted as a Lewis acid to activate the propagating chain end via the halogen-bonding interaction. The reversible activation-deactivation equilibrium was likely established through the reversible abstraction and liberation of halide mediated by the diaryliodonium salts, thereby leading to simultaneous chain growth.

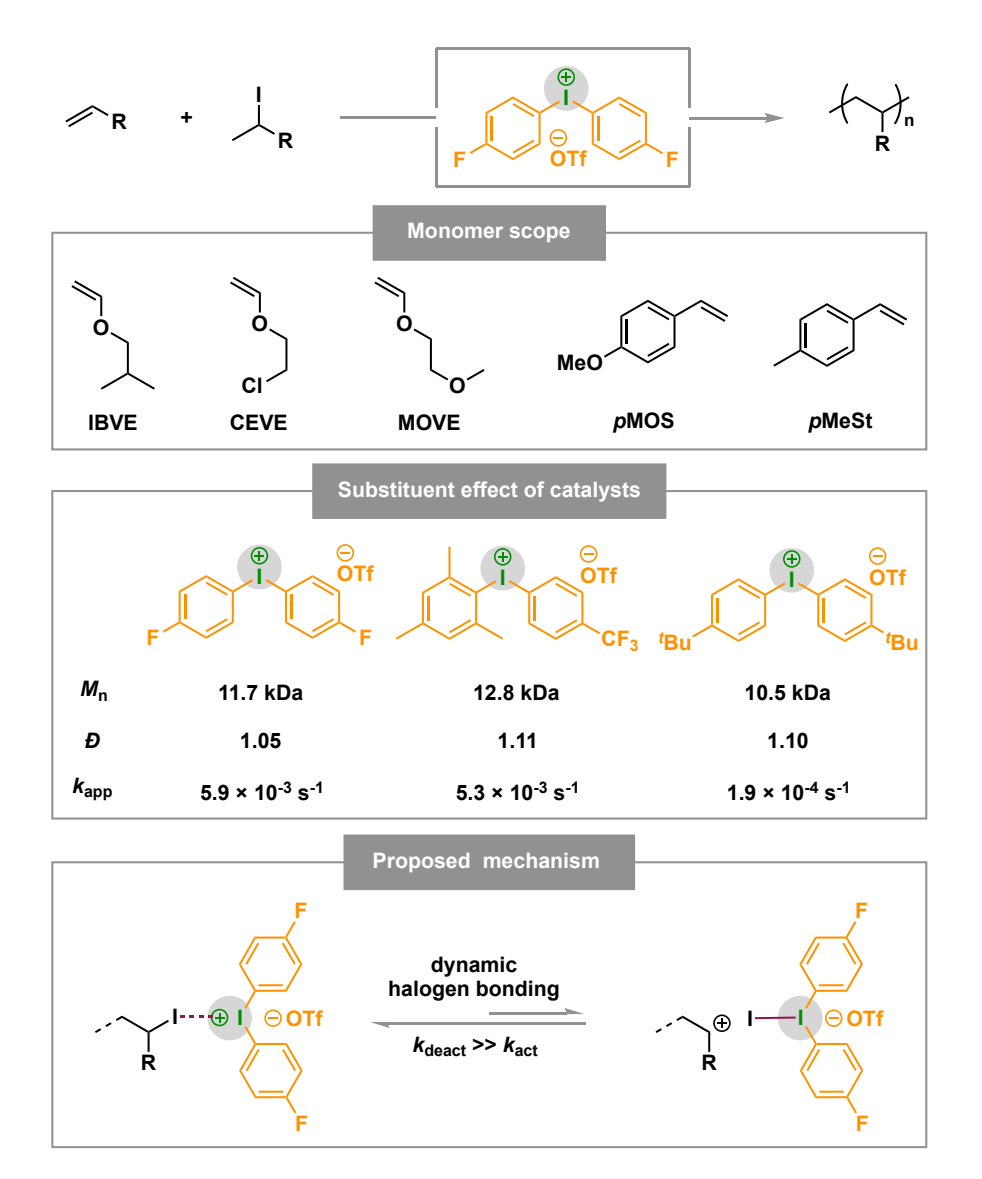


**Fig. 24.** Living cationic polymerization using diaryliodonium salts as halogen-bonding organocatalyst [61].

During their continuous studies on metal-free controlled cationic polymerization, Takagi and coworkers disclosed that chalcogen bonding catalysis could be applied in the living polymerization of pMOS using a mononuclear telluronium cation TeMe-OTf as an organocatalyst (**Fig. 25**) [62]. When an alcohol was used as an initiator, a poly(pMOS) with  $M_n$  of 6.9 kDa and pD of 1.47 was obtained under the optimal condition. The authors claimed that the chalcogen bond between the telluronium cation and the hydroxy group was involved in the reversible activation-deactivation process, which regulated the propagation of the monomer to achieve the simultaneous growth of the polymer chains. More interestingly, the polymerization is water tolerant. For instance, addition

of 6 equivalent of water relative to TeMe-OTf catalyst generated a polymer (D = 1.33) with comparable molecular weight to that of the polymer obtained in the absence of water (D = 1.47). Notably, the organocatalyst could be readily recovered without decomposition. Although this new method displayed moderate control over the polymerization and relatively narrow monomer scope, this finding will open a new avenue for precision polymer synthesis via chalcogen bonding catalysis.

**Fig. 25.** Living cationic polymerization of *p*MOS using tellurium-based chalcogen-bonding organocatalyst. [62], Copyright 2022. Adapted with permission from American Chemical Society.

#### 3.3. Spatiotemporally controlled cationic polymerization

# 3.3.1 Photocontrolled/photoinitiated cationic polymerization

Light is considered as an ideal external stimulus to mediate polymerization processes due to its ubiquitous and non-invasive nature [63]. It provides a powerful approach to regulate the process of precision polymer synthesis and advanced material manufacturing [12]. With the foundation of conventional cationic polymerization, a plethora of photoinitiated and photocontrolled cationic polymerization systems have been developed to control the polymer chain growth spatially and temporally [64]. Recent developments involving both photoinitiated and photocontrolled cationic polymerization of different monomers, including VEs, *p*MOS, and lactones, are highlighted in this section.

Since first reported in the 1970s [65], the investigation of photoinitiated cationic polymerization has rapidly expanded. Many early efforts focused on using onium salts as the photoinitiator to initiate cationic polymerization due to their high oxygen and moisture tolerance [66]. Other photoinitiation systems were also developed in the past few decades [67].

In 2011, Yagci and coworkers developed a novel photoinitiation approach by the photolysis of triaryl vinyl bromide initiator, 1-bromo-1,2,2-tris(p-methoxyphenyl)ethene, in the presence of metallic zinc (**Fig. 26**) [68]. When triaryl vinyl bromide was subjected to UV light irradiation ( $\lambda$  = 350 nm), homolytic cleavage of the C-Br bond followed by spontaneous electron transfer process could generate a vinyl cation species, which then initiated the cationic polymerization of VE. On the other hand, zinc bromide, generating from the reaction of metallic zinc and photochemically produced bromine radicals, could also assist the propagation in a controlled manner. As a result, the polymerization established quasi-living characters and poly(IBVE) with high molecular weight ( $M_{\rm B}$  up to 69 kDa) and moderate dispersity (D < 1.4) was obtained.

**Fig. 26.** Photoinitiated cationic polymerization of IBVE in the presence of triaryl vinyl bromide and metallic zinc. [68], Copyright 2011. Adapted with permission from American Chemical Society.

Later, Yagci and Ciftci developed another improved photoinitiation system to promote the living cationic polymerization of vinyl ethers by visible light (**Fig. 27**) [69]. In this work, the initiation process started with homolytic cleavage of dimanganese decacarbonyl under visible light irradiation ( $\lambda = 400\text{-}500 \text{ nm}$ ), followed by bromine atom abstraction of benzyl bromide led to the generation of a benzyl radical. Further oxidation of benzyl radical by diphenyliodonium bromide

salt, benzyl cation was formed and reacted with IBVE to generate an adduct. The adduct could undergo successive photoinduced radical oxidation and propagation, allowing the preparation of poly(IBVE) with ultra-high molecular weight ( $M_n$  up to 153 kDa, D < 2.0).

**Fig. 27.** Cationic polymerization of IBVE via a photoinduced radical oxidation/activation/deactivation mechanism. [69], Copyright 2017. Adapted with permission from John Wiley & Sons Inc.

The previous photoinitiated cationic polymerization enabled the initiation of polymerization by using light as an external stimulus. However, temporal control was not achievable for the chain growth process due to the difficulty of deactivating the propagating species. Integrated with photoredox catalysis [70], photocontrolled cationic polymerization can reversibly activate and deactivate the propagating chain end and achieve spatiotemporal control over polymerization.

In 2016, Fors and coworkers reported the first photocontrolled cationic polymerization of vinyl ethers (**Fig. 28**) [71]. The combination of 2,4,6-tris(p-methoxyphenyl)pyrylium tetrafluoroborate as the photocatalyst and **CTA-1** as the chain transfer agent enabled the preparation of various well-defined poly(vinyl ether) ( $M_n$  up to 35 kDa and D < 1.3). The proposed mechanism starts with the excitation of photocatalyst by the blue light irradiation ( $\lambda = 450$  nm), the excited photocatalyst oxidized dithiocarbamate chain end and generated a radical cation. The subsequent mesolytic fragmentation event produced a carbocation that polymerized vinyl ethers via a reversible chain-transfer mechanism. Reduction of the concurrently generated radical species by the reduced photocatalyst led to a dithiocarbamate anion, which reversibly deactivated the propagating chain end. The match of the redox potential of the photocatalyst with the dithiocarbamate chain end is

the key for excellent control over polymerization. The polymerization was halted when the light source was removed, while the reaction efficiently reinitiated after exposure to light, which suggested an excellent temporal control.

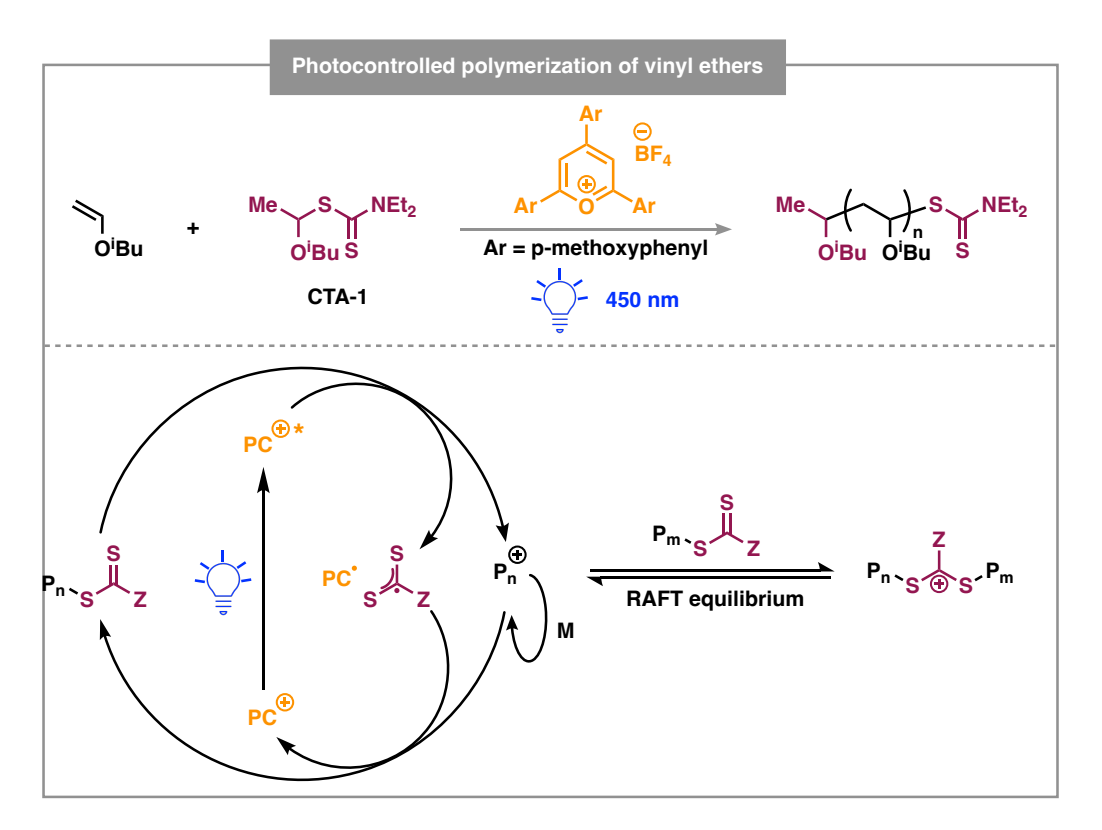


**Fig. 28.** Photocontrolled cationic RAFT polymerization of IBVE and its mechanism. [71], Copyright 2016. Adapted with permission from American Chemical Society.

Further investigation confirmed the proposed mechanism and inspired further exploration of other photocontrolled cationic polymerization systems [72]. For instance, Fors et al. utilized thioacetals as the CTA to initiate and mediate the photocontrolled cationic polymerization of vinyl ethers under blue light irradiation ( $\lambda = 456$  nm) through a reversible chain-transfer mechanism [73]. Notably, using an oxidizing photocatalyst with a higher ground state reduction potential significantly improved the temporal control of the polymerization. In 2021, Fors combined radical and cationic photocontrolled polymerization and enabled the selective incorporation of different type of monomers into a growing chain (**Fig. 29**) [74]. By switching the wavelength of light, this photoswitchable polymerization strategy could selectively polymerize vinyl ethers ( $\lambda = 525$  nm) and acrylates ( $\lambda = 456$  nm) under the cationic and radical mechanism, respectively. The mechanical

properties of the crosslinked polymers were spatially and temporally controlled by modulating the dosage and wavelength of light irradiation. By comparing the value of hardness (H) and reduced modulus ( $E_r$ ), the more crosslinked regions ( $H = 16.36 \pm 0.95$  and  $E_r = 36.69 \pm 2.06$ ) exposed to light irradiation displayed higher stiffness than the unexposed regions ( $H = 0.70 \pm 0.14$  and  $E_r = 1.83 \pm 0.12$ ).

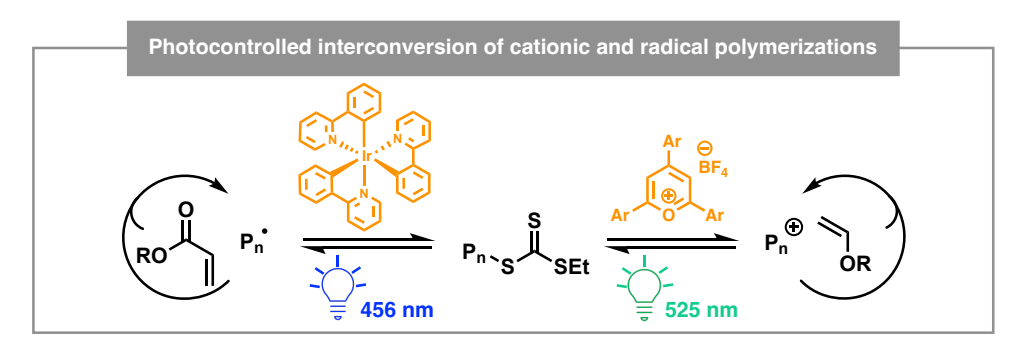
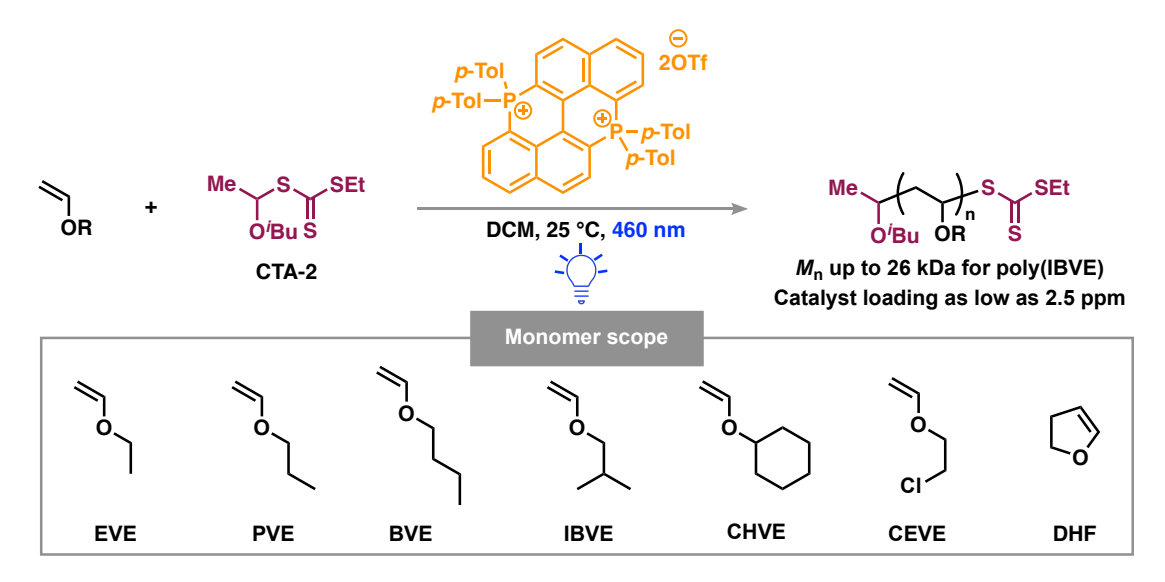


Fig. 29. Photoswitching RAFT cationic and radical Polymerizations [74].

In 2021, Liao and coworkers introduced a new type of organic photocatalyst, bisphosphonium salts, for the photocontrolled polymerization of vinyl ethers (**Fig. 30**) [75]. Compared to pyrylium salts Fors used, higher oxidation potential of the excited photocatalyst and higher reduction potential of the reduced state of bisphosphonium salts enabled highly efficient photocontrolled cationic polymerization of vinyl ethers with catalyst loading as low as 2.5 ppm under blue light irradiation ( $\lambda = 460$  nm). Mediated with **CTA-2**, the polymerization afforded poly(IBVE) with high molecular ( $M_n$  up to 26 kDa) and low dispersity (D < 1.4). In 2023, the same group further developed a class of monophosphonium photocatalysts for the controlled cationic polymerization of vinyl ethers, in which well-defined poly(vinyl ethers) were afforded under excellent temporal control [76]. The mechanism of these catalytic systems was similar to the previous photocontrolled cationic polymerization proposed by Fors [71].



**Fig. 30.** Photocontrolled cationic RAFT polymerization of vinyl ethers with bisphosphonium salts as the photocatalysts [75].

In 2022, Kamigaito and coworkers utilized acridinium salts as strong oxidizing photoredox organocatalysts to mediate the cationic polymerization of vinyl ethers under visible light (blue:  $\lambda_{\text{max}} = 470 \text{ nm}$ ; green:  $\lambda_{\text{max}} = 525 \text{ nm}$ ; white LEDs) (**Fig. 31**) [77]. Poly(IBVE) with high molecular weight ( $M_n = 40.7 \text{ kDa}$ ) and low dispersity (D = 1.28) was obtained when the M/I ratio was 500/1. Temporal control of the photomediated polymerization was partially achieved, despite incomplete halt of the chain growth in the dark period.

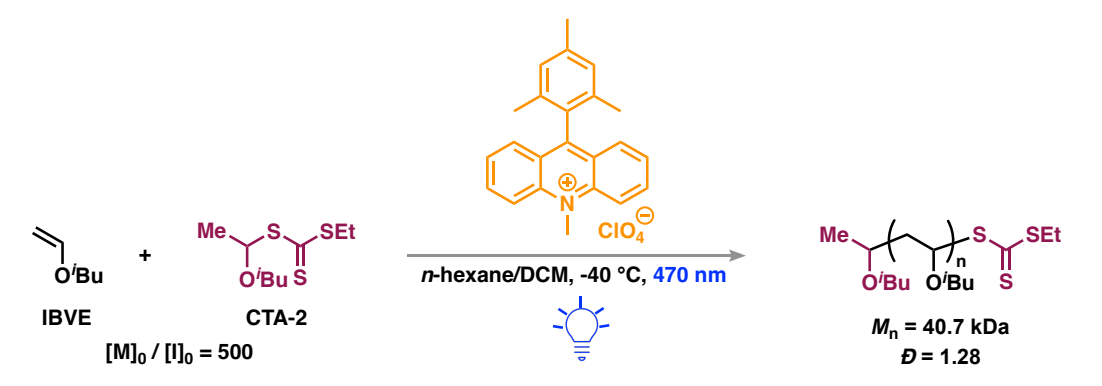


**Fig. 31.** Photocontrolled cationic RAFT polymerization of IBVE with acridinium salts as the photocatalysts [77].

Besides vinyl ethers, photoinduced and photocontrolled cationic polymerization of pMOS was also extensively investigated in the past decade. For instance, Nicewicz and You first discovered the photocontrolled cationic polymerization of pMOS in the presence of pyrylium salt as a photocatalyst and alcohol as the CTA (**Fig. 32**) [78]. The initiation of the polymerization started with the excitation of photocatalyst under blue light irradiation ( $\lambda = 450$  nm) followed by the oxidation of electron-rich pMOS monomer. The resulting styrenyl cation radical then underwent the anti-Markovnikov addition by alcohol, protonation of a monomer led to the initiating cationic species. A rapid chain transfer process, consisting of nucleophilic capture of cation by methanol and subsequent protonation of an additional monomer, proceeded until all methanol was consumed and a relatively small number of active cationic chain ends remained to undergo propagation. With the reversible chain transfer process through oxonium intermediate, the polymerization demonstrated living characteristics, including first-order kinetics, linear increase of molecular weight with respect to monomer conversion, and complete chain extension.

**Fig. 32.** Photoinitiated living cationic polymerization of pMOS in the presence of methanol as the CTA. [78], Copyright 2015. Adapted with permission from American Chemical Society.

Later, Spokoyny et al. utilized a boron-rich cluster  $B_{12}(OR)_{12}$  as a novel photooxidant to initiate the cationic polymerization of St and its derivatives under blue light ( $\lambda = 470$  nm) (Fig. 33) [79]. The polymerization of pMOS achieved ultra-high molecular weight ( $M_n$  up to 198 kDa) with moderate dispersity (D < 1.7). The unprecedented polymerization of styrene derivatives with electron-withdrawing and bulky substituents can also be realized by using these powerful boron-rich cluster photooxidants.

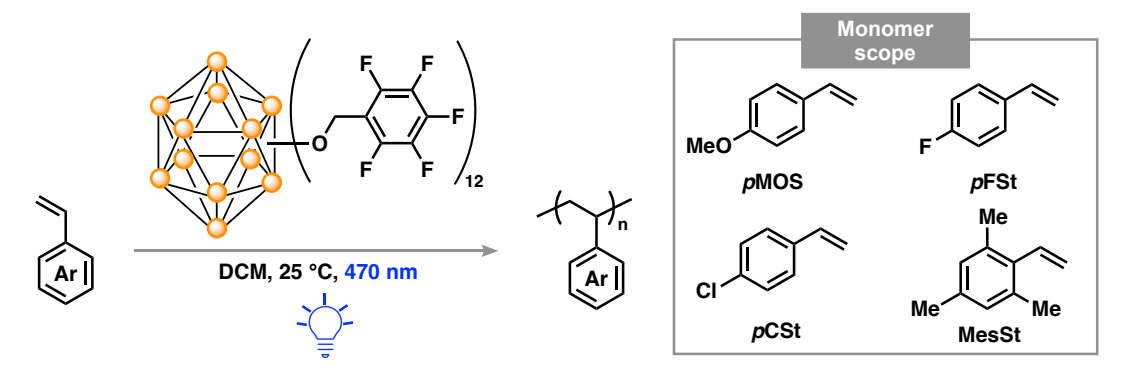


**Fig. 33.** Photoinitiated cationic polymerization of styrene derivatives using a boron-rich cluster as a photooxidant [79].

The aforementioned two examples of photoinitiating systems paved the way for the further development of photocontrolled cationic polymerization of pMOS. In 2022, Zhou and Zhang developed an elegant photocontrolled cationic polymerization of pMOS by using tris(2,4-dimethoxyphenyl)methylium tetrafluoroborate as the photocatalyst and phosphate as the CTA under green light irradiation ( $\lambda = 532$  nm) (**Fig. 34**) [80]. The mechanism was similar to the previous photocontrolled cationic polymerization proposed by Fors, except a phosphonium intermediate was involved in the RAFT process [71]. The polymerization could reach high molecular weights ( $M_n$  up to 53 kDa) and low dispersity (D < 1.3). Notably, the polymerization proceeded under green light irradiation and ceased immediately upon the removal of the light source, suggesting an excellent temporal control.

**Fig. 34.** Photoinitiated cationic RAFT polymerization of pMOS with phosphate as the CTA [80].

The ROP of lactones has become one of the major approaches to producing biodegradable polyesters [81]. However, this method has rarely been regulated by light. In 2013, Barker and Dove utilized triarylsulfonium hexafluorophosphate salts to catalyze the photoinitiated cationic ROP of lactones (**Fig. 35**) [82]. By exposing the photocatalyst to UV light ( $\lambda$  = 365 nm), the resulting H<sup>+</sup> initiated the polymerization, and well-defined polymers with moderate molecular weight ( $M_n$  up to 27 kDa) and low dispersity (D < 1.2) were generated. The high chain-end fidelity was supported by the one-pot synthesis of a triblock copolymer poly( $\delta$ -valerolactone)-b-poly(L-LA)-b-poly( $\delta$ -valerolactone) through a dual basic/acidic catalytic system. In 2020, You and coworkers combined different photocatalysts and onium salts into a series of photoacid composites, which could activate the photoinduced cationic ROP of lactones under visible light irradiation (**Fig. 35**) [83]. By applying different photocatalysts (Ir(ppy)<sub>3</sub>, Eosin Y, ZnTPP), the polymerization can be initiated under different visible lights (blue, green, and red). Moreover, the concurrently generated radical species also facilitated a simultaneous RAFT radical polymerization when a hydroxy group capped trithiocarbonate was used as the initiator.

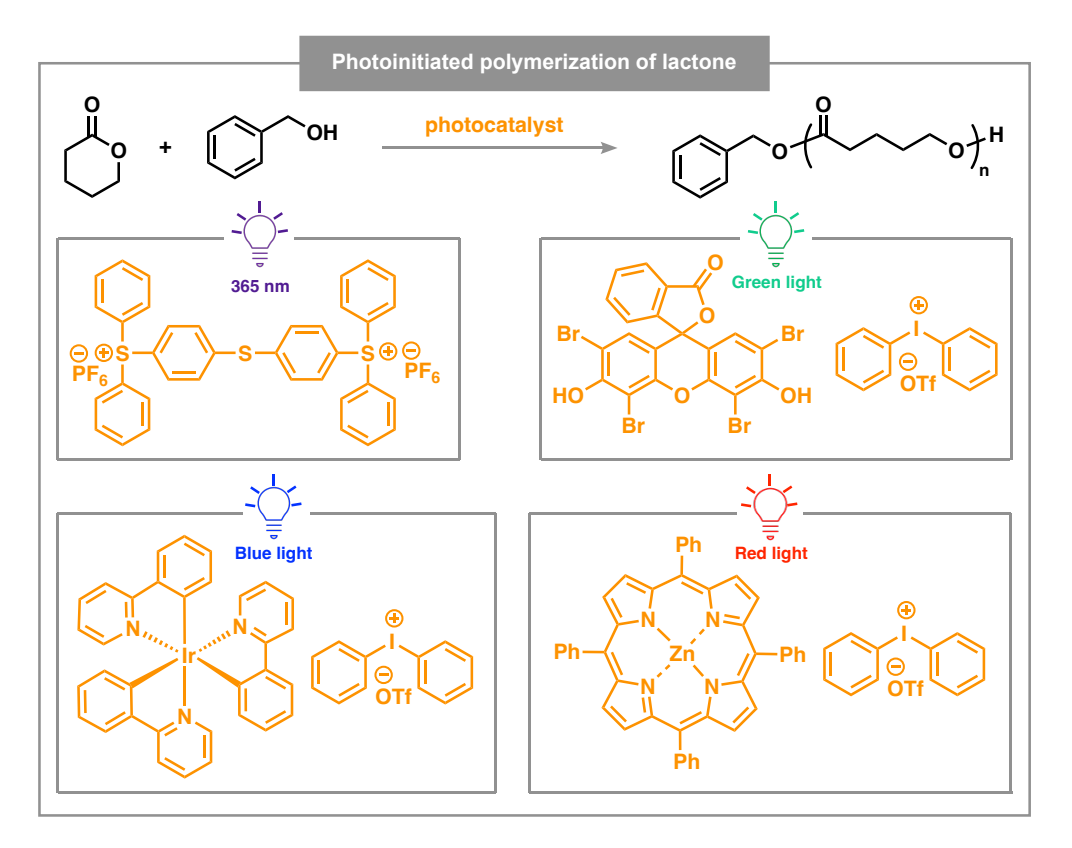


**Fig. 35.** Photoinitiated living cationic ROP of lactones and some representative photocatalysts [82,83].

In 2021, Liao and coworkers developed another interesting visible-light regulated ROP of lactones (**Fig. 36**) [84]. They utilized the increased acidity of the excited aromatic alcohol photocatalyst to catalyze the cationic polymerization under purple light irradiation ( $\lambda = 365$  nm). The polymerization achieved high molecular weight ( $M_n$  up to 39 kDa) under excellent control (D < 1.1). Polymerization under intermittent light exposure demonstrated that the polymerization proceeded under visible light and gradually slowed down in the dark period, indicating of a partially temporal control. Xu and Boyer took a step forward and achieved the photocontrolled cationic ROP of lactones (**Fig. 36**) [85]. In this work, a merocyanine-based photoacid was utilized as the photocatalyst, and the resulting polyesters with moderate molecular weight ( $M_n = 12$  kDa) and low dispersity (D < 1.2) were obtained. The blue light ( $\lambda = 460$  nm) triggered the intramolecular cyclization of the photoacid, releasing H<sup>+</sup> to catalyze the cationic ROP of lactones. The rapid reversible proton dissociation process afforded temporal control of polymerization in the presence/absence of light, suggesting an excellent temporal control was achieved.

Fig. 36. Photocontrolled cationic ROP of lactones using photoacids [84].

#### 3.3.2 Electrocontrolled cationic polymerization

Electrochemistry has emerged as a powerful tool to achieve desired chemical transformations, as it can achieve precise control over redox processes ubiquitous in all fields of chemistry [86]. Moreover, electrochemically controlled reactions can be carried out under mild conditions while maintaining high functional group tolerance and obviating the need for stoichiometric amounts of oxidants or reductants. Recently, electrochemical processes have been applied in polymer science [87-89], and this subsection will highlight the advances in electrocontrolled cationic polymerization.

In 2018, Fors and Lin reported an elegant electrochemically controlled living cationic polymerization of vinyl ethers (**Fig. 37**) [90]. A stable redox nitroxyl radical, namely (2,2,6,6-Tetramethylpiperidin-1-yl)oxy (TEMPO), was used as a mediator to oxidize a dithiocarbamate CTA during polymerization. Application of constant oxidative potential (+325 mV vs. Fc+/Fc) to a mixture of IBVE, **CTA-1**, and TEMPO in a divided electrochemical cell led to the facile synthesis of polymers with low dispersity (D = 1.23) and molecular weight in agreement with theoretical values ( $M_n = 8.4 \text{ kDa}$ ,  $M_{n,\text{Theo}} = 8.3 \text{ kDa}$ ). This system can be employed for additional monomers, including BVE, n-propyl vinyl ether (PVE), EVE, CEVE, and pMOS. Furthermore, utilizing galvanostatic conditions (1 mA anodic current) resulted in the quantitative conversion of monomer within 4 hours, yielding polymers with low dispersity (D < 1.33), predictable  $M_n$  values,

and high chain-end fidelity corroborated by chain extension experiments. The proposed mechanism starts with the oxidation of TEMPO to TEMPO+, which is then trapped by a terminal dithiocarbamate chain end to form an adduct. Followed by a subsequent fragmentation process, generating an oxocarbenium species that can participate in the RAFT process. Notably, this work exhibited excellent temporal control, as changing the external stimulus (oxidizing current or reducing potential) resulted in "On/Off" switching of the polymerization process with high efficiency.

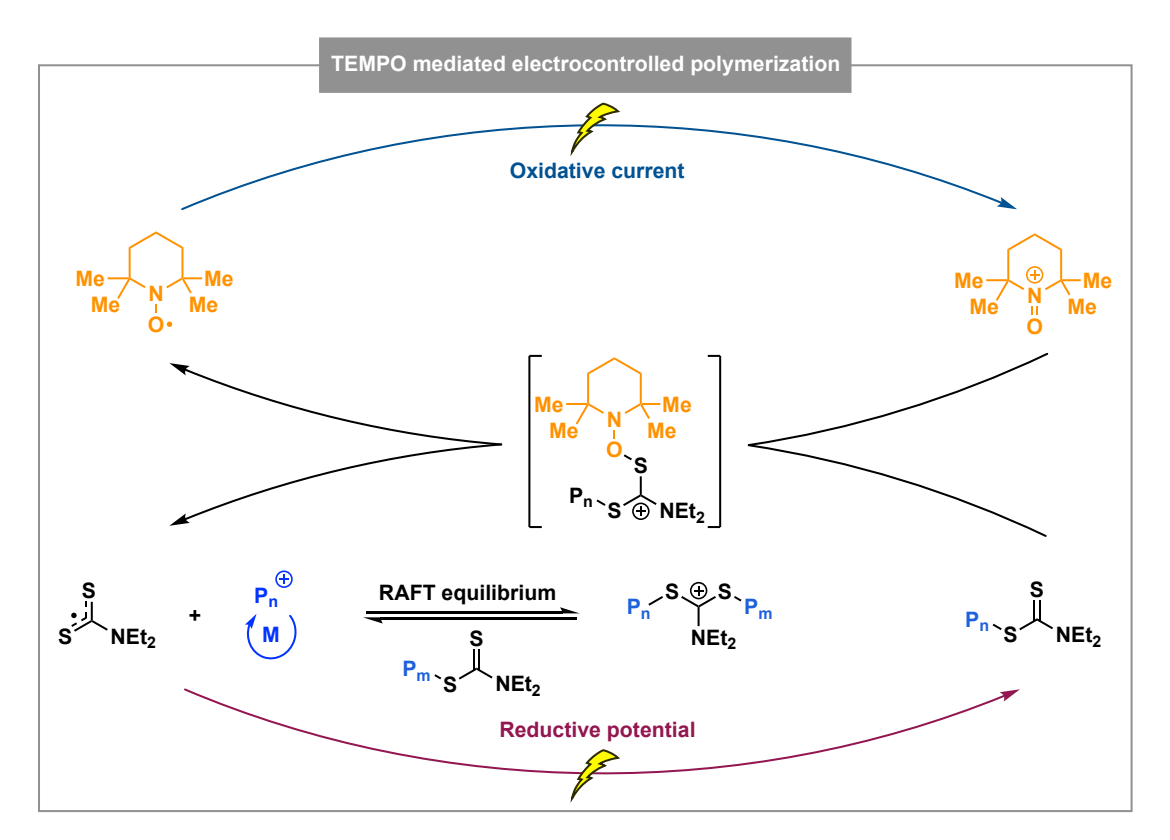


**Fig. 37.** TEMPO as a mediator for the electrocontrolled cationic polymerization of vinyl ethers. [90], Copyright 2018. Adapted with permission from American Chemical Society.

Similarly, Yan and coworkers reported the use of 2,3-Dichloro-5,6-dicyano-1,4-benzoquinone (DDQ) as an organic electrocatalyst that can also facilitate the living cationic polymerization of vinyl ether-type and electron-rich styrene-type monomers (**Fig. 38**) [91,92]. The anionic oxidation of DDQ<sup>2-</sup> catalyst would give DDQ, which can perform a single electron oxidation of a terminal trithiocarbonate chain end, affording an oxocarbenium suitable for propagation. Application of an oxidative potential (+1.2 V vs. Ag+/Ag) to reaction conditions resulted in the efficient synthesis

of well-defined homo- and copolymers under a cationic RAFT mechanism. This system proved to be efficient for the synthesis of polymers with varying monomer to CTA ratios (100-500), while reaching quantitative monomer conversion and maintaining low dispersity (D < 1.28). Furthermore, this method achieved the synthesis of a diblock copolymer poly(IBVE-b-pMOS ( $M_n = 23.3 \text{ kDa}$ , D = 1.21) from poly(IBVE) ( $M_n = 9.7 \text{ kDa}$ , D = 1.15), as confirmed by unimodal profile in size exclusion chromatography (SEC) analysis.

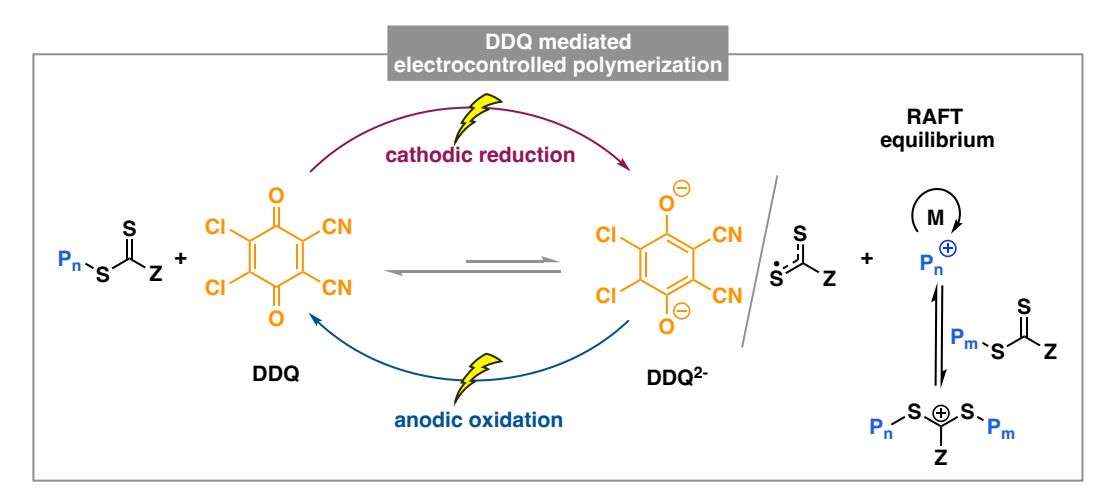


**Fig. 38.** DDQ as a mediator for the electrocontrolled cationic polymerization of VE. [91], Copyright 2018. Adapted with permission from John Wiley & Sons Inc.

Polymerizations controlled by external stimuli have proven effective in generating polymers of more complex architectures. Fors and coworkers reported a dual stimuli system, consisting of electricity and light, for precise synthesis of high-order multiblock copolymers containing acrylates and vinyl ethers (**Fig. 39**) [93]. In this work, Ferrocene (Fc) was utilized as an electromediator for the cationic polymerization of IBVE, while *fac*-Ir(ppy)<sub>3</sub> was chosen as a photocatalyst to regulate the polymerization of methyl acrylate (MA) via a radical mechanism. This dual method proved efficient for synthesizing a variety of block copolymers in situ by alternating the applied stimuli (visible light or electric potential). Several multiblock copolymers were synthesized, such as diblock poly(IBVE-*b*-MA) ( $M_n = 12.5 \text{ kDa}$ , D = 1.40), tetrablock poly(IBVE-*b*-MA-*b*-I

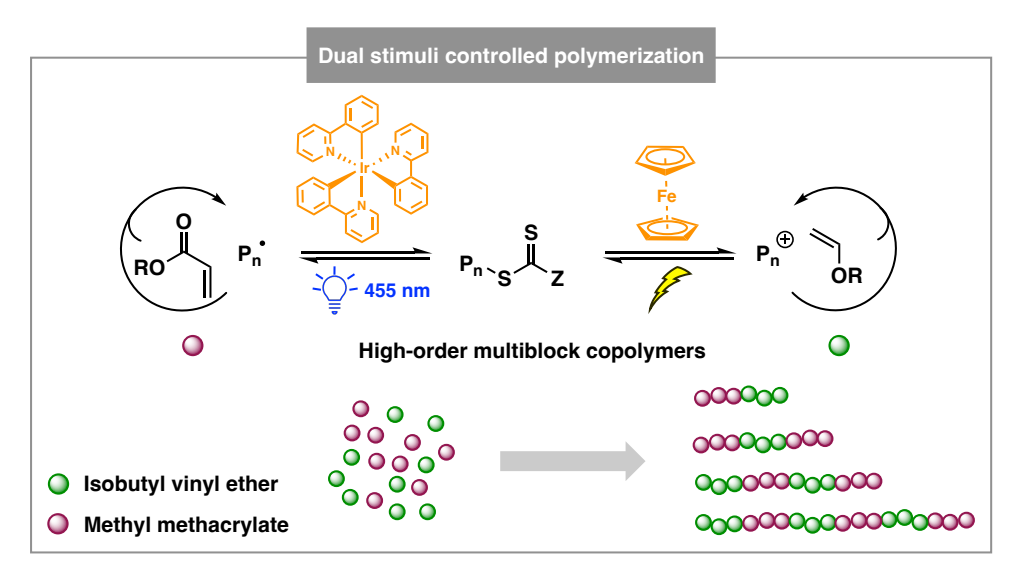
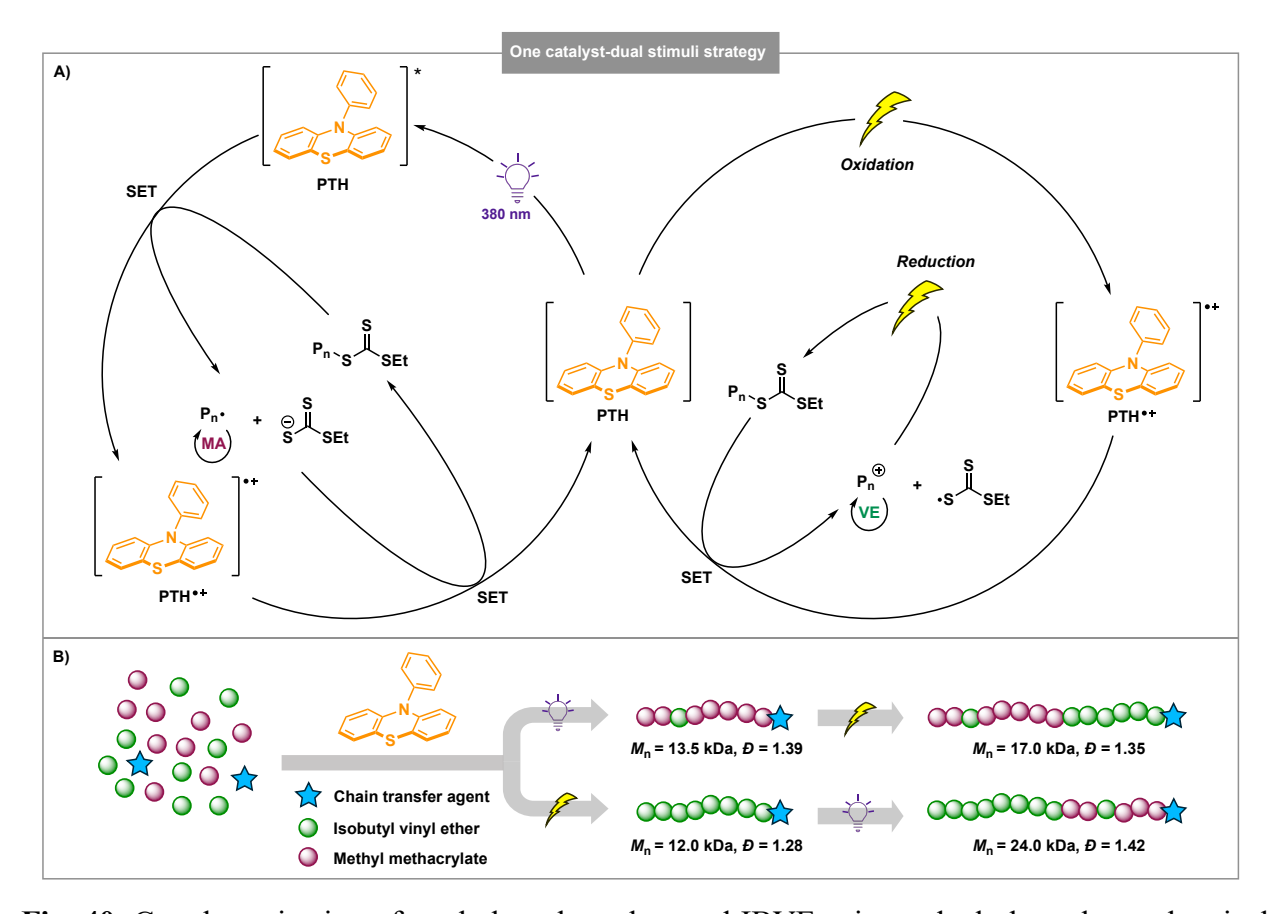


Fig. 39. Copolymerization of methyl methacrylate and IBVE using electricity and light [93].

Parallel to the previous approach reported by Fors and coworkers [93], in 2021, Read de Alaniz and Sepunaru reported an elegant one catalyst-dual stimuli strategy for the synthesis of multiblock copolymers bearing MA and IBVE blocks (Fig. 40) [94]. Harnessing the orthogonal nature of 10phenylphenothiazine (PTH) as a radical and cationic mediator, the on-demand living polymerization of each monomer was achieved upon application of photo- or electrochemical stimuli, generating well-defined multiblock copolymers. Applying an oxidative current (0.1 mA) to reaction conditions can preferably oxidize PTH to generate the radical cation PTH\*+, which can subsequently oxidize a trithiocarbonate compound and control the cationic polymerization of IBVE via RAFT process. Alternatively, light irradiation (380 nm LED) of the reaction mixture led to the excitation of PTH to PTH\*, which is known to be a highly reductive species capable of reducing the trithiocarbonate chain end via a single electron transfer process. The resulting radical propagating species are capable of controlling the radical polymerization of MA. This methodology demonstrated the ability to selectively mediate monomer addition by choice of stimuli applied, which was shown by synthesizing various multiblock copolymers. Most importantly, this system displayed excellent temporal control, allowing for temporal control, as demonstrating by multiple on/off cycles.



**Fig. 40.** Copolymerization of methyl methacrylate and IBVE using a dual photoelectrochemical catalyst. [94], Copyright 2021. Adapted with permission from American Chemical Society.

Additionally, the Fors group also reported using ferrocenyl acids to achieve the living cationic polymerization of cyclic esters (**Fig. 41**) [95]. The ferrocene derivatives with tethered acid moieties could be oxidized electrochemically, thus lowering their pKa and providing the ability to catalyze the cationic ROP of  $\varepsilon$ -CL. This methodology proved efficient to synthesize several polyesters with molecular weights in agreement with their theoretical values, while maintaining low dispersity ( $\theta$  < 1.28).

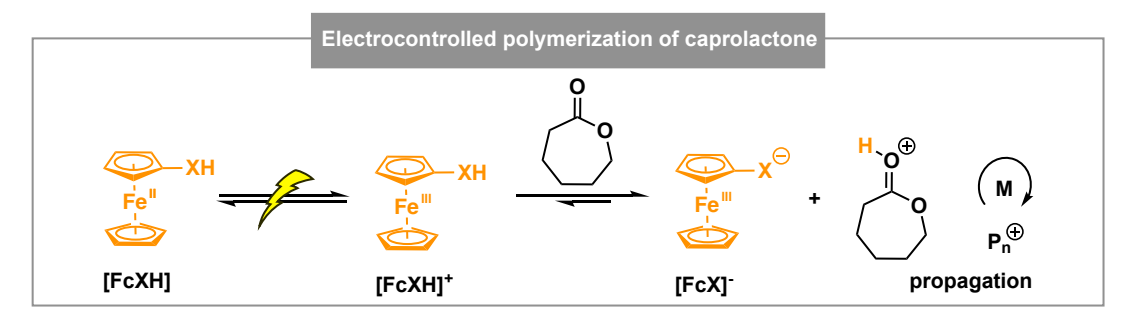


**Fig. 41.** Ferrocenyl acid as a mediator for the electrocontrolled cationic polymerization of lactones [95].

#### 4. Stereocontrolled cationic polymerization

Stereoregularity plays a critical role in determining the physical properties (e.g., mechanical strength, thermal performance, optical property) of polymers [96]. Polypropylene represents the most well-known example (Fig. 42), in which isotactic polypropylene (adjacent methyl groups on successive stereocenters are all of the same configuration) is a semicrystalline and tough thermoplastic [97]. Syndiotactic polypropylene (adjacent methyl groups on successive stereocenters are of perfectly alternating configuration) often has excellent impact strength [98]. In contrast, atactic polypropylene (adjacent methyl groups on successive stereocenters are of a random configuration) usually is as an amorphous material. Thus, achieving on-demand stereocontrol during polymerization remains of high interest [99,100]. Although enormous advances in the stereo-control for anionic [101] and coordination-insertion polymerization [102-104] have been made in the last decades, the stereoregularity control in cationic polymerization remains a formidable challenge. The difficulty in controlling stereochemistry during the cationic polymerization of olefinic monomers is attributed to the undefined stereochemical environment of the planar sp<sup>2</sup>-hybridized growing carbenium species. Therefore, elaborately designed catalysts or counterions are required to achieve stereoregulation in cationic polymerization [105]. In this section, selected seminal discoveries in stereoselective cationic polymerization will be first discussed, followed by a comprehensive summary of recent breakthroughs, and ended with an outlook in this emerging field.

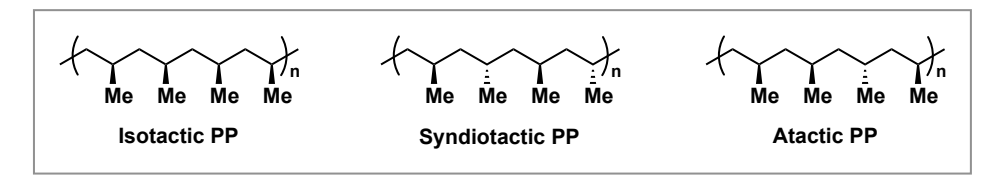


Fig. 42. The structure of isotactic, syndiotactic, and atactic polypropylene (PP).

## 4.1 Stereoselective cationic polymerization of vinyl ethers

Although the stereoselective cationic polymerization of vinyl ethers can be dated back to the 1940s [106,107], high stereoselectivity was still beyond reach at the time. For example, applying BF<sub>3</sub>•Et<sub>2</sub>O as a catalyst, Schildknecht and co-workers found that polymerization of IBVE at low temperature (-78 °C) in neat condition gave rise to semicrystalline materials (**Fig. 43**). Further studies suggested that the polymer crystallinity might arise from the relative stereochemical relationship between adjacent pendant substituents. In the following decades, a variety of catalytic systems have been applied in the polymerization of vinyl ethers to improve the stereoselectivity, such as Ziegler-type catalysts [108,109], metallocene-based transition metal catalysts [110], heterogeneous metal-sulfate complexes [111], and others, however, achieving a high degree of tacticity (e.g.,  $\geq$ 90% m diad, m stands for meso) remained challenging.

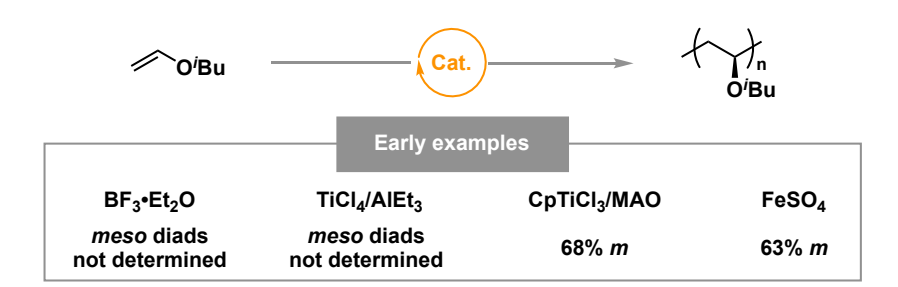


Fig. 43. Early examples in stereoselective cationic polymerization of IBVE [106 - 111].

In their continuing efforts toward stereoselective polymerization, Sawamoto and co-workers described the first highly isotactic (up to 92% *m* diad) cationic polymerization of IBVE in 1999 (**Fig. 44**) [112]. A series of designed phenoxy-bound titanium Lewis acid catalysts were employed to regulate the facial addition of incoming monomer, among which bis(2,6-di-iso-propylphenoxy)titanium dichloride gave the highest *meso* diad contents (92% *m* diad, 83% *mm* 

triad) in hexane at -78 °C with a bulky pyridine (2,6-di-*tert*-butyl-4-methylpyridine) (DTBP) as an additive. Initial mechanistic studies implied that not only the bulkiness of the Lewis acid but also the spatial shape and electronic nature of the forming counterion are responsible for the stereoregulation during the propagation process.

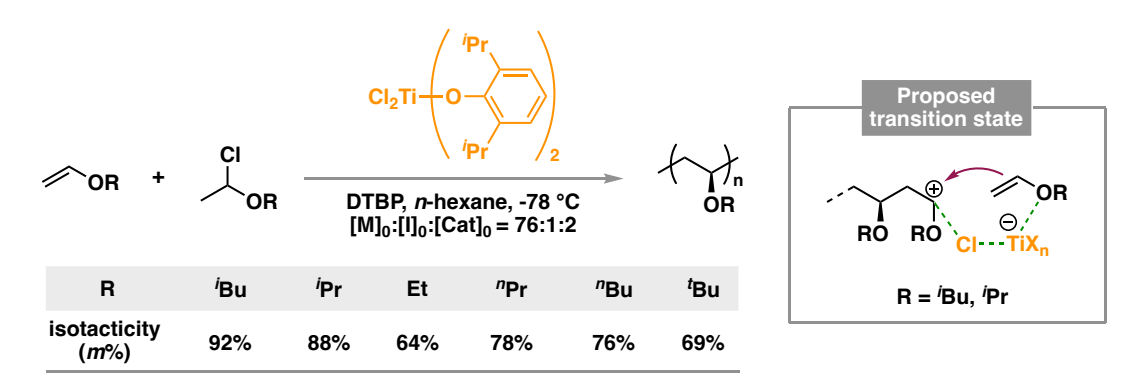


Fig. 44. Stereoselective cationic polymerization of vinyl ethers using phenoxy-Ti complex [113].

Their following studies found that this elaborate catalyst system is not general to all alkyl vinyl ethers (**Fig. 44**) [113]. Instead, the polymers obtained displayed different stereoregularity depending on monomer substitution (*e.g.*, ethyl, 64% *m* diad; *n*-propyl, 78% *m* diad; *iso*-propyl, 88% *m* diad; *n*-butyl, 69% *m* diad; *t*-butyl, 76% *m* diad). A statistical analysis of the triad distributions revealed that low stereoselective systems (69-76% *m* diad) might follow chain-end control, where the stereochemistry of the last enchained monomer influences the facial addition of the incoming monomer. In contrast, the high isospecificity (~90% *m* diad) in the polymerization of IBVE and isopropyl vinyl ether (IPVE) was attributed to the catalyst control, in which bulky catalysts or the corresponding counterions would dictate the facial addition of the monomers (**Fig. 45**). Based on these results, a new transition state was proposed, where the effective interaction between catalyst and monomer could regulate the direction of the incoming monomer to the propagating species to result in the stereoselective propagation.



Fig. 45. Chain-end control and catalyst control in the cationic polymerization of vinyl ethers.

Sawamoto and co-workers additionally disclosed another binary catalytic system, in which a bulky phosphoric acid paired with SnCl<sub>4</sub> gave highly isotactic poly(IBVE) (up to 86% m diad) (**Fig. 46**) [114]. The low polymerization temperature (-78 °C) and low concentration of Lewis acid (1.0 mM) were found to have effects on improving the stereoselectivity. A series of initiators screening revealed that phosphoric acids (RO)<sub>2</sub>POOH with long alkyl chains (R = n-decyl) induced the highest isotacticity (m = 86%) in the SnCl<sub>4</sub>-catalyzed cationic polymerization of IBVE. In addition, Eyring analysis of the stereoselective polymerization demonstrated that enthalpic factor was responsible for the high isotacticity with bulky phosphoric acids. Finally, this seminal work demonstrated that tacticity control is achievable by applying bulky counterions during cationic polymerizations, which lay a strong foundation for following studies.

Fig. 46. Stereoselective cationic polymerization of IBVE using bulky phosphoric acid [114].

Building upon these precedents, in 2019, Leibfarth and co-workers developed an elegant catalyst-controlled stereoselective cationic polymerization system, in which chiral, BINOL-based phosphoric acids counterions could significantly bias the stereochemistry of monomer enchainment and dictate the facial addition of the incoming monomers (**Fig. 47**) [115]. This novel methodology showed a broad monomer scope, vinyl ethers bearing a variety of pendant alkyl substituents all gave highly isotactic polymers (*e.g.*, ethyl, 92% *m* diad; *n*-propyl, 92% *m* diad; *iso*-propyl, 88% *m* diad; *n*-butyl, 93% *m* diad; *iso*-butyl, 93% *m* diad). All the resulting polymers were semicrystalline solids, which is in sharp contrast to the amorphous liquids produced by the chain-

end control model. Additionally, the highly stereoregular polymer poly(IBVE) displayed comparable thermomechanical properties ( $T_{\rm m}=138-150~{\rm ^{\circ}C}$ .  $E=200\pm20~{\rm MPa}$ ,  $\sigma_{\rm y}=8.4\pm0.5~{\rm MPa}$ ,  $\sigma_{\rm b}=8.2\pm0.5~{\rm MPa}$ ,  $\varepsilon_{\rm B}=170\pm20\%$ ) to widely used commodity polymers, such as the low-density polyethylene Dow LDPE 4012 ( $T_{\rm m}=105~{\rm ^{\circ}C}$ .  $E=280\pm40~{\rm MPa}$ ,  $\sigma_{\rm y}=8\pm1~{\rm MPa}$ ,  $\sigma_{\rm b}=10\pm2~{\rm MPa}$ ). Notably, isotactic poly(BVE) also exhibited stronger adhesion to glass than that of the Dow LDPE, as demonstrated by apparent lap shear strengths of  $1600\pm100~{\rm MPa}$  and  $130\pm20~{\rm MPa}$ , respectively. The excellent mechanical and adhesive properties, together with good thermal stabilities ( $T_{\rm d}>325~{\rm ^{\circ}C}$ , defined by 5% weight loss) make these isotactic poly(vinyl ethers) promising candidates for next-generation engineering materials.

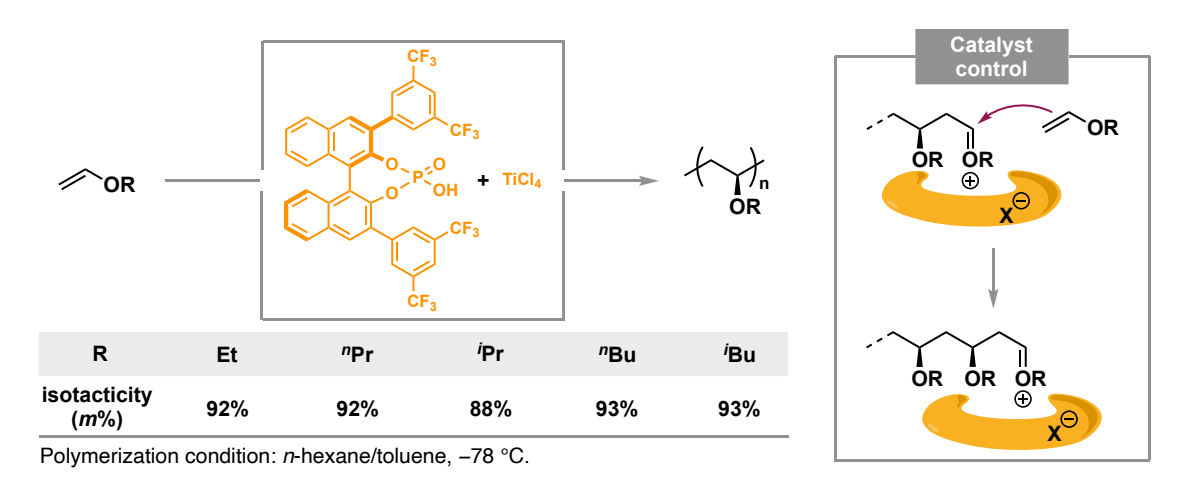
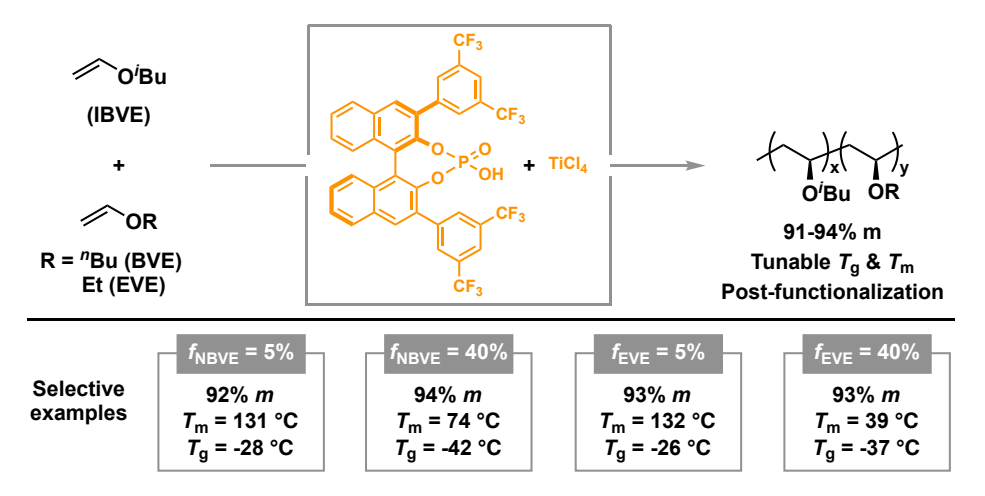


Fig. 47. Stereoselective polymerization of vinyl ethers using BINOL-based phosphoric acid [115].

The generality of this new system with respect to alkyl vinyl ether monomers represent a significant improvement in stereoselective cationic polymerization, leading to the first highly stereoselective copolymerization of vinyl ethers (Fig. 48) [116]. The systematic tuning of both glass transition ( $T_g$ ) and melting temperature ( $T_m$ ) in copolymers could be readily achieved by adjusting the feed ratio of the comonomers, meanwhile the high stereoselectivities were successfully maintained (91-94% m diad). Moreover, a novel pyrene-appended copolymer with interesting fluorescent properties could be obtained when using acyl-protected ethylene glycol vinyl ether as a comonomer, followed by facile post-functionalization reactions. Therefore, this ion-pairing mediated stereoselective cationic polymerization strategy represents a promising approach toward thermoplastics with diverse material properties.



**Fig. 48.** Stereoselective copolymerization of vinyl ethers using BINOL-based phosphoric acids [116].

The comprehensive mechanistic studies provided a deep understanding of the polymerization mechanism [117]. Firstly, the statistical analysis of the triad distributions reveals an evident preference for catalyst control, while chain-end control is the dominant mechanism for stereocontrol in the absence of the chiral phosphoric acid catalyst. Additionally, kinetic analysis indicates a significant ligand deceleration effect, agreeing well with the observation that a molar excess of chiral ligand relative to Lewis acid was necessary to produce the highest tacticity. This observation was supported by density functional theory (DFT) calculations, in which a Ti complex consisting of three coordinated phosphoric acids was identified. Eyring analysis of the stereoselective polymerization showed a good linear relationship between the  $\ln(m/r)$  and 1/T, indicating the overall mechanism remained unchanged between -78 °C and -40 °C. Furthermore, from the Eyring plot, the difference in the energy barrier between meso and racemo addition was calculated to be -0.73 kcal/mol, which was corresponding to 87% m diad. Finally, when enantioenriched vinyl ethers were applied in the stereoselective polymerization, the highest isotacticity (95% m diad) ever reported was achieved, suggesting a fully match system between chiral monomer and catalyst.

In their continuous efforts toward controlled cationic polymerization of vinyl ethers, Aoshima and co-workers have tested an extensive array of ligands, including salen [118], salphen [119], and phenoxyimine [120]. The content of *meso* diad were kept in a range of 65-75% *m* diad, implying

the chain-end control mechanism might be operative in these systems. In 2020, they successfully generated highly isotactic poly(IBVE) (up to 90 diad) by using chiral titanium complexes of tetraaryl-1,3-dioxolane-4,5-dimethanol (TADDOL) (**Fig. 49**) [121]. Owing to their facile preparation from naturally abundant tartaric acid, a series of TADDOLs ligands were evaluated in the stereoselective polymerization of IBVE. The statistical analysis of triad sequences excluded the chain-end control mechanism, implying the high stereoselectivity arises from the catalyst control pathway. More interestingly, the same tacticity was observed when enantiopure (S, S)- or (R, R)-TADDOLs were used as ligands. Therefore, the authors hypothesized that the chiral catalyst should remain within the polymer chain-end and no shuffling of the catalyst was occurring throughout the propagation.

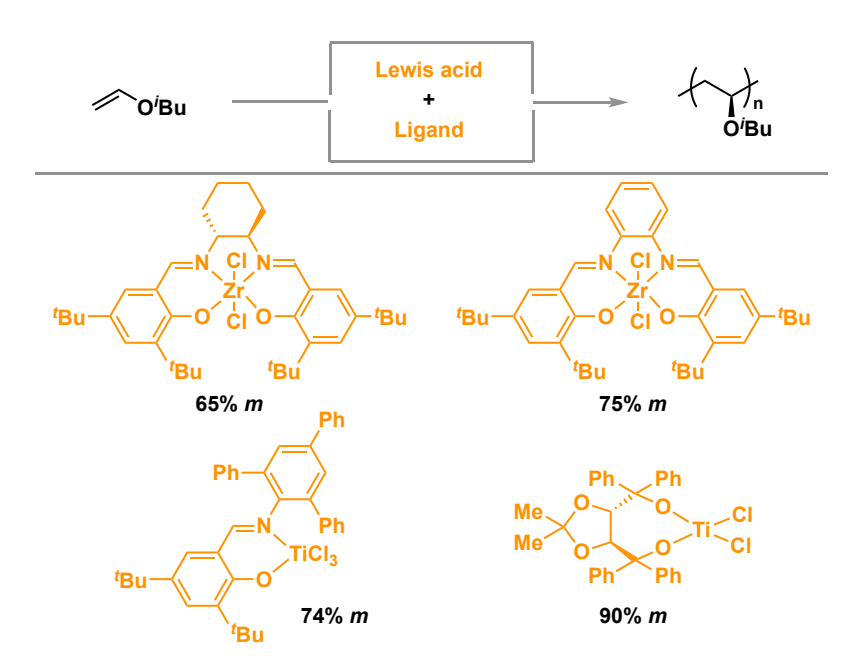
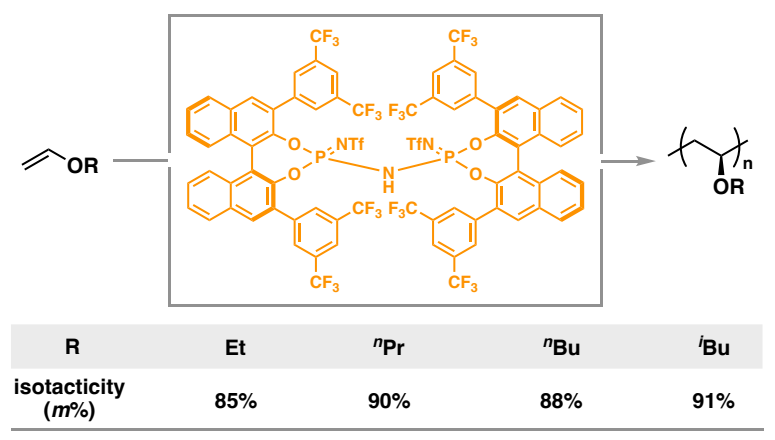


**Fig. 49.** Stereoselective polymerization of IBVE catalyzed by zirconium and titanium complexes [118-121].

In 2022, Liao and co-workers subsequently reported a metal-free stereoselective cationic polymerization of vinyl ethers, in which a class of confined Brønsted acids, imidodiphosphorimidates (IDPi), were used as chiral catalysts (**Fig. 50**) [122]. Examination of a series of chiral Brønsted acids disclosed that the electron-withdrawing trifluoromethyl group was beneficial for improving stereoselectivity, and a stereoregular poly(IBVE) with high isotacticity (91% m diad) and  $M_n$  of 18.9 kDa could be obtained in 30 min at full monomer conversion.

Additionally, this organocatalytic stereoselective polymerization method was compatible to a range of alkyl vinyl ether monomers, affording corresponding polymers with moderate degrees of isotacticity (*e.g.*, ethyl, 85% *m* diad; *n*-propyl, 90% *m* diad; *n*-butyl, 88% *m* diad).



Polymerization condition:  $[\mathbf{M}]_0 / [\mathbf{IDPi}]_0 = 200:1$  at -78 °C for 30 min in toluene.

Fig. 50. Organocatalytic stereoselective polymerization of vinyl ethers [122].

Despite significant advances in the stereoselective cationic polymerization of vinyl ethers, dual control of tacticity and molecular weight have proven more challenging. To achieve highly stereospecific cationic polymerization, bulky or chiral Lewis/Brønsted acids are required to regulate the facial addition of the incoming monomer. However, these catalysts are usually incapable of establishing the reversible activation-deactivation equilibrium between dormant and active species, which is the key to living polymerization. Therefore, developing appropriate catalytic systems in which molecular weight and stereochemistry controls are not disturbed by each other remains challenging [123].

In an early example, Sudhakar and co-workers reported a highly stereoselective living polymerization of vinyl ethers at ambient temperature (**Fig. 51**) [124,125]. Triethanolamine ligated titanium complexes coupled with Methylaluminoxane (MAO) or Ph<sub>3</sub>CB(C<sub>6</sub>F<sub>5</sub>)<sub>4</sub> were capable of polymerizing IBVE in a controllable manner and generated highly stereoregular poly(IBVE) with good isotacticity (90-94% m diad). Furthermore, linear growth of the molecular weights over conversion and low dispersity (D = 1.16-1.25) indicated a living polymerization system. Although

the mechanism of stereocontrol requires further exploration, the initial mechanistic studies suggested that this polymerization likely followed a carbocationic pathway.

Fig. 51. Early example of stereoselective living cationic polymerization of IBVE [124,125].

In 2021, Leibfarth and co-workers showed an elegant catalytic system, in which control of molecular weight and tacticity could be simultaneously achieved (**Fig. 52**) [126]. A bulky Brønsted acid IDPi functioned as the chiral catalyst to direct the stereochemistry of monomer addition, while a thioacetal-type CTA was utilized to modulate the molecular weight. Accordingly, poly(IBVE) with molecular weight ranging from 6.8 to 58.7 kDa could be readily obtained by adjusting the feed ratio between monomer IBVE and CTA, while moderately high stereoselectivity was maintained (88-89% m diad). It is worth nothing that the chiral Brønsted acid could be readily recycled (>95%) and reused in the stereoselective polymerization, without a noticeable change in reactivity and stereoselectivity (89.7 $\pm$ 0.6% m diad).

Fig. 52. Brønsted acids catalyzed stereoselective living cationic polymerization of IBVE [126].

Independently, Liao and co-workers developed another stereoselective living cationic polymerization of vinyl ethers (**Fig. 53**) [127]. They introduced a different type of chiral organic Brønsted acid, 1,1'-bi-2-naphthol-derived N,N'-bis(triflyl)phosphoramidimidates (PADIs), to facilitate the tacticity control. Similarly, a trithiocarbonate-type CTA was employed to control the

molecular weight via cationic RAFT process. As a result, poly(IBVE)s with MW ranging from 4.1 to 14.5 kDa were obtained with relatively low dispersity (D = 1.20-1.46) and moderately high stereoregularity (87-88% m diad). The well-defined structure of poly(IBVE), including the  $\alpha$ -,  $\omega$ -chain ends and main-chain structure, were further demonstrated by  $^{1}$ H NMR. Given the high fidelity (>96%) in the  $\omega$ -chain end, the macromolecular initiator could be used for chain extension to prepare complex stereoblock copolymers. When combined with other polymerization methods, including photo-controlled cationic or radical polymerization and thermo-induced radical RAFT polymerization, a series of diblock copolymers were produced in a controlled manner, as confirmed by unimodal peaks appearing in the high molecular weight regime.

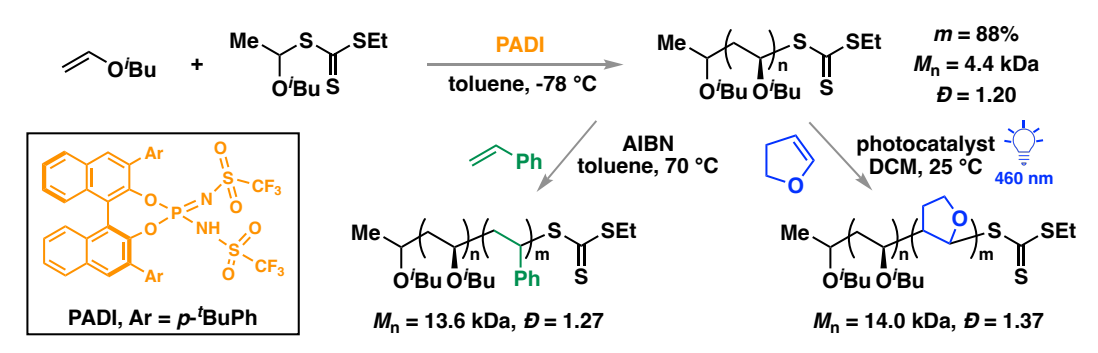


Fig. 53. Organocatalytic stereoselective living polymerization of IBVE via RAFT process [127].

In 2021, Kamigaito and co-workers described the preparation of isotactic poly(vinyl alcohol) via stereoselective cationic RAFT polymerization of bulky vinyl ethers (**Fig. 54**) [128]. When trimethylsilyl vinyl ether (TMSVE) was treated with a Lewis acid (EtAlCl<sub>2</sub>) in the presence of a dithiocarbamate-type CTA, isotactic-rich polymer was obtained ( $M_n = 8.7 \text{ kDa}$ , mm = 70%). The moderately high isotacticity was attributed to the electrostatic repulsion between the bulky side groups and counteranions derived from the Lewis acid catalysts. In addition, the resulting polymer with high  $\omega$ -chain end fidelity can be used as a macroinitiator for radical RAFT polymerization of vinyl acetate (Vac), which engendered a rare isotactic-*b*-atactic stereoblock poly(vinyl alcohol) after the global deprotection of both the silyl and acetyl groups in the copolymer.

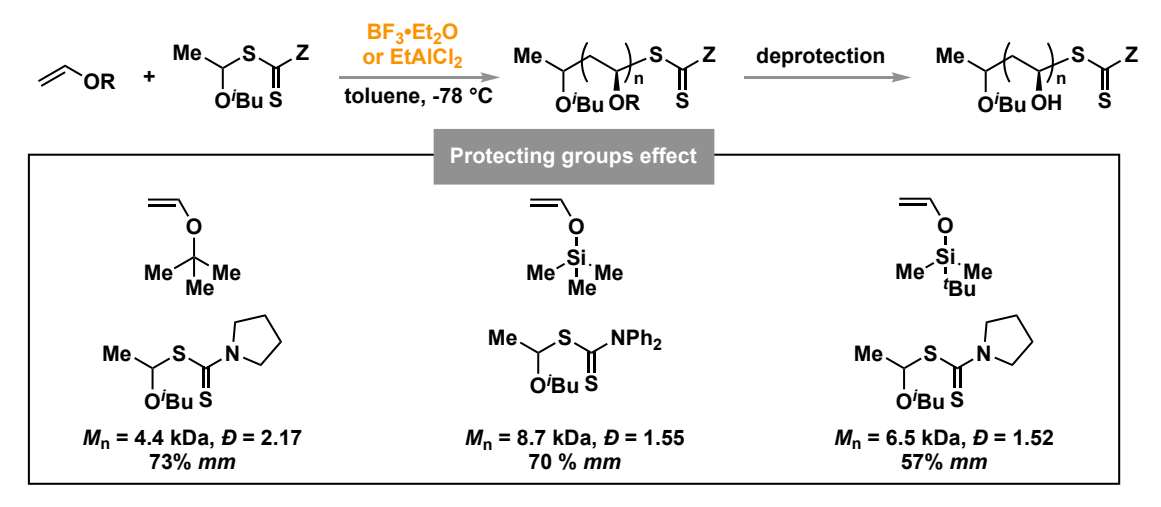


Fig. 54. Stereoselective cationic RAFT polymerization of bulky vinyl ethers [128].

Furthermore, Kamigaito and co-workers discovered the first asymmetric living polymerization of BzF, producing optically active polymers poly(BzF) (**Fig. 55**) [129,130]. In this system, dual control of the molecular weight and optical activity was achieved using thioether as CTA in conjunction with bulky  $\beta$ -amino acid and AlCl<sub>3</sub> as chiral catalyst. The linear relationship between the molecular weights and conversion in conjunction with moderate dispersity (D = 1.36-1.54) indicated a living polymerization system. Interestingly, the optical specific rotations gradually increased with the increasing molecular weights. When each enantiomer of  $\beta$ -amino acid (R or S) was employed in the living polymerization of BzF, the obtained polymers exhibited nearly equal but opposite-in-sign specific rotation values and mirror-image CD spectra. Moreover, a stereoblock copolymer containing opposite absolute configuration segments were first prepared when two enantiomeric  $\beta$ -amino acid (R and S) was added in sequence. Preliminary studies revealed that the propagation should proceed through oxocarbenium ions instead of styryl-type cations. An extensive analysis of <sup>1</sup>H NMR spectra of polymer identified the threo-diisotactic repeating units as the predominant stereostructure within the polymers, which leads to the resulting optical activity.

Fig. 55. Asymmetric cationic RAFT polymerization of BzF [129,130].

# 4.2 Stereoselective cationic polymerization of other monomers

The stereocontrolled cationic polymerization of monomers other than vinyl ethers have been developed since the 1980s. In a pioneering example, Terrell and co-workers reported the first stereoselective polymerization of NVC (**Fig. 56**) [131]. Interestingly, the reaction temperature did not play a major role in the stereoregularity of the polymerization. However, researchers observed significant influence by choice of catalyst and solvent. Polar solvent often gave higher syndiotacticity and 58% r diad was observed when the polymerization was carried out in the presence of BF<sub>3</sub>•Et<sub>2</sub>O catalyst in dichloromethane or diethyl ether at 20 °C. The observed correlation between tacticity and solvent polarity was interpreted to arise from the tightness of the propagating ion pairs, in which tighter ion pairs benefited stereocontrol during the polymerization.

Fig. 56. An early example of stereoselective cationic polymerizations of NVC [131].

In 2017, Aoshima and coworkers reported a systematic analysis on the stereoselective cationic polymerization of NVC (**Fig. 57**) [132]. Using a three-component initiating system consisting of a metal halide (MX<sub>n</sub>), an onium salt (AX), and TfOH, the stereoselective living cationic polymerization of NVC can be achieved, yielding poly(NVC) with excellent stereoregularity (94% mm triad) and narrow dispersity (D = 1.30). Additionally, DFT calculations suggested that the electrostatic interactions between the counteranion, the carbocation propagating species, and the incoming monomers were responsible for the stereoregulation during propagation [133]. The

transition state energy of the *meso* addition was 1.5 kcal/mol lower than the *racemo* addition. Notably, this system also showed the ability to readily synthesize block copolymers consisting of atactic and isotactic blocks of NVC, enabled by different initiating systems.

ZnCl<sub>2</sub>, 
$${}^{n}$$
Bu<sub>4</sub>NCl, CF<sub>3</sub>SO<sub>3</sub>H

DCM, -78 °C

94% mm

 $M_{\rm n} = 8.0 \text{ kDa}, D = 1.27$ 

**Fig. 57.** Stereoselective living cationic polymerization of NVC using the metal halide (MX<sub>n</sub>)/onium halide (AX)/CF<sub>3</sub>SO<sub>3</sub>H initiating systems [132].

In 2022, Leibfarth and coworkers reported a chain-end controlled polymerization of NVC by using chiral Box ligand-metal complexes to result in a helix-sense-selective polymerization (**Fig. 58**) [134]. This seminal work demonstrated that polymer tacticity was controlled by the conformation of the growing polymer chain end. Notably, they found that polymer helicity was deeply influenced by the stereoselectivity of the first monomer propagation event. Using a Box-scandium Lewis acid catalyst and a hemiaminal initiator, highly isotactic (92% *mm* triad) and optically active helical (molar ellipticity  $\theta = 380 \text{ deg} \cdot \text{cm}^2 \cdot \text{dmol}^{-1}$ ) poly(NVC) was obtained.

+ Ph (OTf)<sub>m</sub> Ph 92% mm helical polymers [
$$\theta$$
]<sub>296</sub> = 380 deg·cm<sup>2</sup>·dmol<sup>-1</sup>

Fig. 58. Stereoselective helix-sense-selective cationic polymerizations of NVC [134].

In 2013, Mandal and co-workers succeeded in conducting stereospecific living cationic polymerization of  $\alpha$ -MeSt using FeCl<sub>3</sub> as a catalyst and HBr-St adduct as an initiator (**Fig. 59**) [135]. Notably, an external salt ( $^n$ Bu<sub>4</sub>NBr) was employed to stabilize propagation. First-order reaction kinetics and linear growth of molecular weight over monomer conversion were both observed, suggesting living characteristics of the polymerization. Accordingly, P( $\alpha$ -MeSt) with

molecular weight ranging from 4.3 to 32 kDa could be readily prepared by varying the feed ratio between monomer and initiator, displaying low to moderate syndiotacticity (59%-84% rr). Furthermore, the effect of tacticity on thermal properties was investigated.  $T_{\rm g}$  increased from 115 °C to 159 °C, and  $T_{\rm d}$  increased from ~310 °C to 398 °C as the syndiotacticity increased from 59% rr to 79% rr.

**Fig. 59.** Stereospecific living cationic polymerization of α-MeSt using FeCl<sub>3</sub>/HBr-St/  $^n$ Bu<sub>4</sub>NBr initiating system [135].

In 2010, Chen and coworkers developed a highly isospecific cationic polymerization of nonconjugated chiral oxazolidinone-functionalized alkenes in the presence of Lewis or Brønsted acids, such as  $[Ph_3C][B(C_6F_5)_4]$ ,  $BF_3 \cdot Et_2O$ , and  $[H(Et_2O)_2][B(C_6F_5)_4]$ , providing highly isotactic (a single *mmmm* pentad peak in the C=O region) and optically active ( $[\alpha]_D^{23} = +156^\circ$ ) polymers (**Fig. 60**) [136]. The nonconjugated chiral vinyl oxazolidinone monomer, *N*-vinyl-(*R*)-4-phenyl-2-oxazolidinone (*R*)-VOZ was presumed to adopt a solution-stable one-handed helical conformation during polymerization, therefore showing significant chiral amplifications. The proposed mechanism involves the terminal olefin attacking  $[Ph_3C][B(C_6F_5)_4]$  to form an iminium, followed by a monomer propagation that is dictated by the chiral environment of the chain end. Moreover, the synthesized chiral helical vinyl polymers exhibited high  $T_d$  (435 °C) and crystallinity. A highlight of this work lies on a chiral auxiliary-controlled mechanism at play, which combines side-chain chirality with main-chain chirality affording one-handed helicity polymers.

**Fig. 60.** Stereoselective cationic polymerizations of nonconjugated chiral oxazolidinone-functionalized alkenes. [136], Copyright 2010. Adapted with permission from American Chemical Society.

Despite the great advances have been made in the stereoselective cationic polymerization since last decades, there still exists some limitation in this fast-growing field. Firstly, monomer scope needs to be further expanded, since most of successful examples focused on generating stereoregular poly(vinyl ether). In this context, more elaborate catalysts design and new reaction models are required. Secondly, more precise control over the polymerization structure is highly desirable, such as simultaneous control of the tacticity, molecular weight, and dispersity. Finally, the unique material properties associated with the stereoregular polymer needs to be further investigated, which will lead to the discovery of functional polymeric materials.

### 5. Chemically recyclable/degradable polymers

Synthetic polymers play an essential role in the modern human society due to their low cost, chemical robustness, thermal stability, and high mechanical strength. However, the increasingly serious environmental issue, caused by unsustainable generation (~320 Mt in 2015) and disposal of single-use commodity plastics [137,138], compels polymer scientists to find efficient approaches to address the end-of-life dilemma of plastics from the perspective of circular economy [139]. Therefore, the development of polymers with on-demand degradability or inherent chemical recyclability is highly desirable to alleviate the current global issues on polymer-waste pollution [140-144]. In the last decades, numerous polymer platforms have been established, and the

sustainability of these polymers was systematically investigated [145-147]. This section will illustrate the recent efforts toward developing cationic polymerization platforms that are chemically recyclable or degradable [148-151]. Particularly, different classes of polymers will be discussed, including polyacetals, polysaccharides, polyvinyl ethers, and polyethers.

# 5.1 Polyacetals

Polyacetals are promising as degradable materials due to the inherent chemical recyclability of acetal functional groups, which can readily undergo depolymerization [152]. Among them, poly(o-phthalaldehyde) (PPA) is one of the most easily accessible polymers via both cationic and anionic homopolymerization of o-phthalaldehyde (o-PA) [153,154]. Since the 1960s, it has been investigated as a potential material for lithography [155-157], but the low ceiling temperature ( $T_c$  =  $\sim$  -40 °C) made actualizing its potential challenging [154].

In 2009, Ribitsch and coworkers disclosed that PPA synthesized *via* cationic polymerization was thermally stable, as demonstrated by moderate degradation temperature of 150 °C [158]. In contrast, PPA obtained by anionic polymerization required end-capping to prevent degradation upon purification. Furthermore, cationic conditions achieved a moderate molecular weight polymer ( $M_n = 46 \text{ kDa}$ ) by using BF<sub>3</sub> as a catalyst, whereas anionic polymerization was limited to lower molecular weight polymer ( $M_n = 6.8 \text{ kDa}$ ) when <sup>n</sup>BuLi was used as a catalyst.

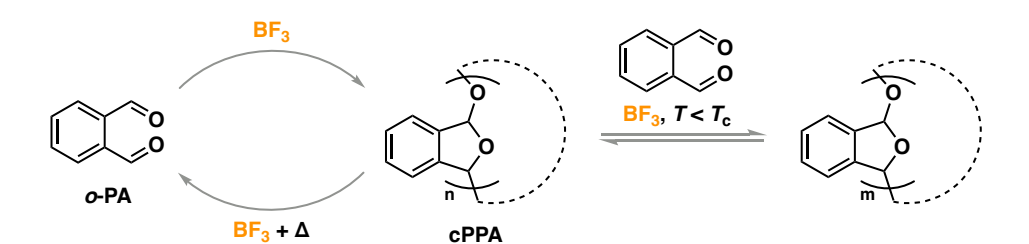


**Fig. 61.** Reversible cationic polymerization of *o*-PA catalyzed by BF<sub>3</sub> and expansion of the resulting polymer [159].

In 2013, Moore and coworkers launched a detailed investigation into the synthesis of PPA by cationic polymerization using BF<sub>3</sub> as the catalyst at -78 °C (**Fig. 61**) [159]. MALDI-TOF analysis indicated that cationic polymerization of *o*-PA yields a cyclic PPA polymer (cPPA). Importantly,

cyclization was discovered to be reversible. Addition of BF<sub>3</sub> and monomer to cPPA at low concentration (0.6 M) enabled the acetal backbone to reopen and expand even below the ceiling temperature ( $T_c = -43$  °C at 1.0 M). More importantly, a complete depolymerization of cPPA was achieved, in which 97% of monomer was recovered with BF<sub>3</sub> and heat [160].

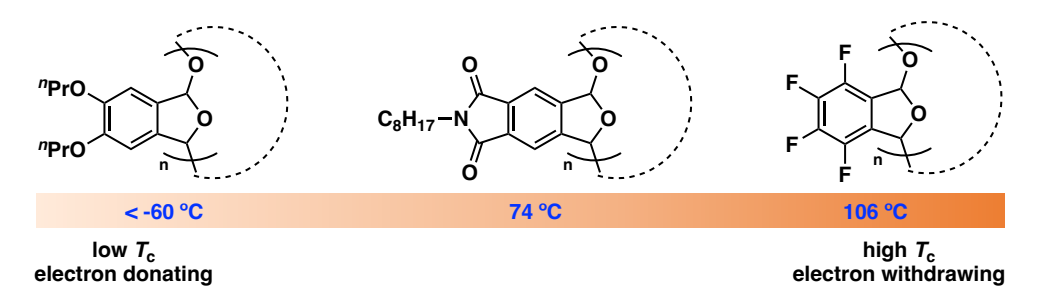
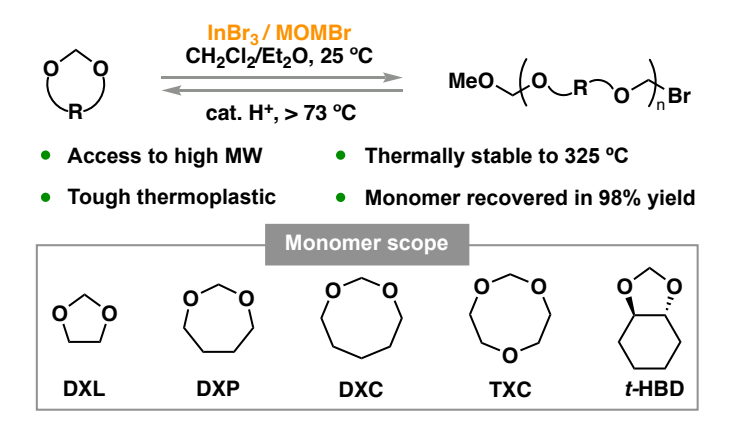


Fig. 62. Effect of o-PA substituents on the ceiling temperature of the resulting cPPA [161].

In 2019, McNeil and coworkers carried out a comprehensive study of the effect of substituted o-PA monomers on the properties of the resulting cPPA (**Fig. 62**) [161]. In the presence of SnCl<sub>4</sub> as a catalyst, polymerization of 2-octyl-1,3-dioxoisoindoline-5,6-dicarbaldehyde generated a cyclic polymer ( $M_n = 25$  kDa, D = 1.9). The thermodynamic analysis revealed that electron-donating substituents lowered the  $T_c$  of cPPA, whereas electron-withdrawing substituents increased the  $T_c$ , with  $T_c$  ranging from below -60 to 106 °C. Notably, poly(tetrafluorophthalaldehyde) with electron-withdrawing substituent group exhibited higher decomposition temperature ( $T_d = 196$  °C) than glass transition temperature ( $T_g = 106$  °C), positioning it as a promising material for processing. Methods to improve the thermal stability of cPPA were further developed by Moore and coworkers [162]. It was found that addition of TEMPO stabilized the polymer by raising the degradation temperature to 131 °C. Furthermore, the combined addition of diethyl phthalate (DEP, a plasticizer) and N,N'-di-sec-butyl-1,2-phenylenediamine (DBPDA) resulted in a robust cPPA suitable for thermal processing with minimal degradation. In addition to improved thermal processing, complete depolymerization of cPPA could also be achieved with addition of TfOH as a catalyst.

Cyclic acetal monomers present an alternative path to accessing polyacetal materials. One such material, poly(1,3-dioxolane) (PDXL) is a tough thermoplastic which has been used since the 1940s for a variety of applications, such as wax substitutes, plasticizers for rubber, and water-

soluble lubricant [163]. PDXL can be readily obtained by rapid polymerization of 1,3-dioxolane (DXL) under acidic conditions. However, actualizing the potential of PDXL has proven to be challenging, as polyacetals with high molecular weights are difficult to access [164].



**Fig. 63.** Living cationic polymerization of cyclic acetals mediated by InBr<sub>3</sub> and bromomethyl methyl ether (MOMBr) [165].

In 2021, Coates et al. established a living cationic polymerization approach to high molecular weight PDXL (Fig. 63) [165]. MOMBr and InBr<sub>3</sub> were identified as an efficient initiator/catalyst pair for controlled cationic polymerization of DXL. This system was also applicable to other cyclic acetal monomers with different ring sizes, such as 1,3-dioxepane (DXP), 1,3-dioxocane (DXC), 1,3,7-trioxocane (TXC), and trans-hexahydro-1,3-benzodioxole (t-HBD). The polymerization met the characteristics for living polymerization, including a linear relationship between  $M_n$  and [M]<sub>0</sub>:[I]<sub>0</sub>, and successful chain extension. The thermogravimetric analysis (TGA) indicated good thermal stability for each polyacetal derivative, with degradation temperatures measured to be >337 °C. Notably, the semicrystalline PDXL displayed similar thermal properties to several commercial plastics, such as poly(lactic) acid and poly(ethylene) oxide ( $T_g = -63$  °C,  $T_m = 58$  °C). A high MW PDXL (180 kDa) exhibited excellent mechanical properties ( $\sigma_B = 40.4 \pm 1.2$  MPa,  $\varepsilon_B$ = 720 ± 20%), comparable to those of isotactic propylene and high-density polyethylene. Moreover, the addition of catalytic amount of camphorsulfonic acid (2 mol %) to neat PDXL at 150 °C efficiently depolymerized PDXL back to DXL, which was collected by simple distillation in nearly quantitative yield. Repolymerization of the recovered monomer resulted in PDXL with tensile properties identical to pristine PDXL of similar molecular weight, suggesting a circular monomer-polymer-monomer life cycle of the polyacetals materials. In 2023, by using meerwein salts  $[Et_3O^+][PF_6^-]$  as an initiator and DTBP as a proton trap, Coates and coworkers accessed for the first time ultra-high-molecular-weight PDXL (UHMW PDXL) [166]. This UHMW PDXL material ( $M_n > 2000 \text{ kDa}$ ) displayed comparable mechanical properties to ultra-high-molecular-weight polyethylene.

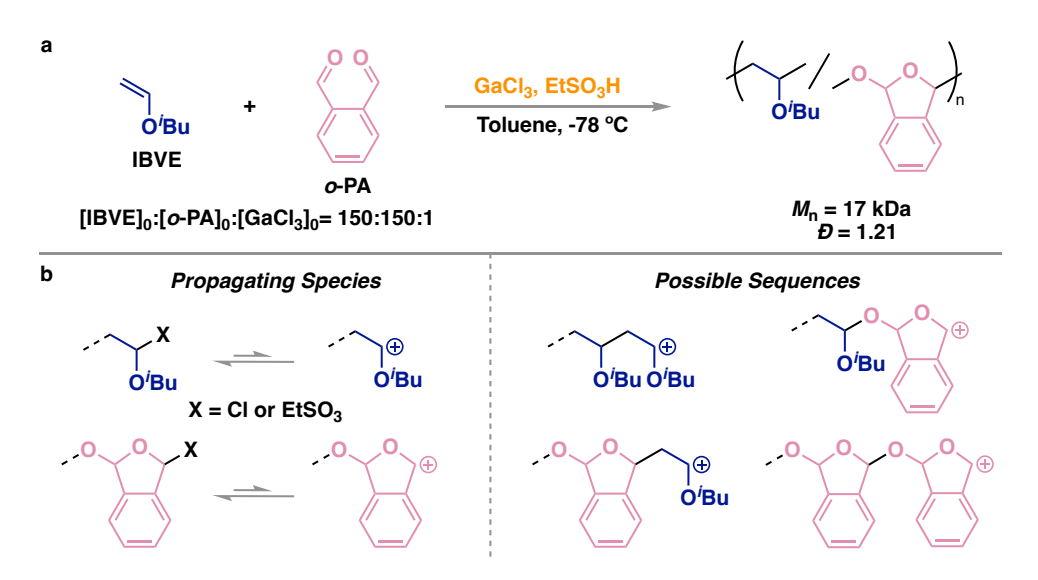


**Fig. 64.** (a) Cationic copolymerization of IBVE and *o*-PA catalyzed by GaCl<sub>3</sub> and EtSO<sub>3</sub>H. (b) Possible sequences generated by homo- and cross-propagation [167].

Copolymerization of vinyl ethers and aldehydes offers another route to accessing degradable polyacetals. To this end, Aoshima and coworkers developed the cationic copolymerization of IBVE and o-PA in the presence of GaCl<sub>3</sub> as a Lewis acid catalyst and EtSO<sub>3</sub>H as a proton source (**Fig. 64a**) [167]. A copolymer with moderate molecular weight ( $M_n = 17 \text{ kDa}$ , D = 1.21) was readily obtained. The reactivity ratios calculated using the Kelen-Tüdõs method ( $r_{\text{IBVE}} = 0.49$ ,  $r_o$ - $p_A = 0.09$ ) indicated frequent crossover reactions were involved during the polymerization (**Fig. 64b**). Owing to the labile acetal groups in the main chain, acid hydrolysis of the copolymer ( $M_n = 17 \text{ kDa}$ , D = 1.21) produced oligomers which showed significantly lower molecular weight ( $M_n = 0.36 \text{ kDa}$ , D = 1.44).

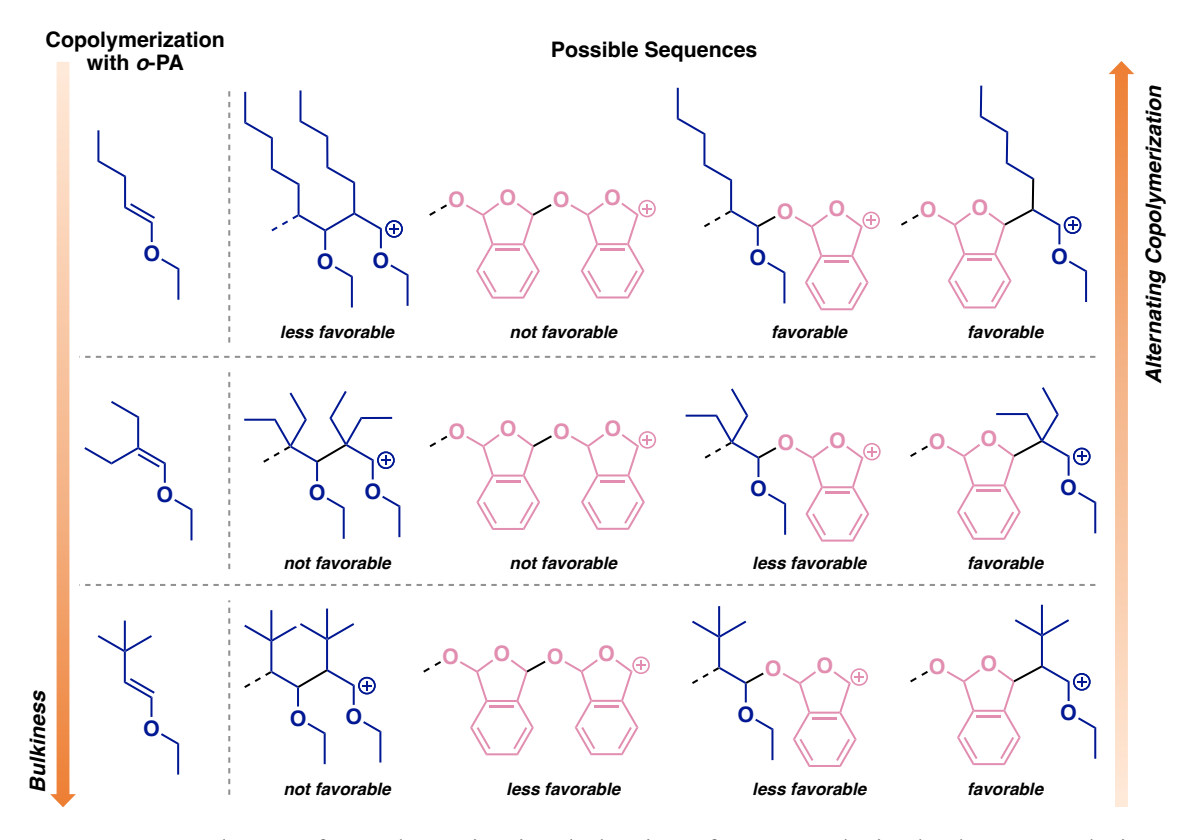


**Fig. 65.** Dependency of copolymerization behavior of *o*-PA and vinyl ethers on relative rates of homo- and crossover-propagation, which are affected by relative bulkiness of monomers [168].

Copolymerization of o-PA with vinyl ethers was further expanded to various bulky enol ethers. The copolymerizability depended on the substituent groups of the vinyl ether comonomers (**Fig. 65**) [168]. Less bulky alkyl substituents correlated with better alternating propagation, vinyl ethers with secondary cyclic substituents also generated alternating copolymer. In contrast, vinyl ethers with non-locking secondary or tertiary substituents negatively impacted alternating copolymerization. Different propagation mechanisms were proposed to understand the impact of steric hinderance on homo- and crossover reactivity (**Fig. 65**). As the vinyl ether monomer becomes bulkier, steric hinderance suppresses the crossover reaction from o-PA to vinyl ethers, thus generating homopolymer of o-PA. On the other hand, less bulky vinyl ether monomers preferably react with o-PA, resulting in the copolymer formation. Moreover, all copolymers degraded to oligomers via acidic methanolysis or hydrolysis. For instance, a copolymer of isopropyl-EVE and o-PA ( $M_n = 9.3$  kDa, D = 1.68) underwent complete methanolysis to yield an oligomer ( $M_n = 0.2$  kDa).

$$\begin{array}{c} \text{Ane} \\ \text{Ane} \\ \text{[Ane]}_0:[o\text{-PA]}_0:[\text{SnCl}_4]_0 = 40:40:1 \end{array}$$

Fig. 66. Cationic copolymerization of o-PA and Ane catalyzed by SnCl<sub>4</sub> or GaCl<sub>3</sub> [169].

In 2022, Aoshima and coworkers extended the comonomer scope to styrene derivatives [169]. Copolymerization of *trans*-anethole (Ane) and *o*-PA proceeded well in the presence of SnCl<sub>4</sub> or GaCl<sub>3</sub>, generating moderate molecular weight copolymers ( $M_n = 12 \text{ kDa}$ , D = 1.70;  $M_n = 9.8 \text{ kDa}$ , D = 1.91, respectively) (**Fig. 66**). The copolymer synthesized by SnCl<sub>4</sub> consisted of 47% Ane units and 53% *o*-PA units, as calculated by <sup>1</sup>H NMR analysis. Thermal degradation of poly(Ane-*co-o-PA*) began around 200 °C and a glass transition temperature was not observed below 180 °C. Moreover, the copolymer was also chemically degradable. An oligomer ( $M_n = 0.2 \text{ kDa}$ ) was obtained under methanolysis conditions.

**Fig. 67.** Synthesis of a polyacetal copolymer with discrete cleavable units *via* controlled cationic copolymerization of CEVE and *p*MeBzA catalyzed by GaCl<sub>3</sub> [170].

To place the cleavable acetal linkage in the specific position, Aoshima et al. developed an elegant living copolymerization of vinyl ehters with aldehydes (**Fig. 67**) [170]. Specially, living polymerization of CEVE was carried out to reach 32% conversion with  $GaCl_3$  as catalyst. This was followed by sequential addition of five equivalents of 4-methylbenzaldehyde (pMeBzA). After full consumption of pMeBzA, the polymerization was allowed to continue until the lengths of two poly(CEVE) block ends were similar. Acid hydrolysis reflected that the CEVE-pMeBzA

alternating sequence was incorporated into the middle of the main chain. The degradation resulted in an oligomer ( $M_n = 5.1$  kDa, D = 1.10), which suggested the copolymer ( $M_n = 10$  kDa, D = 1.08) was cleaved in half. Furthermore, this strategy was applied to the synthesis of star-shaped polymers with degradable cores. Therefore, this method has potential applications for the development of stimuli-responsive polymers.

**Fig. 68.** Synthesis of an alternating polyacetal copolymer with pendent imidazole ionic-liquid type vinyl ether units *via* controlled cationic copolymerization of CEVE and *p*MeBzA catalyzed by GaCl<sub>3</sub>. [171], Copyright 2019. Adapted with permission from American Chemical Society.

The facile copolymerization of vinyl ethers with aldehydes allows for easy access to customized copolymers by post-polymerization functionalization. To this end, an alternative copolymerization of CEVE and pMeBzA was carried out. Followed by a  $S_N2$  reaction, a novel copolymer with pendent imidazole ionic-liquid type vinyl ether units was obtained (**Fig. 68**) [171]. Solubility tests in water demonstrated that UCST-type phase separation behaviors of these alternating copolymers were similar to that of the imidazole homopolymer poly([Me<sub>2</sub>Im][BF<sub>4</sub>]). Moreover, all the substituted alternating copolymers underwent complete degradation upon acid hydrolysis, yielding p-methylcinnamaldehyde and alcohol in quantitative yield.

(a)
$$DOP$$

$$CI$$

$$TiCl_4/SnCl_4$$

$$Toluene/CH_2Cl_2, -78 °C$$

$$CEVE$$

$$[CEVE]_0:[cyclic acetal]_0:[TiCl_4]_0:[SnCl_4]_0$$

$$80:80:1:4$$
(b)
$$M_n = 7.1 \text{ kDa}$$

$$DOP$$

$$CI$$

$$M_n = 5.2 \text{ kDa}$$

$$DOP$$

$$M_n = 5.2 \text{ kDa}$$

$$DOP$$

$$M_n = 5.4 \text{ kDa}$$

$$DOP$$

$$M_n = 5.4 \text{ kDa}$$

$$DOP$$

$$CI$$

$$M_n = 5.4 \text{ kDa}$$

$$DOP$$

$$CI$$

$$M_n = 5.4 \text{ kDa}$$

$$DOP$$

$$DOP$$

$$CI$$

$$M_n = 5.4 \text{ kDa}$$

$$DOP$$

**Fig. 69.** Cationic copolymerization of CEVE with (a) 1,3-dioxepane (DOP), (b) 2-methyl-1,3-dioxolane (MDOL), and (c) 2-(4-methoxyphenyl)-1,3-dioxolane (PMPDOL) catalyzed by TiCl<sub>4</sub>/SnCl<sub>4</sub> [172,173].

In addition to aldehydes, vinyl ethers can be copolymerized with cyclic acetals to prepare degradable polyacetals. The controlled copolymerization of vinyl ethers and cyclic acetals was first studied by the Aoshima group in 2016 [172]. In this work, CEVE was copolymerized with 1,3-dioxepane (DOP) using TiCl<sub>4</sub>/SnCl<sub>4</sub> as a catalyst system and IBEA (the adduct of IBVE and acetic acid) as an initiator (Fig. 69a). When fixing the feed ratio to be 1:1, a copolymer ( $M_n = 7.1$ kDa, D = 2.45) with 91% DOP conversion and 73% CEVE conversion was obtained. Acid hydrolysis of this copolymer resulted in an oligomer ( $M_n = 0.6$  kDa, D = 2.44). Notably, the clear preference for DOP incorporation indicated higher reactivities of DOP comonomers and insufficient crossover reactions. To generate copolymers with more degradable acetal units dispersed throughout the chain, 2-methyl-1,3-dioxolane (MDOL) was utilized as comonomer in their following works (Fig. 69b). Homopropagation of MDOL was negligible, as indicated by insignificant integration of the <sup>1</sup>H NMR peak unique to the MDOL-MDOL sequence. Moreover, the reactivity ratio measured by the Kelen-Tüdõs method was 0.06 for MDOL ( $r_{\text{MDOL}} = 0.06$ ), and 2.6 for CEVE ( $r_{\text{CEVE}} = 2.6$ ). As a result, acid hydrolysis of poly(CEVE-co-MDOL) ( $M_n = 5.2 \text{ kDa}$ , D = 1.48) resulted in oligomer with low molecular weight ( $M_n = 0.2$  kDa, D = 1.33). In 2022, by employing a bulkier cyclic acetal, 2-(4-Methoxyphenyl)-1,3-dioxolane (PMPDOL), as a comonomer, a degradable alternating copolymer was obtained ( $M_n = 5.4 \text{ kDa}$ , D = 1.23) (Fig. 69c)

[173]. <sup>1</sup>H NMR analysis revealed that homopropagation of PMPDOL was absent and nearly alternative copolymers were produced. Further, all the peaks in the <sup>1</sup>H NMR of the acid hydrolysis product ( $M_n = 0.1 \text{ kDa}$ , D = 1.04) belonged to the cinnamaldehyde derivative from the alternating CEVE/PMPDOL sequence.

**Fig. 70.** (a) Controlled cationic copolymerization of VAc and 5-methyl-1,3-dioxolan-4-one (DOLO) catalyzed by GaCl<sub>3</sub> and (b) The proposed crossover reactions in the propagation step. [174], Copyright 2022. Adapted with permission from American Chemical Society.

In 2022, the cationic copolymerization of VAc with 5-methyl-1,3-dioxolan-4-one (DOLO) was also achieved by the Aoshima group (**Fig. 70a**) [174]. A low molecular weight copolymer ( $M_n = 3.4 \,\mathrm{kDa}$ , D = 2.20) was obtained using GaCl<sub>3</sub> as a catalyst at -40 °C. Additionally, <sup>1</sup>H NMR analysis showed well-defined copolymer structure without the presence of DOLO and VAc homosequences, suggesting the formation of nearly alternating copolymers. The authors suggested a possible mechanism in which the carbocationic species generating from VAc would preferably react with DOLO, whereas the carbocation derives from DOLO fully prevents it from homopolymerization (**Fig. 70b**). As a result, alternative chain growth was readily achieved, engendering degradable copolymers.

A highly branched copolymer ( $M_n = 1.5 \text{ kDa}$ , D = 7.65) was prepared from copolymerization of VAc and a non-substituted cyclic acetal 1,3-dioxane (**DOX**) (**Fig. 71**) [174]. The acetoxy moieties

in the polymer chains could be abstracted by an electrophile, generating oxocarbenium species and thus resulting in branching polymerization. The copolymer was degradable by both acid and base. The addition of hydrochloric acid and propanol resulted in an oligomer ( $M_n = 0.4$  kDa, D = 2.2). Subjecting the copolymer to  $K_2CO_3$  caused degradation of hemiacetal moieties, leading to dramatic reduction of the molecular weight ( $M_n = 0.2$  kDa, D = 1.5).

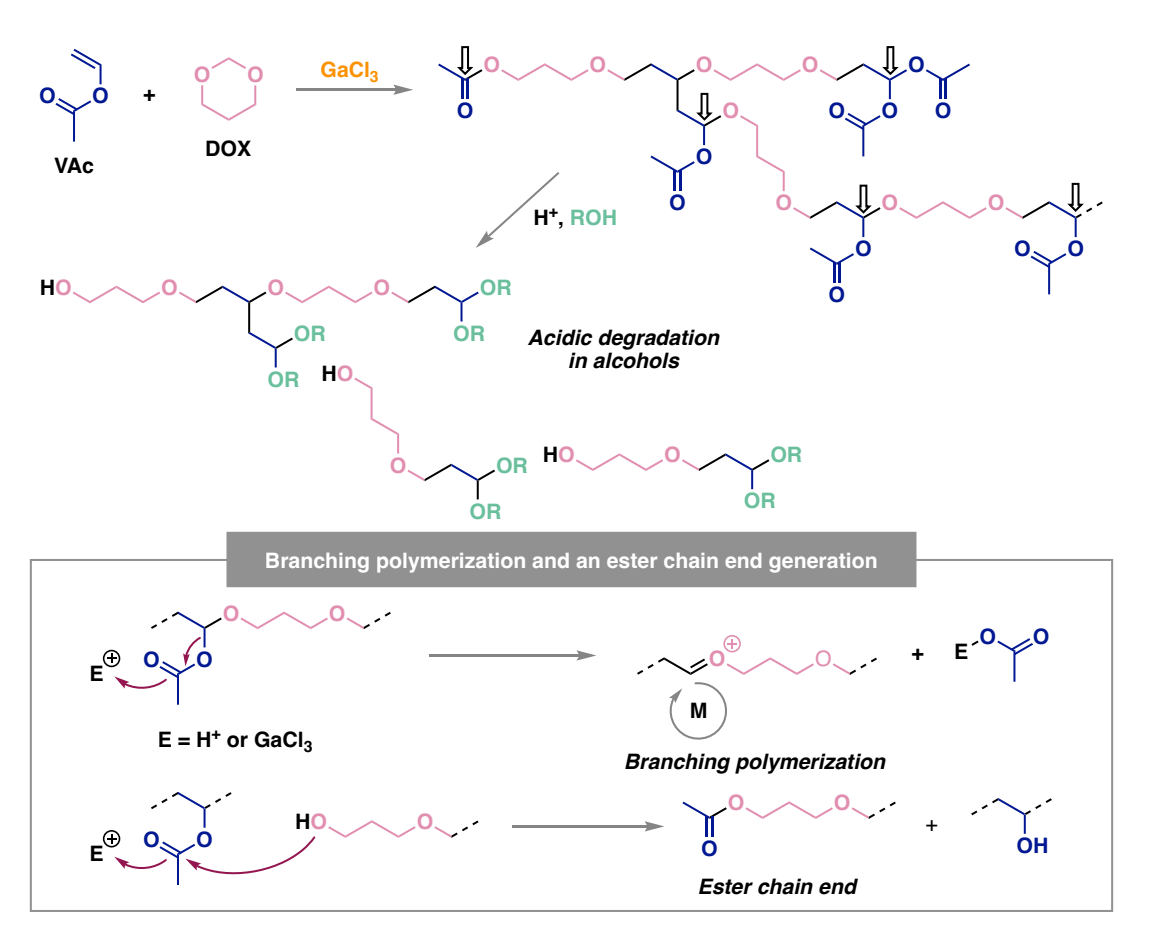


**Fig. 71.** Cationic copolymerization of VAc and 1,3-dioxane (DOX) catalyzed by GaCl<sub>3</sub> and acidic degradation of branched copolymer in alcohols. [174], Copyright 2022. Adapted with permission from American Chemical Society.

In 2023, Kamigaito and coworkers developed the precision synthesis of degradable vinyl copolymers via cationic RAFT copolymerization of vinyl ethers and 2-methyl-1,3-oxathiepane (MOTP) [175]. A moderate molecular weight copolymer poly(EVE-b-MOTP) ( $M_n = 22 \text{ kDa}$ , D = 1.59) was synthesized using ZnCl<sub>2</sub> as a catalyst at -40 °C (**Fig. 72**). When poly(EVE-b-MOTP) was treated by AgNO<sub>3</sub> or p-toluenesulfonic acid, an oligomer with low-molecular weight ( $M_n = 1.59$ ) was synthesized using ZnCl<sub>2</sub> as a catalyst at -40 °C (**Fig. 72**).

2.0 kDa) was obtained. Notably, a unimodal SEC peak and low dispersity (D = 1.3) were observed for the resulting oligomer, implying the even distribution of poly(EVE) segments throughout the pristine copolymer.

$$CI \\ O/Bu \\ CH_2Cl_2/n-Hexanes/Et_2O \\ -40 °C$$

$$CH_2Cl_2/n-Hexanes/Et_2O \\ -40 °C$$

$$CH_2Cl_2/n-Hexan$$

**Fig. 72.** Cationic RAFT copolymerization of EVE and 2-methyl-1,3-oxathiepane (MOTP) catalyzed by ZnCl<sub>2</sub> and acidic degradation of the copolymer. [175], Copyright 2023. Adapted with permission from John Wiley & Sons Inc.

#### 5.2 Polysaccharides and carbohydrate polymers

Polysaccharides are the most abundant class of biopolymers on Earth and play important roles in biology [176], renewable energy [177], and sustainable materials [178]. These polymers are attractive, since the labile functionality within backbones provide a good handle to trigger efficient degradation or depolymerization. Recently, many carbohydrate-derived monomers have been designed to generate (bio)degradable carbohydrate polymers, such as isosorbide [179], xylose [180], isohexide [181], and monosaccharide-derived cyclic carbonates [182] and lactams [183]. However, anionic polymerization or step growth polymerization are usually involved in these examples, preparing degradable polysaccharides and carbohydrate polymers via cationic polymerization have rarely been explored [184,185].

Schlaad and co-workers discovered a degradable polysaccharide mimetic from the cationic polymerization of a cellulose-derived monomer levoglucosenyl methyl ether (Fig. 73) [186]. A

semicrystalline polymer ( $M_n$ = 36 kDa) could be obtained when boron trifluoride etherate was used as an initiator. The double bonds in the polymer backbone provided a good handle for post-polymerization functionalization. For example, addition of methyl 3-mercaptopropionate to the polymer backbone was furnished via a photo-induced thiol-ene reaction. More importantly, because of the inherent acid-lability of acetal group, the resulting polymer could be completely degraded in the presence of BF<sub>3</sub>•Et<sub>2</sub>O and methanol. The facile degradability andversatile reactivity of the double bonds makes this semicrystalline polymer a promising candidate for next-generation functional materials.

**Fig. 73.** Cellulose-derived functional polyacetal from cationic polymerization of levoglucosenyl methyl ether [186].

Inspired by the reversible-deactivation mechanism in living cationic polymerization, we developed a chemical approach to precision polysaccharides with native glycosidic linkages via living cationic ROP of 1,6-anhydrosugars (**Fig. 74**) [187]. A series of well-defined polysaccharides with tunable molecular weight, low dispersity, and excellent regio- and stereoselectivity were prepared using a boron trifluoride etherate catalyst and glycosyl fluoride initiators. The livingness of the polymerization was supported by a series of experiments, including first-order reaction kinetics, linear growth of the molecular weight over conversion, controlled molecular weights proportional to [M]<sub>0</sub>/[I]<sub>0</sub> ratio, and successful chain extension and chain end modification. This methodology also displayed broad monomer scope, *O*-alkylated 1,6-anhydroglucose with various alkyl side chains (Me, Et, "Pr, "Bu, "Pen, allyl), 1,6-anhydromannose, and 1,6-anhydrogalactose all exhibited good reactivities and excellent control over the polymerization. Notably, the synthetic protocol could be readily scaled up, and 1.1 grams of precise polysaccharide was obtained without loss of control. A well-defined α-1,6-D-glucan was prepared after global deprotection, which showed identical <sup>1</sup>H NMR and <sup>13</sup>C NMR spectra to the natural α-1,6-D-glucan. Finally, these precision

polysaccharides also demonstrated excellent chemical recyclability. The quantitative depolymerization was observed at 80 °C in the presence of a catalytic amount of BF<sub>3</sub>•Et<sub>2</sub>O. Additionally, the recovered monomer was repolymerized to give corresponding polymer with an efficiency comparable to the pristine monomer, providing a circular monomer-polymer-monomer life cycle of the precision polysaccharides.

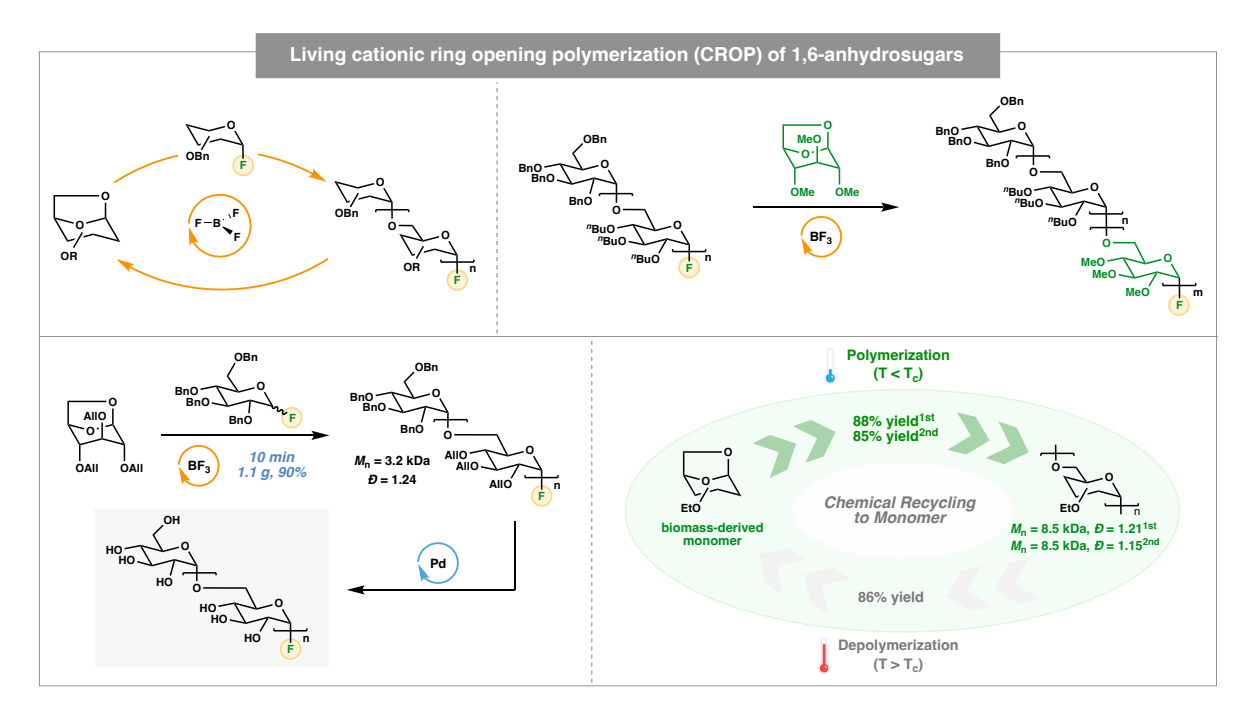


**Fig. 74.** Chemically recyclable polysaccharides from living cationic polymerization of 1,6-anhydrosugars. [187], Copyright 2023. Adapted with permission from Springer Nature Limited.

# 5.3 Polyvinyl ethers and polyethers

Due to the lack of labile functional groups, poly(vinyl ether) and polyethers are usually challenging to be degraded or depolymerized. Despite these challenges, considerable efforts have been made in the degradation/depolymerization of these polymers, which will be highlighted in the following subsection.

In 2022, Fors and co-workers created a strong and tough plastic from the cationic polymerization of DHF (**Fig. 75**) [188]. Using PCCP as an acidic initiator, a high molecular weight poly(DHF) with  $M_n$  of up to 256 kDa could be readily prepared in decagram scale at room temperature. The

high molecular weight sample displayed comparable tensile properties to commodity polycarbonate, with an ultimate tensile strength (UTS) of 70 MPa, a toughness of 14 MPa, and elongation at break of 52%. Moreover, the free-standing films showed excellent transparency with 89% transmittance across visible light (380-700 nm). Furthermore, the gas permeation measurements suggested poly(DHF) attractive for food packing applications, given its moderate gas (e.g. O<sub>2</sub>, CO<sub>2</sub>) and water permeability. More importantly, it was found that poly(DHF) could undergo smooth degradation in the presence of hydrogen peroxide and (NH<sub>4</sub>)<sub>2</sub>Fe(SO<sub>4</sub>)<sub>2</sub>•6H<sub>2</sub>O (known as Fenton's reagent). A reduction in molecular weight from 50 to ~1 kDa over 48 h was observed after treating polymer with Fenton's reagent. The initial mechanistic studies demonstrated that a radical chain scission mechanism was likely involved in this accelerated oxidative degradation process. Therefore, the scalable preparation from biomass-derived monomer, excellent mechanical properties, high optical clarity, low oxygen and water permeability, and facile degradability make this material appealing for sustainable engineering thermoplastic manufacture.

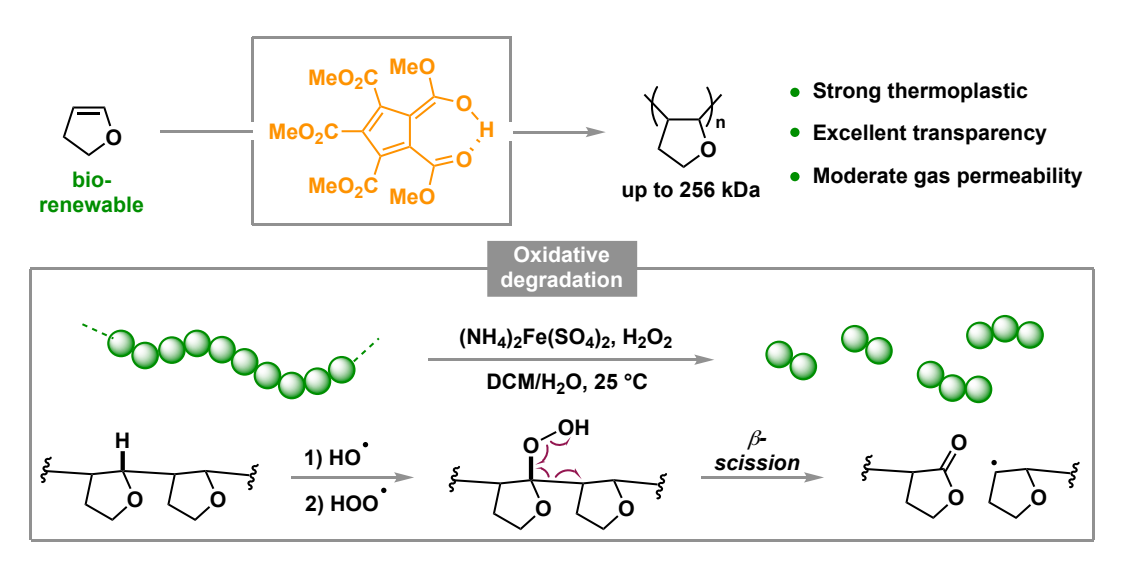


**Fig. 75.** A strong and degradable thermoplastic from living cationic polymerization of DHF. [188], Copyright 2022. Adapted with permission from American Chemical Society.

In their pursuit of preparing 5-substituted benzofuran, Hua and co-workers found an unprecedented monomer-polymer-monomer process of poly(BzF) (**Fig. 76**) [189]. In the presence of 0.2 mol% of TFA in 1,1,1,3,3,3-hexafluoro-2-propanol (HFIP), the cationic polymerization of BzF

proceeded efficiently, generating a poly(BzF) ( $M_n = 36$  kDa) with 99% yield. The complete depolymerization of the polymer was achieved using practical pyrolysis conditions (320 °C, N<sub>2</sub>), and 95% of monomer could be readily recovered in gram scale. More interestingly, they also demonstrated that the poly(BzF) could undergo highly regioselective electrophilic aromatic substitution (S<sub>E</sub>Ar), yielding a variety of functional polymer poly(E-BzF) with electrophiles para to the "alkoxy" group. Additionally, these functional polymers could also be completely depolymerized to engender various 5-substituted benzofuran in a range of yield of 36-91%. According to the DFT calculations, a radical chain scission mechanism was proposed during the depolymerization. Due to the relatively low bond dissociation energy (BDE = 46.2 kcal/mol at 600.0 K), homolytic cleavage of the polymer chain readily occurred to give a pair of radicals. Followed by a facile β-scission pathway, monomer was generated together with another macroradical, which would undergo complete depolymerization in the same manner. Therefore, this novel monomer-polymer-monomer strategy not only served as an efficient approach for functional benzofuran synthesis, but also provided an ideal end-of-life solution for poly(BzF) materials.

**Fig. 76.** A circular monomer-polymer-monomer life cycle of poly(BzF). [189], Copyright 2021. Adapted with permission from John Wiley & Sons Inc.

In 2022, Aoshima and co-workers disclosed an alternating-like cationic copolymerization of styrene derivatives and benzaldehyde (BzA) to create degradable polystyrene materials (**Fig. 77**) [190]. In the presence of GaCl<sub>3</sub> as a catalyst and tetrahydropyran as a base additive, the

copolymerization of pMeSt and BzA proceeded efficiently to generate copolymers with predetermined molecular weight and moderate dispersity. More significantly, the resulting copolymer featured a nearly alternating sequence, which was due to the frequent crossover reaction during the polymerization. Particularly, the pMeSt-derived carbocation favorably reacts with a BzA monomer. On the other hand, the resulting BzA-derived carbocation was exclusively captured by another pMeSt monomer, due to the non-homopolymerizability of BzA. Detailed analysis of the copolymer composition by the Kelen-Tüdõs method suggested that the monomer reactivity ratios were 0.42 and 0 for pMeSt and BzA, respectively. As a result, the labile sec-benzylic ether functionality was incorporated into the polymer main chain evenly, providing a good opportunity for polymer degradation. After treated by TFA (0.5 M) in dichloromethane at room temperature for 3 h, a significant reduction of molecular weight from 15.0 to 0.4 kDa was observed. Furthermore, the authors also demonstrated that the obtained copolymer showed comparable thermal properties to pMeSt homopolymer with a T<sub>g</sub> of 86 °C and a T<sub>d</sub> of 353 °C. Although this method is incompatible with styrene copolymerization, further optimization of the conditions, such as Lewis acid and benzaldehydes screening, might overcome the limitation to generate degradable polystyrene materials.

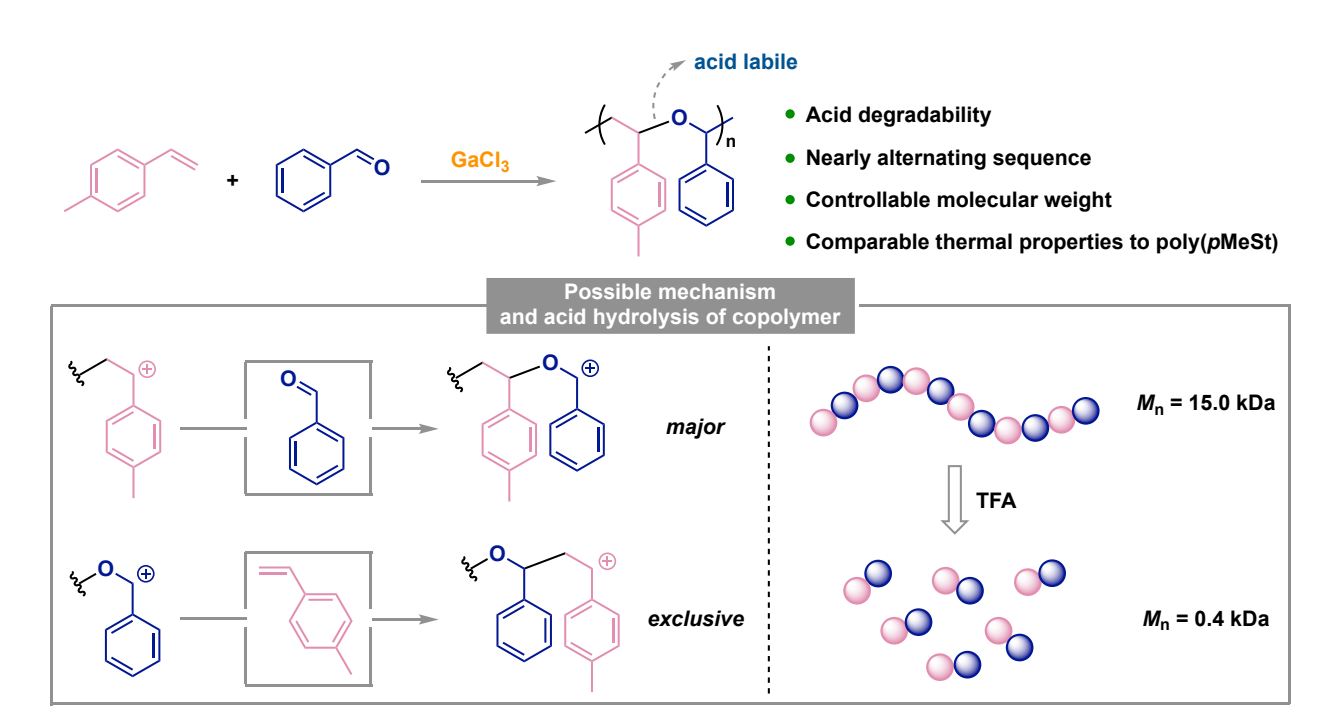


**Fig. 77.** Precise synthesis of degradable copoly(styrene) via cationic copolymerization of styrene derivative and benzaldehyde [190].

### 6. Conclusion and outlook

In this review, representative recent developments of catalysts, initiating methods, control mechanisms, and new monomers are discussed. These advances together have allowed for a dramatic growth of research in cationic polymerization. Unprecedented precision polymeric materials with well-controlled molecular weight, dispersity, chain end group, stereochemistry, and backbone architecture have been generated, with some having already entered commercial production. Many of these materials have also demonstrated new properties that go beyond what can be achieved by traditional synthetic polymers, making them great candidates for emerging applications that gear toward sustainability and biocompatibility. While these successes deserve much celebration, developments in the following aspects could propel cationic polymerization technologies into a new phase that matches the ever-increasing demands for future materials.

Integration of photo- and electro-catalysis. Using photocatalysis and electrocatalysis to initiate and control cationic polymerizations represents a significant advance in the last decades. They enable more efficient and precise control over the polymerization, thanks to the ability to fine-tune the redox potentials to match the reactivities of photo/electrocatalysts, monomers, and CTAs, creating the opportunity for achieving spatiotemporal regulation and surface patterning for advanced material synthesis. The recent works by Fors [71], Yan [91,92], Liao [75], and Read de Alaniz [94] provide inspirations for future developments in this area.

New monomers. While it is likely that petroleum-based monomers will continue playing an important role in developing cationic polymerization techniques in academia and industry, the movements toward sustainable monomers and green chemistry are unstoppable. The renaissance of bio-based monomers such as anhydrosugars [184,185,187] and DHF [188] are a strong testimony of this growing trend. Compared to their petroleum-derived counterparts, bio-based monomers often contain higher fractions of heteroatoms, presenting new challenges as well as opportunities for the development of cationic polymerization techniques. Correspondingly, the development of new catalytic systems in response to the use of bio-based monomers in cationic polymerization will dramatically accelerate.

New control mechanisms and agents. The cationic RAFT polymerization developed by Kamigaito [11] in 2015 has spurred the rapid development of a variety of CTAs capable of mediating cationic reversible deactivation polymerization. This development is concurrent with the developments of new initiating methods and new monomers, creating the possibility to modulate the reaction conditions of cationic polymerization based on monomer reactivity and the demand for spatiotemporal control. Following this trend, control systems that match the reactivities of new monomer classes and can effectively interface with photo- and electro-catalysis would likely become focus of future studies.

Stereochemical control. Seminal contributions by Sawamoto [112], Aoshima [121], Kamigaito [129], Leibfarth [115], Chen [136], and Liao [127] have revealed key insights into the catalyst and monomer design for controlling tacticity in cationic polymerization. Their works also demonstrated the profound impact of tacticity on the properties of the polymers generated from cationic polymerization. Significant progress can be expected in both catalyst-controlled and substrate-controlled stereoselective polymerization. Catalyst-controlled approaches are expected to benefit significantly from the cutting-edge asymmetric catalysis techniques developed in synthetic organic chemistry, with many chiral catalysts and reagents being applied to control stereochemistry during polymerization. Development of substrate-controlled approaches for biobased monomers, e.g., anhydrosugars, will likely require synergies with chemical biology and carbohydrate chemistry.

## **Declaration of Competing Interests**

The authors declare that they have no known competing financial interests or personal relationships that could have appeared to influence the work reported in this paper.

## Acknowledgments

We gratefully acknowledge the support from the CAREER Award from the National Science Foundation (CHE-1944512) to J.N. and the Beckman Young Investigator Award from the Arnold and Mabel Beckman Foundation to J.N.

#### References

- [1] Higashimura T, Kishiro O. Possible Formation of Living Polymers of *p*-Methoxystyrene by Iodine. Macromolecules 1977;9:87–93.
- [2] Miyamoto M, Sawamoto M, Higashimura T. Living Polymerization of Isobutyl Vinyl Ether with the Hydrogen Iodide/Iodine Initiating System. Macromolecules 1984;17:265–8.
- [3] Miyamoto M, Sawamoto M, Higashimura T. Synthesis of Monodisperse Living Poly(vinyl ethers) and Block Copolymers by the Hydrogen Iodide/Iodine Initiating System. Macromolecules 1984;17:2228–30.
- [4] Sawamoto M, Fujimori J, Higashimura T. Living Cationic Polymerization of *N*-Vinylcarbazole Initiated by Hydrogen Iodide. Macromolecules 1987;20:916–20.
- [5] Faust R, Kennedy JP. Living Carbocationic Polymerization III. Demonstration of the Living Polymerization of Isobutylene. Poly Bull 1986;15:317–23.
- [6] Faust R, Kennedy JP. Living carbocationic polymerization. IV. Living polymerization of isobutylene. J Polym Sci A Polym Chem 1987;25:1847–69.
- [7] Sawamoto M. Modern cationic vinyl polymerization. Prog Polym Sci 1991;16:111–72.
- [8] Aoshima S, Kanaoka S. A renaissance in living cationic polymerization. Chem Rev 2009;109:5245–87.
- [9] Kamigaito M, Sawamoto M. Synergistic Advances in Living Cationic and Radical Polymerizations. Macromolecules 2020;53:6749–53.
- [10] Goethals EJ, Du Prez F. Carbocationic polymerizations. Prog Polym Sci 2007;32:220–46.
- [11] Uchiyama M, Satoh K, Kamigaito M. Cationic RAFT and DT polymerization. Prog Polym Sci 2022;124:101485.
- [12] Yagci Y, Jockusch S, Turro NJ. Photoinitiated polymerization: Advances, challenges, and opportunities. Macromolecules 2010;43:6245–60.

- [13] Xiao P, Zhang J, Dumur F, Tehfe MA, Morlet-Savary F, Graff B, Gigmes D, Fouassier JP, Lalevée J. Visible light sensitive photoinitiating systems: Recent progress in cationic and radical photopolymerization reactions under soft conditions. Prog Polym Sci 2015;41:32–66.
- [14] Michaudel Q, Kottisch V, Fors BP. Cationic Polymerization: From Photoinitiation to Photocontrol. Angew Chem Int Ed 2017;56:9670–9.
- [15] Chen Y, Zhang L, Jin Y, Lin X, Chen M. Recent Advances in Living Cationic Polymerization with Emerging Initiation/Controlling Systems. Macromol Rapid Commun 2021;42:2100148.
- [16] Kanazawa A, Kanaoka S, Aoshima S. Recent progress in living cationic polymerization of vinyl ethers. Chem Lett 2010;39:1232–7.
- [17] Kckxetkov NK. Synthesis of polysaccharides with a regular structure. Tetrahedron 1987;43:2389–436.
- [18] Uryu T. Artificial polysaccharides and their biological activities. Prog Polym Sci 1993;18:717–61.
- [19] Sawamoto M, Fujimori ichi, Higashimura T. Living Cationic Polymerization of N-Vinylcarbazole Initiated by Hydrogen Iodide. Macromolecules 1987;20:916–20.
- [20] Grubbs RB, Grubbs RH. 50th Anniversary Perspective: Living Polymerization Emphasizing the Molecule in Macromolecules. Macromolecules 2017;50:6979–97.
- [21] Chiefari J, Chong YK, Ercole F, Krstina J, Jeffery J, Le TPT, Mayadunne RTA, Meijs GF, Moad CL, Moad G, Rizzardo E, Thang SH. Living Free-Radical Polymerization by Reversible Addition-Fragmentation Chain Transfer: The RAFT Process. Macromolecules 1998;31:5559–62.
- [22] Perrier S. 50th Anniversary Perspective: RAFT Polymerization A User Guide. Macromolecules 2017;50:7433–47.
- [23] Uchiyama M, Satoh K, Kamigaito M. Cationic RAFT polymerization using ppm concentrations of organic acid. Angew Chem Int Ed 2015;54:1924–8.
- [24] Uchiyama M, Satoh K, Kamigaito M. Thioether-Mediated Degenerative Chain-Transfer Cationic Polymerization: A Simple Metal-Free System for Living Cationic Polymerization. Macromolecules 2015;48:5533–42.

- [25] Uchiyama M, Sakaguchi M, Satoh K, Kamigaito M. A User-friendly Living Cationic Polymerization: Degenerative Chain-transfer Polymerization of Vinyl Ethers by Simply Using Mixtures of Weak and Superstrong Protonic Acids. Chinese J Polym Sci 2019;37:851–7.
- [26] Boeck PT, Tanaka J, Liu S, You W. Importance of Nucleophilicity of Chain-Transfer Agents for Controlled Cationic Degenerative Chain-Transfer Polymerization.

  Macromolecules 2020;53:4303–11.
- [27] Uchiyama M, Satoh K, Kamigaito M. A phosphonium intermediate for cationic RAFT polymerization. Polym Chem 2016;7:1387–96.
- [28] Müller AE, Zhuang R, Yan D, Litvinenko G. Kinetic Analysis of "Living" Polymerization Processes Exhibiting Slow Equilibria. 1. Degenerative Transfer (Direct Activity Exchange between Active and "Dormant" Species). Application to Group Transfer Polymerization. vol. 28. 1995. Macromolecules 1995;28:4326–33.
- [29] Kricheldorf HR, Dunsing R. Mechanism of the cationic polymeriztion of L,L-dilactide. Makromol Chem 1986;187:1611–25.
- [30] Kricheldorf HR, Kreker I. Cationic copolymerization of glycolide with L,L-dilactide. Makromol Chem 1987;188:1861–73.
- [31] Kiesewetter MK, Shin EJ, Hedrick JL, Waymouth RM. Organocatalysis: Opportunities and challenges for polymer synthesis. Macromolecules 2010;43:2093–107.
- [32] Kamber NE, Jeong W, Waymouth RM, Pratt RC, Lohmeijer BGG, Hedrick JL. Organocatalytic ring-opening polymerization. Chem Rev 2007;107:5813–40.
- [33] Shibasaki Y, Sanada H, Yokoi M, Sanda F, Endo T. Activated monomer cationic polymerization of lactones and the application to well-defined block copolymer synthesis with seven-membered cyclic carbonate. Macromolecules 2000;33:4316–20.
- [34] Bourissou D, Martin-Vaca B, Dumitrescu A, Graullier M, Lacombe F. Controlled cationic polymerization of lactide. Macromolecules 2005;38:9993–8.
- [35] Kakuchi R, Tsuji Y, Chiba K, Fuchise K, Sakai R, Satoh T, Kakuchi T. Controlled/living ring-opening polymerization of δ-valerolactone using triflylimide as an efficient cationic organocatalyst. Macromolecules 2010;43:7090–4.

- [36] Gazeau-Bureau S, Delcroix D, Martín-Vaca B, Bourissou D, Navarro C, Magnet S. Organo-catalyzed ROP of ε-caprolactone: Methanesulfonic acid competes with trifluoromethanesulfonic acid. Macromolecules 2008;41:3782–4.
- [37] Oledzka E, Narine SS. Organic acids catalyzed polymerization of ε-caprolactone: Synthesis and characterization. J Appl Polym Sci 2011;119:1873–82.
- [38] Grondal C, Jeanty M, Enders D. Organocatalytic cascade reactions as a new tool in total synthesis. Nat Chem 2010;2:167–78.
- [39] Qin Y, Zhu L, Luo S. Organocatalysis in Inert C-H Bond Functionalization. Chem Rev 2017;117:9433–520.
- [40] van der Helm MP, Klemm B, Eelkema R. Organocatalysis in aqueous media. Nat Rev Chem 2019;3:491–508.
- [41] Makiguchi K, Ogasawara Y, Kikuchi S, Satoh T, Kakuchi T. Diphenyl phosphate as an efficient acidic organocatalyst for controlled/living ring-opening polymerization of trimethylene carbonates leading to block, end-functionalized, and macrocyclic polycarbonates. Macromolecules 2013;46:1772–82.
- [42] Kan S, Jin Y, He X, Chen J, Wu H, Ouyang P, Guo K, Li Z. Imidodiphosphoric acid as a bifunctional catalyst for the controlled ring-opening polymerization of δ-valerolactone and ε-caprolactone. Polym Chem 2013;4:5432–9.
- [43] Liu J, Zhang C, Li Z, Zhang L, Xu J, Wang H, Xu S, Guo T, Yang K, Guo K. Dibutyl phosphate catalyzed commercial relevant ring-opening polymerizations to bio-based polyesters. Eur Polym J 2019;113:197–207.
- [44] Adoumaz I, Boutriouia EH, Beniazza R, Qayouh H, El Kadib A, Khoukh A, Save M, Lahcini M. Phosphorus pentoxide as a cost-effective, metal-free catalyst for ring opening polymerization of ε-caprolactone. RSC Adv 2020;10:23498–502.
- [45] Zhang X, Jiang Y, Ma Q, Hu S, Wang Q, Liao S. Imidodiphosphorimidate (IDPi) as an efficient organocatalyst for controlled/living ring-opening polymerization of lactones. Eur Polym J 2020;123:109449.
- [46] Delcroix D, Couffin A, Susperregui N, Navarro C, Maron L, Martin-Vaca B, Bourissou D. Phosphoric and phosphoramidic acids as bifunctional catalysts for the ring-opening polymerization of ε-caprolactone: A combined experimental and theoretical study. Polym Chem 2011;2:2249–56.

- [47] Siu PW, Hazin K, Gates DP. H(OEt<sub>2</sub>)<sub>2</sub>[P(1,2-O<sub>2</sub>C<sub>6</sub>Cl<sub>4</sub>)<sub>3</sub>]: Synthesis, characterization, and application as a single-component initiator for the carbocationic polymerization of olefins. Chem Eur J 2013;19:9005–14.
- [48] Song J, Xu J, Tang D. Rapid living cationic polymerization of vinyl ethers by a single-molecular initiating system. J Polym Sci A Polym Chem 2016;54:1373–7.
- [49] Kottisch V, O'Leary J, Michaudel Q, Stache EE, Lambert TH, Fors BP. Controlled Cationic Polymerization: Single-Component Initiation under Ambient Conditions. J Am Chem Soc 2019;141:10605–9.
- [50] Gheewala CD, Collins BE, Lambert TH. An aromatic ion platform for enantioselective Brønsted acid catalysis. Science 2016;351:961–5.
- [51] Kottisch V, Jermaks J, Mak JY, Woltornist RA, Lambert TH, Fors BP. Hydrogen Bond Donor Catalyzed Cationic Polymerization of Vinyl Ethers. Angew Chem Int Ed 2021;60:4535–9.
- [52] Shankel SL, Lambert TH, Fors BP. Moisture tolerant cationic RAFT polymerization of vinyl ethers. Polym Chem 2022;13:5974–9.
- [53] Li M, Zhang Z, Yan Y, Lv W, Li Z, Wang X, Tao Y. Anion-binding catalysis enables living cationic polymerization. Nature Synthesis 2022;1:815–23.
- [54] Xu Y, Wang L, Chen C, Huang P, Dai H, Jiang W, Zhou Y. Living Cationic Polymerization of ε-Caprolactone Catalyzed by a Metal-free Lewis Acid of Trityl Tetrafluoroborate. Macromolecules 2023;56:501-9.
- [55] Yan X, Zhang S, Zhang P, Wu X, Liu A, Guo G, Dong Y, Li X. [Ph<sub>3</sub>C][B(C<sub>6</sub>F<sub>5</sub>)<sub>4</sub>]: A Highly Efficient Metal-Free Single-Component Initiator for the Helical-Sense-Selective Cationic Copolymerization of Chiral Aryl Isocyanides and Achiral Aryl Isocyanides. Angew Chem Int Ed 2018;57:8947–52.
- [56] Bulfield D, Huber SM. Halogen Bonding in Organic Synthesis and Organocatalysis. Chem Eur J 2016;22:14434–50.
- [57] Vogel L, Wonner P, Huber SM. Chalcogen Bonding: An Overview. Angew Chem Int Ed 2019;58:1880–91.
- [58] Takagi K, Yamauchi K, Murakata H. Halogen-Bonding-Mediated and Controlled Cationic Polymerization of Isobutyl Vinyl Ether: Expanding the Catalytic Scope of 2-Iodoimidazolium Salts. Chem Eur J 2017;23:9495–500.

- [59] Takagi K, Murakata H, Yamauchi K, Hashimoto K. Cationic polymerization of vinyl monomers using halogen bonding organocatalysts with varied activity. Polym Chem 2020;11:6739–44.
- [60] Takagi K, Okamura K. Cationic polymerization of n-hexyloxyallene by using halogen-bonding organocatalysts. J Polym Sci A Polym Chem 2019;57:2436–41.
- [61] Haraguchi R, Nishikawa T, Kanazawa A, Aoshima S. Metal-Free Living Cationic Polymerization Using Diaryliodonium Salts as Organic Lewis Acid Catalysts. Macromolecules 2020;53:4185–92.
- [62] Takagi K, Sakakibara N, Hasegawa T, Hayashi S. Controlled/Living Cationic Polymerization of p-Methoxystyrene Using Tellurium-Based Chalcogen Bonding Catalyst-Discovery of a New Water-Tolerant Lewis Acid Catalyst. Macromolecules 2022;55:3671.
- [63] Leibfarth FA, Mattson KM, Fors BP, Collins HA, Hawker CJ. External regulation of controlled polymerizations. Angew Chem Int Ed 2013;52:199–210.
- [64] Sifri RJ, Ma Y, Fors BP. Photoredox Catalysis in Photocontrolled Cationic Polymerizations of Vinyl Ethers. Acc Chem Res 2022;55:1960–71.
- [65] Crivello JV, Lam JHW. Diaryliodonium salts. A new class of photoinitiators for cationic polymerization. Macromolecules 1977;10:1307–15.
- [66] Crivello J V. The discovery and development of onium salt cationic photoinitiators. J Polym Sci A Polym Chem 1999;37:4241–54.
- [67] Dadashi-Silab S, Doran S, Yagci Y. Photoinduced Electron Transfer Reactions for Macromolecular Syntheses. Chem Rev 2016;116:10212–75.
- [68] Kahveci MU, Yagci Y. Photoinitiated cationic polymerization of vinyl ethers using substituted vinyl halides in the presence of metallic zinc. Macromolecules 2011;44:5569–72.
- [69] Ciftci M, Yoshikawa Y, Yagci Y. Living Cationic Polymerization of Vinyl Ethers through a Photoinduced Radical Oxidation/Addition/Deactivation Sequence. Angew Chem Int Ed 2017;56:519–23.
- [70] Prier CK, Rankic DA, MacMillan DWC. Visible light photoredox catalysis with transition metal complexes: Applications in organic synthesis. Chem Rev 2013;113:5322–63.
- [71] Kottisch V, Michaudel Q, Fors BP. Cationic Polymerization of Vinyl Ethers Controlled by Visible Light. J Am Chem Soc 2016;138:15535–8.

- [72] Michaudel Q, Chauviré T, Kottisch V, Supej MJ, Stawiasz KJ, Shen L, Zipfel WR, Abruña HD, Freed JH, Fors BP. Mechanistic Insight into the Photocontrolled Cationic Polymerization of Vinyl Ethers. J Am Chem Soc 2017;139:15530–8.
- [73] Sifri RJ, Kennedy AJ, Fors BP. Photocontrolled cationic degenerate chain transfer polymerizations: Via thioacetal initiators. Polym Chem 2020;11:6499–504.
- [74] Ma Y, Kottisch V, McLoughlin EA, Rouse ZW, Supej MJ, Baker SP, Fors BP. Photoswitching Cationic and Radical Polymerizations: Spatiotemporal Control of Thermoset Properties. J Am Chem Soc 2021;143:21200–5.
- [75] Zhang X, Jiang Y, Ma Q, Hu S, Liao S. Metal-Free Cationic Polymerization of Vinyl Ethers with Strict Temporal Control by Employing an Organophotocatalyst. J Am Chem Soc 2021;143:6357–62.
- [76] Chen J, Lin J, Yang Z, Wu Y, Liao S. The development of highly efficient monophosphonium photocatalysts for the visible light-regulated metal-free cationic polymerization of vinyl ethers. Polym Chem 2022.
- [77] Matsuda M, Uchiyama M, Itabashi Y, Ohkubo K, Kamigaito M. Acridinium salts as photoredox organocatalysts for photomediated cationic RAFT and DT polymerizations of vinyl ethers. Polym Chem 2022;13:1031–9.
- [78] Perkowski AJ, You W, Nicewicz DA. Visible Light Photoinitiated Metal-Free Living Cationic Polymerization of 4-Methoxystyrene. J Am Chem Soc 2015;137:7580–3.
- [79] Messina MS, Axtell JC, Wang Y, Chong P, Wixtrom AI, Kirlikovali KO, Upton BM, Hunter BM, Shafaat OS, Khan SI, Winkler JR, Gray HB, Alexandrova AN, Maynard HD, Spokoyny AM. Visible-Light-Induced Olefin Activation Using 3D Aromatic Boron-Rich Cluster Photooxidants. J Am Chem Soc 2016;138:6952–5.
- [80] Wang L, Xu Y, Zuo Q, Dai H, Huang L, Zhang M, Zheng Y, Yu C, Zhang S, Zhou Y. Visible light-controlled living cationic polymerization of methoxystyrene. Nat Commun 2022;13:3621.
- [81] Tang X, Chen EYX. Toward Infinitely Recyclable Plastics Derived from Renewable Cyclic Esters. Chem 2019;5:284–312.
- [82] Barker IA, Dove AP. Triarylsulfonium hexafluorophosphate salts as photoactivated acidic catalysts for ring-opening polymerisation. Chem Commun 2013;49:1205–7.

- [83] Xia L, Zhang Z, You YZ. Visible light-induced living/controlled cationic ring-opening polymerization of lactones. Polym J 2020;52:1323–31.
- [84] Zhang X, Ma Q, Jiang Y, Hu S, Li J, Liao S. Visible light-regulated organocatalytic ring-opening polymerization of lactones by harnessing excited state acidity. Polym Chem 2021;12:885–92.
- [85] Fu C, Xu J, Boyer C. Photoacid-mediated ring opening polymerization driven by visible light. Chem Commun 2016;52:7126–9.
- [86] Yan M, Kawamata Y, Baran PS. Synthetic Organic Electrochemical Methods since 2000: On the Verge of a Renaissance. Chem Rev 2017;117:13230–319.
- [87] Magenau AJD, Strandwitz NC, Gennaro A, Matyjaszewski K. Electrochemically Mediated Atom Transfer Radical Polymerization. Science 2011;332:81–4.
- [88] Sang W, Xu M, Yan Q. Coenzyme-Catalyzed Electro-RAFT Polymerization. ACS Macro Lett 2017;6:1337–41.
- [89] Qi M, Dong Q, Wang D, Byers JA. Electrochemically Switchable Ring-Opening Polymerization of Lactide and Cyclohexene Oxide. J Am Chem Soc 2018;140:5686–90.
- [90] Peterson BM, Lin S, Fors BP. Electrochemically Controlled Cationic Polymerization of Vinyl Ethers. J Am Chem Soc 2018;140:2076–9.
- [91] Sang W, Yan Q. Electro-Controlled Living Cationic Polymerization. Angew Chem Int Ed 2018;57:4907–11.
- [92] Zhu J, Hao X, Yan Q. Electro-selective interconversion of living cationic and radical polymerizations. Sci China Chem 2019;62:1023–9.
- [93] Supej MJ, Peterson BM, Fors BP. Dual Stimuli Switching: Interconverting Cationic and Radical Polymerizations with Electricity and Light. Chem 2020;6:1794–803.
- [94] Nikolaev A, Lu Z, Chakraborty A, Sepunaru L, De Alaniz JR. Interconvertible Living Radical and Cationic Polymerization using a Dual Photoelectrochemical Catalyst. J Am Chem Soc 2021;143:12278–85.
- [95] Supej MJ, McLoughlin EA, Hsu JH, Fors BP. Reversible redox controlled acids for cationic ring-opening polymerization. Chem Sci 2021;12:10544–9.
- [96] Worch JC, Prydderch H, Jimaja S, Bexis P, Becker ML, Dove AP. Stereochemical enhancement of polymer properties. Nat Rev Chem 2019;3:514–35.

- [97] Busico V. Giulio Natta and the development of stereoselective propene polymerization. In: Kaminsky W, editor. Polyolefins: 50 years after Ziegler and Natta I. Berlin: Springer, 2013. pp. pp 37–57.
- [98] De Rosa C, Auriemma F. Structure and physical properties of syndiotactic polypropylene: A highly crystalline thermoplastic elastomer. Prog Polym Sci 2006;31:145–237.
- [99] Okamoto Y, Nakano T. Asymmetric Polymerization. Chem Rev 1994;94:349–72.
- [100] Teator AJ, Varner TP, Knutson PC, Sorensen CC, Leibfarth FA. 100th Anniversary of Macromolecular Science Viewpoint: The Past, Present, and Future of Stereocontrolled Vinyl Polymerization. ACS Macro Lett 2020;9:1638–54.
- [101] Baskaran D, Müller AHE. Anionic vinyl polymerization-50 years after Michael Szwarc. Prog Polym Sci 2007;32:173–219.
- [102] Coates GW. Precise control of polyolefin stereochemistry using single-site metal catalysts. Chem Rev 2000;100:1223–52.
- [103] Chen EYX. Coordination polymerization of polar vinyl monomers by single-site metal catalysts. Chem Rev 2009;109:5157–214.
- [104] Chen C. Designing catalysts for olefin polymerization and copolymerization: beyond electronic and steric tuning. Nat Rev Chem 2018;2:6–14.
- [105] Sorensen CC, Kozuszek CT, Borden MA, Leibfarth FA. Asymmetric Ion-Pairing in Stereoselective Vinyl Polymerization. ACS Catal 2023;13:3272–84.
- [106] Schildknecht CE, Zoss AO, Mckinley C. Vinyl Alkyl Ethers. Ind Eng Chem 1947;39: 180-6.
- [107] Schildknecht CE, Gross ST, Davidson HR, Lambert JM, Zoss AO. Polyvinyl Isobutyl Ethers. Ind Eng Chem 1948;40:2104–15.
- [108] Lal J. Polymerization of vinyl ethers by Ziegler catalysts. J Polym Sci 1958;31:179–81.
- [109] Vandenberg EJ, Heck RF, Breslow DS. Crystalline vinyl ether polymers. J Polym Sci 1959;41:519–20.
- [110] Kawaguchi T, Sanda F, Masuda T. Polymerization of vinyl ethers with transition-metal catalysts: An examination of the stereoregularity of the formed polymers. J Polym Sci A Polym Chem 2002;40:3938–43.

- [111] Kanazawa A, Kanaoka S, Aoshima S. A stepping stone to stereospecific living cationic polymerization: Cationic polymerization of vinyl ethers using iron(II) sulfate. J Polym Sci A Polym Chem 2010;48:3702–8.
- [112] Ouchi M, Kamigaito M, Sawamoto M. Stereoregulation in cationic polymerization by designed Lewis acids. 1. Highly isotactic poly(isobutyl vinyl ether) with titanium-based Lewis acids. Macromolecules 1999;32:6407–11.
- [113] Ouchi M, Kamigaito M, Sawamoto M. Stereoregulation in cationic polymerization by designed Lewis acids. II. Effects of alkyl vinyl ether structure. J Polym Sci A Polym Chem 2001;39:1060–6.
- [114] Ouchi M, Sueoka M, Kamigaito M, Sawamoto M. Stereoregulation in cationic polymerization. III. High isospecificity with the bulky phosphoric acid [(RO)<sub>2</sub>PO<sub>2</sub>H]/SnCl<sub>4</sub> initiating systems: Design of counteranions via initiators. J Polym Sci A Polym Chem 2001;39:1067–74.
- [115] Teator AJ, Leibfarth FA. Catalyst-controlled stereoselective cationic polymerization of vinyl ethers. Science 2019;363:1439–43.
- [116] Teator AJ, Varner TP, Jacky PE, Sheyko KA, Leibfarth FA. Polar Thermoplastics with Tunable Physical Properties Enabled by the Stereoselective Copolymerization of Vinyl Ethers. ACS Macro Lett 2019;8:1559–63.
- [117] Leibfarth FA, Varner TP, Teator AJ, Reddi Y, Jacky PE, Cramer CJ. Mechanistic insight into the stereoselective cationic polymerization of vinyl ethers. J Am Chem Soc 2020;142:17175–86.
- [118] Kigoshi S, Kanazawa A, Kanaoka S, Aoshima S. Tetradentate schiff base ligand/MCl<sub>n</sub> initiating systems for the controlled cationic polymerization of isobutyl vinyl ether: Effects of the ligand framework. J Polym Sci A Polym Chem 2019;57:989–96.
- [119] Kigoshi S, Kanazawa A, Kanaoka S, Aoshima S. In situ and readily prepared metal catalysts and initiators for living cationic polymerization of isobutyl vinyl ether: Dual-purpose salphen as a ligand framework for ZrCl<sub>4</sub> and an initiating proton source. Polym Chem 2015;6:30–4.
- [120] Kigoshi S, Kanazawa A, Kanaoka S, Aoshima S. Structure–property relationship of phenoxyimine ligands/metal chloride initiating systems for controlled cationic polymerizations of alkyl vinyl ethers. J Polym Sci A Polym Chem 2019;57:2021–9.

- [121] Watanabe H, Yamamoto T, Kanazawa A, Aoshima S. Stereoselective cationic polymerization of vinyl ethers by easily and finely tunable titanium complexes prepared from tartrate-derived diols: Isospecific polymerization and recognition of chiral side chains. Polym Chem 2020;11:3398–403.
- [122] Yang Z, Zhang X, Jiang Y, Ma Q, Liao S. Organocatalytic stereoselective cationic polymerization of vinyl ethers by employing a confined brønsted acid as the catalyst. Sci China Chem 2022;65:304–8.
- [123] Oishi M, Yamamoto H. Polymerization of t-Butyl Vinyl Ether Mediated by an Aluminum Lewis Acid-TrF System and Its Complex Structure-Tacticity Correlation Cationic Polymerization. Bull Chem Soc Jpn 2001;74,1–10.
- [124] Sudhakar P, Vijayakrishna K. Polymerization of vinyl ethers using titanium catalysts containing tridentate triamine ligand of the type N[CH<sub>2</sub>CH(Ph)(Ts)N]<sub>2</sub><sup>2</sup>. Polymer 2009;50:783–8.
- [125] Sudhakar P, Vijayakrishna K. Highly stereoselective living polymerization of vinyl ethers at ambient temperature mediated by chiral titanium complexes. ChemCatChem 2010;2:649–52.
- [126] Knutson PC, Teator AJ, Varner TP, Kozuszek CT, Jacky PE, Leibfarth FA. Brønsted Acid Catalyzed Stereoselective Polymerization of Vinyl Ethers. J Am Chem Soc 2021;143:16388–93.
- [127] Zhang X, Yang Z, Jiang Y, Liao S. Organocatalytic, Stereoselective, Cationic Reversible Addition–Fragmentation Chain-Transfer Polymerization of Vinyl Ethers. J Am Chem Soc 2022;144:679–84.
- [128] Uchiyama M, Satoh K, Kamigaito M. Stereospecific cationic RAFT polymerization of bulky vinyl ethers and stereoblock poly(vinyl alcohol) via mechanistic transformation to radical RAFT polymerization of vinyl acetate. Giant 2021;5:100047.
- [129] Uchiyama M, Watanabe D, Tanaka Y, Satoh K, Kamigaito M. Asymmetric Cationic Polymerization of Benzofuran through a Reversible Chain-Transfer Mechanism: Optically Active Polybenzofuran with Controlled Molecular Weights. J Am Chem Soc 2022;144:10429–37.
- [130] Natta G, Farina M, Peraldo M, Bressan G. Asymmetric Synthesis of Optically Active Diisotactic Polymers from Cyclic Monomers. Makromol Chem 1961;43:68–75.

- [131] Terrell DR, Evers F. Stereocontrol in the Cationic Polymerization of N-Vinylcarbazole. J Polym Sci Polym Chem Ed 1982;20:2529–43.
- [132] Watanabe H, Kanazawa A, Aoshima S. Stereospecific Living Cationic Polymerization of N-Vinylcarbazole through the Design of ZnCl<sub>2</sub>-Derived Counteranions. ACS Macro Lett 2017;6:463–7.
- [133] Watanabe H, Kanazawa A, Okumoto S, Aoshima S. Role of the Counteranion in the Stereospecific Living Cationic Polymerization of N-Vinylcarbazole and Vinyl Ethers: Mechanistic Investigation and Synthesis of Stereo-Designed Polymers. Macromolecules 2022;55:4378–88.
- [134] Sorensen CC, Leibfarth FA. Stereoselective Helix-Sense-Selective Cationic Polymerization of N-Vinylcarbazole Using Chiral Lewis Acid Catalysis. J Am Chem Soc 2022;144:8487– 92.
- [135] Banerjee S, Paira TK, Mandal TK. Control of molecular weight and tacticity in stereospecific living cationic polymerization of α-methylstyrene at 0 °C using FeCl<sub>3</sub>-based initiators: Effect of tacticity on thermal properties. Macromol Chem Phys 2013;214:1332–44.
- [136] Miyake GM, DiRocco DA, Liu Q, Oberg KM, Bayram E, Finke RG, Rovis T, Chen EYX. Stereospecific polymerization of chiral oxazolidinone-functionalized alkenes. Macromolecules 2010;43:7504–14.
- [137] Geyer R, Jambeck JR, Law KL. Production, use, and fate of all plastics ever made. Sci Adv 2017;3:e170078.
- [138] Borrelle SB, Ringma J, Law KL, Monnahan CC, Lebreton L, Mcgivern A, Murphy E, Jambeck J, Leonard GH, Hilleary MA, Eriksen M, Possingham HP, De Frond H, Gerber LR, Polidoro B, Tahir A, Bernard M, Mallos N, Barnes M, Rochman CM. Predicted growth in plastic waste exceeds efforts to mitigate plastic pollution. Science 2020;369: 1515–8.
- [139] Shi C, Reilly LT, Phani Kumar VS, Coile MW, Nicholson SR, Broadbelt LJ, Beckham GT, Chen EYX. Design principles for intrinsically circular polymers with tunable properties. Chem 2021;7:2896–912.
- [140] Coates GW, Getzler YDYL. Chemical recycling to monomer for an ideal, circular polymer economy. Nat Rev Mater 2020;5:501–16.

- [141] Rahimi AR, Garciá JM. Chemical recycling of waste plastics for new materials production. Nat Rev Chem 2017;1:0046.
- [142] Hong M, Chen EYX. Chemically recyclable polymers: A circular economy approach to sustainability. Green Chemistry 2017;19:3692–706.
- [143] Worch JC, Dove AP. 100th Anniversary of Macromolecular Science Viewpoint: Toward Catalytic Chemical Recycling of Waste (and Future) Plastics. ACS Macro Lett 2020;9:1494–506.
- [144] Kaitz JA, Lee OP, Moore JS. Depolymerizable polymers: Preparation, applications, and future outlook. MRS Commun 2015;5:191–204.
- [145] Schneiderman DK, Hillmyer MA. 50th Anniversary Perspective: There Is a Great Future in Sustainable Polymers. Macromolecules 2017;50:3733–49.
- [146] Zhang X, Fevre M, Jones GO, Waymouth RM. Catalysis as an Enabling Science for Sustainable Polymers. Chem Rev 2018;118:839–85.
- [147] Fagnani DE, Tami JL, Copley G, Clemons MN, Getzler YDYL, McNeil AJ. 100th Anniversary of Macromolecular Science Viewpoint: Redefining Sustainable Polymers. ACS Macro Lett 2021;10:41–53.
- [148] Nishida T, Satoh K, Tamura M, Li Y, Tomishige K, Kamigaito M. Model and Terpenoid-Derived *exo*-Methylene Six-Membered Conjugated Dienes: Comprehensive Studies on Cationic and Radical Polymerizations of Substituted 3-Methylenecyclohexenes. Macromolecules 2022;55:2300–9.
- [149] Nishida T, Satoh K, Nagano S, Seki T, Tamura M, Li Y, Tomishige K, Kamigaito M. Biobased cycloolefin polymers: Carvone-derived cyclic conjugated diene with reactive *exo*-methylene group for regioselective and stereospecific living cationic polymerization. ACS Macro Lett 2020;9:1178–83.
- [150] Takeshima H, Satoh K, Kamigaito M. R-Cl/SnCl<sub>4</sub>/*n*-Bu<sub>4</sub>NCl-induced direct living cationic polymerization of naturally-derived unprotected 4-vinylphenol, 4-vinylguaiacol, and 4-vinylcatechol in CH<sub>3</sub>CN. Polym Chem 2019;10:1192–201.
- [151] Nishida T, Satoh K, Tamura M, Li Y, Tomishige K, Caillol S, Ladmiral V, Vayer M, Mahut F, Sinturel C, Kamigaito M. Terpenoid-derived conjugated dienes with: *exo*-methylene and a 6-membered ring: High cationic reactivity, regioselective living cationic

- polymerization, and random and block copolymerization with vinyl ethers. Polym Chem 2021;12:1186–98.
- [152] Hufendiek A, Lingier S, Du Prez FE. Thermoplastic polyacetals: Chemistry from the past for a sustainable future? Polym Chem 2019;10:9–33.
- [153] Aso C, Tagami S. Polymerization of Aromatic Aldehydes. III. The Cyclopolymerization of Phthaldehyde and the Structure of the Polymer. Macromolecules 1969;2:414–9.
- [154] Aso C, Tagami S, Kunitake T. Polymerization of aromatic aldehydes. II. Cationic cyclopolymerization of phthalaldehyde. J Polym Sci A Polym Chem 1969;7:497–511.
- [155] Tsuda M, Hata M, Nishida R, Oikawa S. Acid-Catalyzed Degradation Mechanism of Poly(phthalaldehyde): Unzipping Reaction of Chemical Amplification Resist. J Polym Sci A Polym Chem. 1997;35:77–89.
- [156] Ito H, Willson CG. Chemical amplification in the design of dry developing resist materials. Polym Eng Sci 1983;23:1012–8.
- [157] Knoll AW, Pires D, Coulembier O, Dubois P, Hedrick JL, Frommer J, Duerig U. Probebased 3-D nanolithography using self-amplified depolymerization polymers. Adv Mater 2010;22:3361–5.
- [158] Köstler S, Zechner B, Trathnigc B, Fasl H, Kern W, Ribitsch V. Amphiphilic block copolymers containing thermally degradable poly(phthalaldehyde) blocks. J Polym Sci A Polym Chem 2009;47:1499–509.
- [159] Kaitz JA, Diesendruck CE, Moore JS. End group characterization of poly(phthalaldehyde): Surprising discovery of a reversible, cationic macrocyclization mechanism. J Am Chem Soc 2013;135:12755–61.
- [160] Lloyd EM, Lopez Hernandez H, Feinberg AM, Yourdkhani M, Zen EK, Mejia EB, Sottos NR, Moore JS, White SR. Fully Recyclable Metastable Polymers and Composites. Chem Mater 2019;31:398–406.
- [161] Lutz JP, Davydovich O, Hannigan MD, Moore JS, Zimmerman PM, McNeil AJ. Functionalized and Degradable Polyphthalaldehyde Derivatives. J Am Chem Soc 2019;141:14544–8.
- [162] Feinberg AM, Hernandez HL, Plantz CL, Mejia EB, Sottos NR, White SR, Moore JS. Cyclic Poly(phthalaldehyde): Thermoforming a Bulk Transient Material. ACS Macro Lett 2018;7:47–52.

- [163] Gresham WF. Preparation of polydioxolane. US Patent: 2394910. 1946.
- [164] Qiu H, Yang Z, Köhler M, Ling J, Schacher FH. Synthesis and Solution Self-Assembly of Poly(1,3-dioxolane). Macromolecules 2019;52:3359–66.
- [165] Abel BA, Snyder RL, Coates GW. Chemically recyclable thermoplastics from reversible-deactivation polymerization of cyclic acetals. Science 2021;373:783-9.
- [166] Hester HG, Abel BA, Coates GW. Ultra-High-Molecular-Weight Poly(Dioxolane): Enhancing the Mechanical Performance of a Chemically Recyclable Polymer. J Am Chem Soc 2023;145:8800–4.
- [167] Hayashi K, Kanazawa A, Aoshima S. Exceptional copolymerizability of o-phthalaldehyde in cationic copolymerization with vinyl monomers. Polym Chem 2019;10:3712–7.
- [168] Hayashi K, Kanazawa A, Aoshima S. Living and Alternating Cationic Copolymerization of o-Phthalaldehyde and Various Bulky Enol Ethers: Elucidation of the "Limit" of Polymerizable Monomers. Macromolecules 2022;55:1365–75.
- [169] Hayashi K, Kanazawa A, Aoshima S. Cationic Copolymerization of o-Phthalaldehyde and Vinyl Monomers with Various Substituents on the Vinyl Group or in the Pendant: Effects of the Structure and Reactivity of Vinyl Monomers on Copolymerization Behavior. Macromolecules 2022;55:3276–86.
- [170] Kawamura M, Kanazawa A, Kanaoka S, Aoshima S. Sequence-controlled degradable polymers by controlled cationic copolymerization of vinyl ethers and aldehydes: Precise placement of cleavable units at predetermined positions. Polym Chem 2015;6:4102–8.
- [171] Yokota D, Kanazawa A, Aoshima S. Alternating Degradable Copolymers of an Ionic Liquid-Type Vinyl Ether and a Conjugated Aldehyde: Precise Synthesis by Living Cationic Copolymerization and Dual Rare Thermosensitive Behavior in Solution. Macromolecules 2019;52:6241–9.
- [172] Shirouchi T, Kanazawa A, Kanaoka S, Aoshima S. Controlled cationic copolymerization of vinyl monomers and cyclic acetals via concurrent vinyl-addition and ring-opening mechanisms. Macromolecules 2016;49:7184–95.
- [173] Maruyama K, Kanazawa A, Aoshima S. Alternating Cationic Copolymerization of Vinyl Ethers and Aryl-Substituted Cyclic Acetals: Structural Investigation of Effects of Cyclic Acetals on Copolymerizability. Macromolecules 2022;55:4034–45.

- [174] Azuma J, Kanazawa A, Aoshima S. Cationic Polymerizability of Vinyl Acetate: Alternating Copolymerization with 1,3-Dioxolan-4-ones and Branched Copolymer Formation with Cyclic Acetals. Macromolecules 2022;55:6110–9.
- [175] Uchiyama M, Murakami Y, Satoh K, Kamigaito M. Synthesis and Degradation of Vinyl Polymers with Evenly Distributed Thioacetal Bonds in Main Chains: Cationic DT Copolymerization of Vinyl Ethers and Cyclic Thioacetals. Angew Chem Int Ed 2023;62:e202215021.
- [176] Varki A, Cummings RD, Esko JD, Freeze HH, Stanley P, Bertozzi CR, Hart GW, Etzler ME, Essentials of Glycobiology, 2<sup>nd</sup> edition. New York: Cold Spring Harbor Laboratory Press 2009.
- [177] Ragauskas AJ, Williams CK, Davison BH, Britovsek G, Cairney J, Eckert CA, Frederick Jr. WJ, Hallett JP, Leak DJ, Liotta CL, Mielenz JR, Murphy R, Templer R, Tschaplinski T. The Path Forward for Biofuels and Biomaterials. Science 2006;311:484–9.
- [178] Zhu Y, Romain C, Williams CK. Sustainable polymers from renewable resources. Nature 2016;540:354–62.
- [179] Saxon DJ, Nasiri M, Mandal M, Maduskar S, Dauenhauer PJ, Cramer CJ, Lapointe AM, Reineke TM. Architectural Control of Isosorbide-Based Polyethers via Ring-Opening Polymerization. J Am Chem Soc 2019;141:5107–11.
- [180] McGuire TM, Bowles J, Deane E, Farrar EHE, Grayson MN, Buchard A. Control of Crystallinity and Stereocomplexation of Synthetic Carbohydrate Polymers from D- and L-Xylose. Angew Chem Int Ed 2021;60:4524–8.
- [181] Stubbs CJ, Worch JC, Prydderch H, Wang Z, Mathers RT, Dobrynin AV, Becker ML, Dove AP. Sugar-Based Polymers with Stereochemistry-Dependent Degradability and Mechanical Properties. J Am Chem Soc 2022;144:1243–50.
- [182] Mikami K, Lonnecker AT, Gustafson TP, Zinnel NF, Pai PJ, Russell DH, Wooley KL. Polycarbonates derived from glucose via an organocatalytic approach. J Am Chem Soc 2013;135:6826–9.
- [183] Dane EL, Grinstaff MW. Poly-amido-saccharides: Synthesis via Anionic Polymerization of a β-Lactam Sugar Monomer. J Am Chem Soc 2012;134:16255–64.
- [184] Xiao R, Grinstaff MW. Chemical synthesis of polysaccharides and polysaccharide mimetics. Prog Polym Sci 2017;74:78–116.

- [185] Porwal MK, Reddi Y, Saxon DJ, Cramer CJ, Ellison CJ, Reineke TM. Stereoregular functionalized polysaccharides via cationic ring-opening polymerization of biomass-derived levoglucosan. Chem Sci 2022;13:4512–22.
- [186] Debsharma T, Yagci Y, Schlaad H. Cellulose-Derived Functional Polyacetal by Cationic Ring-Opening Polymerization of Levoglucosenyl Methyl Ether. Angew Chem Int Ed 2019;58:18492–5.
- [187] Wu L, Zhou ZF, Sathe D, Zhou J, Reich S, Zhao ZS, Wang J, Niu J. Precision native polysaccharides from living polymerization of anhydrosugars. Nat Chem 2023; DOI: https://doi.org/10.1038/s41557-023-01193-2.
- [188] Spring SW, Hsu JH, Sifri RJ, Yang SM, Cerione CS, Lambert TH, Ellison CJ, Fors BP. Poly(2,3-Dihydrofuran): A Strong, Biorenewable, and Degradable Thermoplastic Synthesized via Room Temperature Cationic Polymerization. J Am Chem Soc 2022;144:15727–34.
- [189] Lu L, Hua R. A Monomer-Polymer-Monomer (MPM) Organic Synthesis Strategy: Synthesis and Application of Polybenzofuran for Functionalizing Benzene Ring of Benzofuran. Asian J Org Chem 2021;10:2137–42.
- [190] Nara T, Kanazawa A, Aoshima S. Alternating-like Cationic Copolymerization of Styrene Derivatives and Benzaldehyde: Precise Synthesis of Selectively Degradable Copoly(styrenes). Macromolecules 2022;55:6852–9.